Aus der Klinik für Dermatologie, Venerologie und Allergologie,
Immunologisches Zentrum
des Städtischen Klinikums Dessau

DISSERTATION

INVOLVEMENT OF HUMAN FIBROBLASTS IN ADIPOSE TISSUE DEVELOPMENT

zur Erlangung des akademischen Grades
Doctor medicinae (Dr. med.)

vorgelegt der Medizinischen Fakultät
Charité-Universitätsmedizin Berlin

von
Vasiliki A. Zampeli
aus Preveza, Griechenland

Datum der Promotion: 22.06.2014

«It does not matter how slow you go, as long as you do not stop»

Confucius

Chinese philosopher, 551–479 BCE

To the most important people of my life;
my beloved parents, Anastasios and Thaleia,
my dearest grandmother, Vasiliki
and my precious sister, Rodoula.

« After climbing a great hill, one only finds
that there are many more hills to climb »
Nelson Mandela
South African politician, 1918-

ABSTRACT

Human adult somatic stem cells, residing in almost every human tissue, have currently attracted attention due to their multipotent abilities, and those of the skin due to their easy access. Fibroblasts, cells of mesodermal origin and major structural cells of the dermis, have been over decades regarded as "terminally differentiated" cells. More recently, dermal fibroblasts were shown to possess multilineage potential, giving rise to fat-, cartilage- and bone-like cells in numerous experiments. On the other hand, many authors continue to believe that fibroblasts do not possess such differentiation potential, although fibroblasts have been reported to be capable to differentiate into adipocytes. However, it has been disputed whether these adipocytes, indeed, derive from fibroblasts or from progenitor cells that reside in the dermis. Nevertheless, it still remains unclear whether fibroblasts, an easily accessible cell population, without being transformed into induced pluripotent cells, can themselves serve as a pool of multidynamic cells with universal – rather than isolated - cell plasticity.

The aim of my thesis was to investigate the differentiation capacity of human dermal fibroblasts, specifically towards an adipogenic phenotype and to establish a method, which makes it possible to pbtain satisfactory numbers of adipocytes from differentiated human primary skin fibroblasts. These cells could be used in therapeutic needs in regenerative medicine, for example in cases of extended lipodystrophy (facial rehabilitation in HIV-positive patients, steroid-induced lipoatrophy, scleroderma), as well as in scientific cosmetic dermatology to fill voids (skin ageing or rare genetic diseases, such as progeria syndromes). Furthermore, the differentiation capacity of dermal fibroblasts from young donors versus older ones was assessed. Moreover, the gene expression profile of adipogenic induced fibroblasts was conducted in order to gain insight into the transcriptional phenotype of differentiated cells and to map important molecular pathways during the differentiation process.

Primary fibroblasts were obtained from skin specimens of human foreskin and of the light-protected area of the inner upper arm of 30– and 76-year old women. An adipocyte induction system was applied and lipid accumulation and cell morphology in induced and control fibroblasts was analysed by fluorescence microscopy, flow cytometric analysis

(FACS) and transmission electron microscopy. Lastly, after the induction towards an adipogenic lineage, the transcriptional phenotype of the cells was determined via microarrays and compared with that of control cultures and genuine adipose tissue. The time-related expression levels of a comprehensive group of adipocyte-specific genes were further assessed by a sensitive real-time RT-PCR.

My results suggest that under special culture conditions, human dermal fibroblasts are able to accumulate intracellular lipids and to acquire an adipocyte-like morphology and transcriptional phenotype *in vitro*. This ability is stronger in cells derived from young skin in comparison to those derived from older skin. Fibroblasts from younger donors express a considerable amount of major transcription factors of adipogenesis, master regulatory genes, as well as adipocyte-specific genes. On the other hand, although adipogenesis is also initiated in fibroblasts from older donors, it is likely to remain incomplete. We conclude that dermal fibroblasts could be a suitable cell source for purposes of regenerative medicine, however younger donors should be preferred and regenerative treatments should be performed at early ages.

ZUSAMMENFASSUNG

Aufgrund Ihrer multipotenten Fähigkeiten gelangten die erwachsenen humanen somatischen Stammzellen in den Fokus des wissenschaftlichen Interesse. Von besonderer Bedeutung sind hier die dermalen Stammzellen, da für diese eine einfache Entnahmemöglichkeit besteht. Fibroblasten sind Zellen mesodermalen Ursprungs und die Hauptstrukturzellen der Dermis. Sie werden als nahezu entdifferenzierte Zellen betrachtet. Es gab bislang wenige Berichte, dass Fibroblasten zu Adipozyten differenzieren können. Es konnte in bisherigen Experimenten nicht geklärt werden, ob diese Adipozyten von Fibroblasten oder Präadipozyten abstammen, welche eine Vorstufe der Adipozyten darstellen.

Ziel des Projektes war die Etablierung einer Methode, um aus primären Fibroblasten menschlicher Haut eine größere Anzahl von Adipozyten zu erhalten und die experimentelle Überprüfung der Hypothese, dass sich primäre Fibroblasten menschlicher Haut in Adipozyten umwandeln können. Die induziertne Fibroblasten und daraus gewonnenen Adipozyten könnten sowohl für therapeutische Zwecke der regenerativen Medizin (z.B. in Zell- und Gewebetransplantation, Lipoatrophien bei HIV-positiv Patienten, steroid-induzierte Lipoatrophien, Sklerodermie) als auch für die wissenschaftliche kosmetische Dermatologie (z.B. Hautalterung oder bei Syndromen mit extremer, vorzeitiger Alterung der Patienten wie zum Beispiel dem Progerie-Syndrome) genutzt werden.

Primäre Fibroblasten wurden aus humaner Vorhaut und aus lichtgeschützer Haut an der Oberarminnenseite von 30 und 76 Jahre alten Frauen gewonnen. Eine Induktion der Fibroblasten zu Adipozyten wurde durchgeführt und die Lipidspeicherung in den induzierten Fibroblasten mittels Fluoreszenzmikroskopie, Durchflusszytometrie und Elektronenmikroskopie beurteilt. Zuletzt wurde der transkriptionelle Phänotyp der Zellen bestimmt und mit Kontrollzellen (nativen Fibroblasten) und Fettgewebsadipozyten verglichen. Adipozytenspezifische Gene wurden mit real-time PCR und microarray Genanalyse untersucht.

Unsere Ergebnisse zeigen, dass unter speziellen Kulturbedingungen kultivierte humane Hautfibroblasten fähig sind, zu Adipozyten-ähnlichen Zellen zu differenzieren. Diese Fähigkeit zur Differenzierung ist bei Fibroblasten von jüngeren Spenderinnen stärker als bei Fibroblasten von älteren Spenderinnen. „Junge“ sowie „alte“ Fibroblasten exprimieren nach der adipogenen Induktion eine signifikante Anzahl von wichtigen Transkriptionsfaktoren und regulatorischen Genen der Adipogenese, sowie Adipozyten-spezifischen Gene und

Differenzierungsmarker. Allerdings exprimieren die induzierten „alten“ Fibroblasten eine kleinere Anzahl von Genen als „junge“ Fibroblasten mit schwächerer Expression als bei den „jungen“ induzierten Zellen.

Zusammenfassend könnten dermale Fibroblasten eine geeignete Quelle für Zellen sein, die für Zwecke der regenerativen Medizin gebraucht werden. Jüngere Spender sollten hierbei bevorzugt werden und regenerative Behandlungen frühzeitig durchgeführt werden.

«Alles Gescheite ist schon gedacht worden, man
muss nur versuchen, es noch einmal zu denken»
«Everything worthwhile and intelligent has already
been thought. One can only try to think it over again»
Johann Wolfgang von Goethe
German poet and philosopher, 1749-1832

1. INTRODUCTION

1.1. Human stem cells

Tissue bioengineering and regenerative medicine have attracted much attention in the past few years and have become an intriguing and promising field of medical technology. The cornerstone of regenerative medicine is without question the stem cell, which represents a non-specialized, undifferentiated cell that preserves the ability of self-renewal in an undifferentiated state or, by generating progenitor cells (which are widely also regarded as stem cells), being able to produce any type of specialized cell (Zouboulis et al., 2008). Three categories of naturally occurring stem cells have been identified to date: embryonic stem cells (ES) (blastocyst, epiblast-derived or germ cell-derived), adult stem cells (AS) (tissue-specific or cord blood), and cancer stem cells (Boheler, 2009; Gundry et al., 2011). A fourth class of stem cells, which derive *in vitro* from fetal or adult cells types through reprogramming, are known as induced pluripotent stem cells (iPS) (Prigione et al., 2011).

1.1.1. Stem cell potency

Cell potency is the term used to describe the differentiation capacity of a cell or otherwise said of a cell's capacity to differentiate into different cell types. Scells can be categorised in a functional hierarchy according to their differentiation potency (Fig. 1.1.1.). Mammalian development commences with the totipotent zygote, which is a self-contained entity that can give rise to a whole organism. As development unfolds, cells of the early embryo proliferate and gradually lose their totipotency. This restriction in developmental potential indicates the irreversible differentiation and specialization of early embryonic cells into the first two lineages, the inner cell mass, that includes cells that will give rise to the fetus and the trophectoderm, and an outer layer of cells that is destined to an extraembryonic fate (Mitalipov and Wolf, 2009). Pluripotent embryonic or embryonal cells (ES) display the

broadest developmental potential after the zygote and can differentiate into all cells of a developing embryo (Boheler, 2009). A step further, multipotent stem cells are more fate-restricted and can generate cells only from a limited number of cell lineages. A lineage stem cell is considered to be permanently committed to a specific function and a specific lineage, thus oligopotent, whereas tissue-determined stem cells are only tri- or bipotent being able to differentiate only in one or two different cell types of the tissue they belong to. Unipotent or progenitor cells have the capacity only to generate one specific cell type. At the end of this long series of cell divisions that form the embryo are the so called terminally differentiated cells that are nullpotent, meaning they possess no differential capacity.

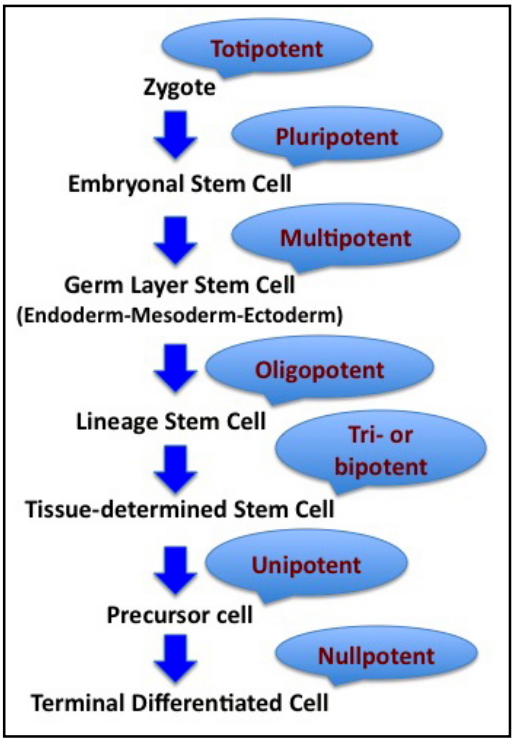

Fig. 1.1.1. Stem cell hierarchy according to differentiation potency.

1.1.2. Human embryonic stem cells (ES)

The discovery of human ES cells in 1998 has been one of the most exciting developments of recent years (Thomson et al., 1998). Human ES are characterized by important aspects, such as self-renewal, which means that they can undergo numerous cycles of cell division while maintaining their undifferentiated state; long life; high proliferative potential and therefore they are characterised as pluripotent cells. The term “pluripotency” originates from the Latin word *plurimus*, which means “many” and the word *potent*, meaning “having great power” and describes the capacity of a pluripotent cell to differentiate into specialized cell types representing all three primary germ layers - endoderm, ectoderm and mesoderm. Replication of ES cells can occur either symmetrically when a stem cell division gives rise to two identical stem cells or asymmetrically when a stem cell produces an identical and a more differentiated daughter cell. ES cells divide symmetrically, whereas asymmetrical cell division can be found in adult stem cells (Morrison and Kimble, 2006).

The potential applications of these cells to repair, replace or regenerate failing tissues and organs delivered a revolution in terms of how we treat cardiovascular disease, neurodegenerative disease, cancer, diabetes, and the like. Derivatives of the first human ES

line, obtained by J. Thomson's research group, have been used in clinical trials in patients with spinal cord injury (ClinicalTrials.gov, 2010), whereas since their isolation many other human ES lines have been produced and have been already used, for example to generate cells in treating blindness (Schwartz et al., 2012).

However, experimenting on embryonic stem cells derivating either from embryos created for in vitro fertilization but left unused, or embryos created especially for research has raised major ethical questions and created controversies in the scientific circles, thus leading scientists to discover new strategies in order to bypass the ethical debate (de Vries et al., 2008; Sugarman, 2008).

1.1.3. Induced pluripotent stem cells (iPS)

Two independently working research groups have reported, almost simultaneously, in 2007 a breakthrough in human stem cell technology. Yu and his colleagues managed to reprogram, in vitro, somatic cell nuclei (IMR90 cell-line human Caucasian fetal lung fibroblasts) to an undifferentiated state by using four factors (OCT4, SOX2, NANOG, and LIN28). The induced cells were shown to exhibit the essential characteristics of ES cells, including pluripotency, had normal karyotypes, expressed telomerase activity, cell surface markers and genes that normally characterize human ES cells, and lastly they maintained the developmental potential to differentiate into advanced derivatives of all three primary germ layers. Therefore, the cells were named “induced pluripotent stem cells” (iPS) (Yu et al., 2007).

Takahashi’s group, after reporting in 2006 the generation of iPS cells capable of germline transmission, from mouse somatic cells by transduction of four defined transcription factors (Takahashi and Yamanaka, 2006), they managed to demonstrate the generation of iPS cells, also from adult human dermal fibroblasts, with the same four factors: OCT 3/4, SOX2, KLF4, and c-MYC. In the same work these cells were reported to possess all the essential features of human ES cells, and therefore it was demonstrated that iPS cells could be generated from adult human fibroblasts (Takahashi et al., 2007).

Following the same pattern, many other groups have reported the reprogramming of either human or murine somatic cells to pluripotency; in most cases, direct reprogramming has been achieved by forced expression of defined factors using multiple viral vectors (Wernig et al., 2007; Maherali et al., 2007; Park et al., 2008; Okita et al., 2007). However, it has been reported that such iPS cells may contain a large number of viral vector integrations, which

could cause unpredictable genetic dysfunction (Takahashi and Yamanaka, 2006). In order to overcome this obstacle, new protocols for the induction of pluripotent stem cells have been generated, which deploy non-viral transfection of a single multiprotein expression vector, which comprises the coding sequences of c-MYC, KLF4, OCT4 and SOX2 linked with peptides which are able to reprogram both mouse and human fibroblasts (Kaji et al., 2009).

Furthermore, most of the initial studies on iPS cell generation have relied, among other genes, on the use of c-MYC and KLF4, two well-known oncogenes (Yu et al., 2007). The presence of such genes in the reprogramming cocktail has been strongly linked to tumorigenesis due to oncogene re-activation and accumulation of point mutations (Sun et al., 2010; Gore et al., 2011). In order to moderate these side effects and to produce "safer" iPS cells, a great range of different protocols has been reported in the literature. These include a reduction in the number of factors used for reprogramming, the engineering of more potent transcription factors, the combination of chemical compounds alongside different reprogramming factors, as well as non-integrative approaches (reviewed by Montserrat et al., 2012). Furthermore, in 2012, the group of Montserrat et al. reported the rapid, reproducible and highly efficient generation of iPS cells derived from endogenous kidney tubular renal epithelial cells with only two transcriptional factors: OCT4 and SOX2 (Montserrat et al., 2012).

In summary, although iPS cells have introduced a new era in the stem cell technology field and provided hope for new therapeutic strategies by regenerating failing tissues, a number of different considerations have to be taken into account. The methodologies employed should avoid the use of oncogenes, such as c-Myc, while the number of integrations, and thus the number of independent viral particles encoding each reprogramming factor, has to be kept to a minimum while allowing for robust expression of the transgenes in the initial reprogramming phase and the reprogramming procedure has to be fast and efficient in terms of reproducibility and number of iPS cell colonies generated (Montserrat et al., 2012).

1.1.4. Human adult stem (AS) cells

Adult stem cells (AS) are also known as somatic cells, deriving from the Greek word «σωματικός», which means "of or relating to the body". AS cells are undifferentiated cells, found throughout the human body among differentiated cells that multiply mainly through asymmetrical cell division to replace and renew dying cells and regenerate damaged tissues.

AS cells have been identified in fetal, mature and geriatric humans (Young et al., 2001) and in multiple organs and tissues, such as umbilical cord, endometrial polyps, menses blood, bone marrow, adipose tissue, brain, peripheral blood, blood vessels, skeletal muscle, skin, teeth, heart, gut, liver, ovarian epithelium, testis, etc (Jiang et al., 2002; Ding et al., 2011). The ease of harvest and the quantity obtained make these sources most practical for experimental and possible clinical applications, and therefore AS cells have attracted a huge amount of scientific attention in the last decade.

These rare and specialized AS cells are required for tissue replacement throughout the lifespan of an organism. Stem cells in several tissues are largely retained in a quiescent state but can be coaxed back into the cell cycle in response to extracellular cues. Once stimulated to divide, AS cells yield undifferentiated progenitors, which are relatively undifferentiated cell types that are derived from asymmetric stem cell division and lack the capacity to self-renew. The progenitors in turn produce differentiated effector cells through subsequent rounds of proliferation. Resident self-renewing cells are thought to have a significant role in the homeostatic maintenance of many organs and tissues (reviewed by Zouboulis et al., 2008).

AS cells are thought to reside in a specific area of each tissue called a "stem cell niche" (reviewed by Zouboulis et al. 2008). Stem cell niches are composed of microenvironmental cells that nurture stem cells and enable them to maintain tissue homeostasis (Moore and Lemischka, 2006).

1.1.4.1. Multipotency of human AS cells

Compared with ES cells, tissue-specific AS cells have been demonstrated to posses characteristics of ES cells, such as self-renewal, long life, high proliferative potential, but on the other hand, they have been reported to be more fate-restricted, and therefore characterised as multipotent cells (in contrast to pluripotent ES cells) (Hematti, 2011; Si et al., 2011). Multipotency is the capacity of an undifferentiated cell found in a differentiated tissue to renew itself and differentiate into all the specialized cell types of the tissue from which it originated, in contrast to pluripotency, whereby the cells can generate any kind of human body tissue cells under the appropriate environmental conditions. An example of a multipotent AS cell is a hematopoietic cell, which can generate all types of blood cells (intra-lineage differentiation), but is unable to transform into a cell of a different origin (over-lineage differentiation). After multiple divisions, the terminally differentiated cells are

permanently committed to a specific function, for example in the case of erythrocytes, to transport oxygen and carbon dioxide in the blood (Fig. 1.1.4.1.).

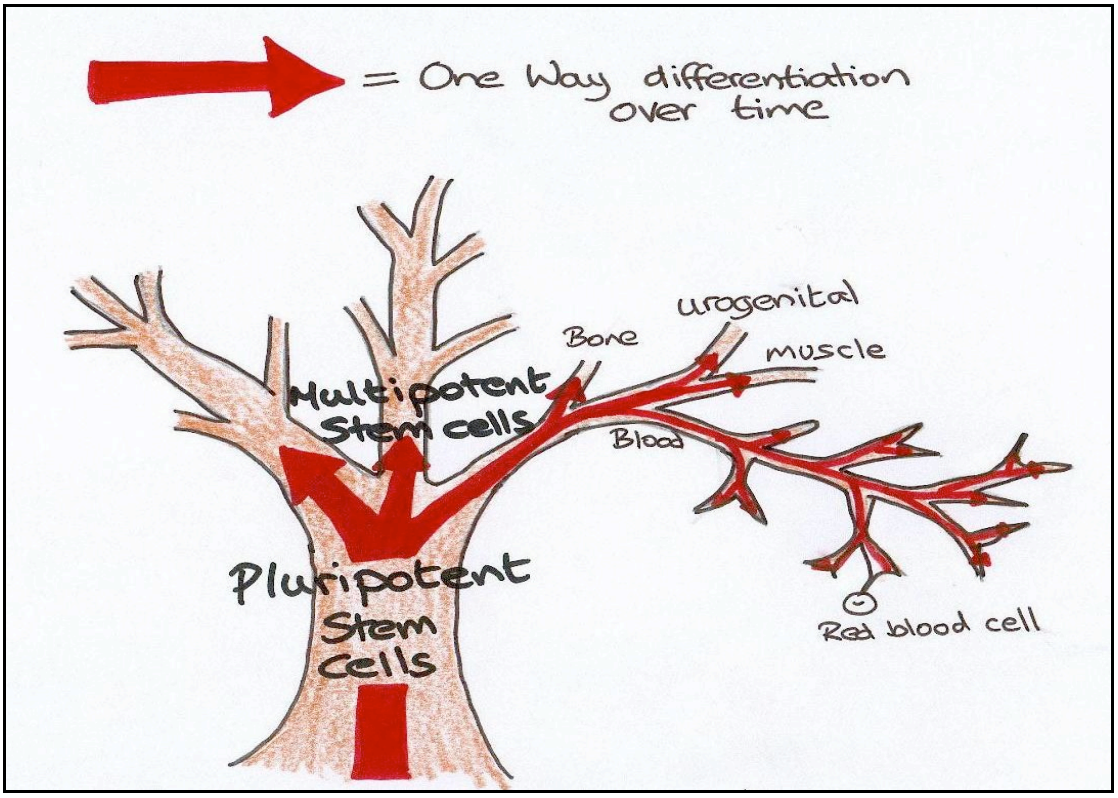

Fig. 1.1.4.1. A simplified schematic representation of the terms "pluripotency" and "multipotency". The "pluripotent stem cells" represent the trunk of the tree, being able to give rise to all possible branches (multiple cell types), whereas "multipotent stem cells" are placed at the beginning of the tree branch, implying the commitment of these cells to a specific cell lineage. (Picture from www.sarahwray.com/page6.htm)

However, many recent published studies have suggested that AS cells may have the ability to give rise to cell types of tissues from unrelated organs, thus being able to transdifferentiate and achieve an over-lineage transformation (Verfaillie CM, 2005; Chien et al., 2006; Sieber-Blum et al., 2004; Lysy et al., 2007). As a result, many authors describe the AS cells as being pluripotent instead of multipotent, referring to their ability to generate multiple cell types (Sieber-Blum et al., 2004). On the other hand, there have also been reports of AS cell populations in adult animals being lineage-committed and referred to as tripotent, bipotent or even unipotent, demonstrating only a limited capacity for differentiation (Young and Black, 2004). This controversy demonstrates the challenges of studying AS cells and suggests that additional research using adult stem cells is necessary to understand their full potential as future therapeutic targets.

1.1.4.2. Classification of human AS cells

AS cells can be classified into multiple broad types mainly based on their origin (Fig. 1.1.4.2.). As scientists continue to discover and report new AS cell sources in every possible human tissue, more AS cell type groups are added to this classification. It is worth mentioning that some scientists believe that AS cells actually evolved from ES cells and that the stem cells observed in adult organs are the remains of original ES cells that gave up in the race to differentiate into developing organs or remained in cell niches in the organs which are called upon for repair during tissue injury (Anderson et al., 2001).

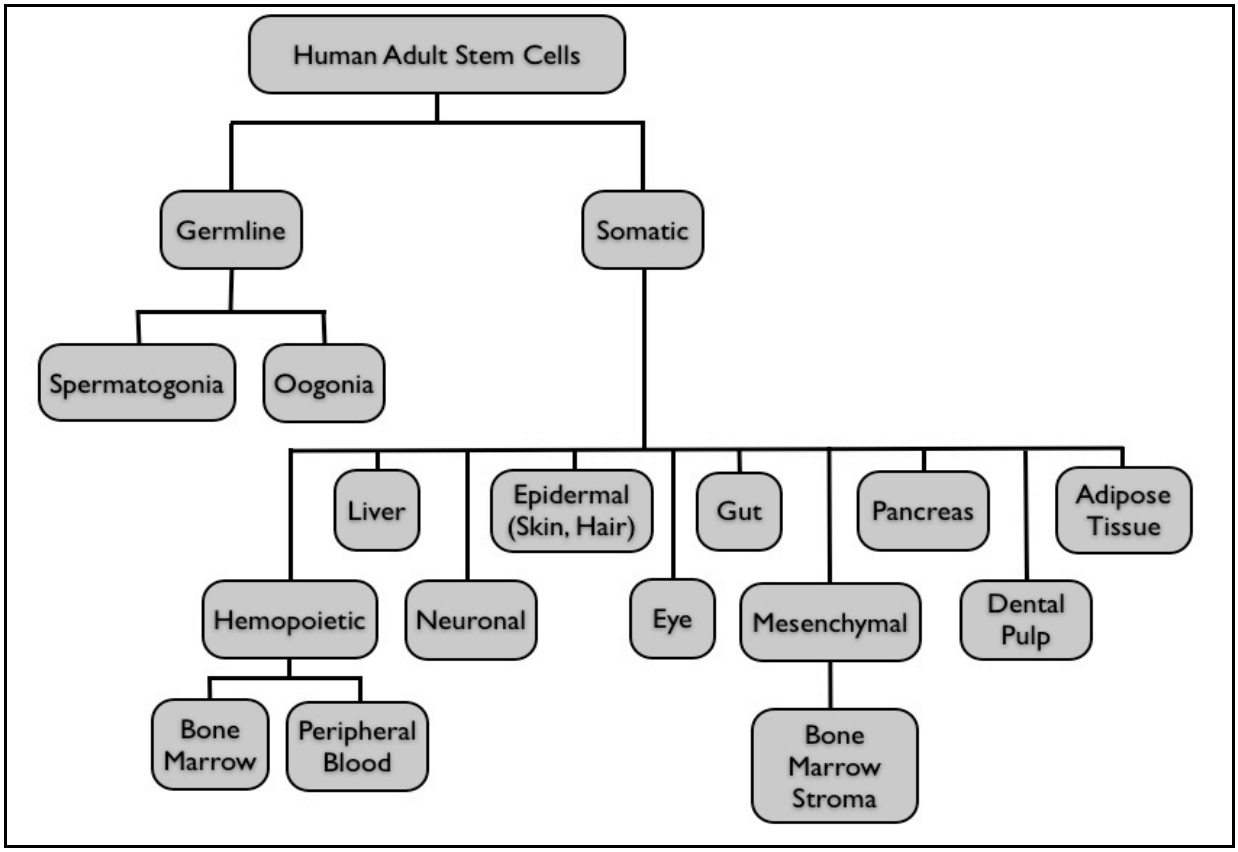

Fig. 1.1.4.2. Classification of human adult stem cells based on their tissue origin.
(*Based on*: Bongso and Lee, 2005)

1.1.5. Cancer stem cells (CS)

Cancer stem cells (CS) are a subpopulation of tumor cells with distinct stem-like properties, which are responsible for tumor initiation, invasive growth, and metastasis formation. CS cells appear to be resistant to chemotherapy, may remain quiescent for extended periods, and have affinity for hypoxic environments (Tirino et al., 2012). There is mounting evidence from cell purification studies that these cancer-initiating cells, that are distinct from the bulk of the

tumor, are responsible for long-term maintenance of tumor growth in several cancers, such as acute leukemias, although recent studies have identified CS cells in an increasingly longer list of solid tumors, including brain, breast, and colon (Ailles and Weissman, 2007; Dalerba et al., 2007; Dick, 2008). CS cells are therefore considered to be highly oncogenic and cannot be considered for therapeutic purposes, however they have managed to give us further insight into understanding the pathogenetic mechanisms underlying cancer initiation and progression.

1.2. Human skin and adult stem cells

1.2.1. General – Human skin

Skin is our largest organ, weighing in an average adult about 3.6 kilograms and covering a surface area of an average of 2 square meters. It exhibits multiple functions, with the most important being that it serves as a protective barrier between internal organs and the environment. Three basic layers are identified: epidermis, dermis and subcutaneous tissue.

Epidermis

The outermost layer of the skin is the epidermis, which is in fact a stratified squamous epithelium, composed of proliferating basal and differentiated suprabasal keratinocytes. The epidermis is morphologically subdivided into four different layers; the stratum basale, the stratum spinosum, the stratum granulosum and the stratum corneum. The outermost layer of the epidermis is the stratum corneum, where keratinocytes migrate to and lose nuclei and cytoplasmic organelles (then also called corneocytes) and finally detach in a progress known as desquamation. The cellular progression from the basal layer to the skin surface takes about 30 days in normal skin conditions but can be accelerated in various skin defects (McGrath and Uitto, 2010). It has been actually reported that the epidermis is maintained and repaired by a population of resident somatic stem cells, which reside in the proliferative basal cell layer and are believed to persist for the lifetime of an individual (Stern and Bickenbach, 2007). Other cells of the epidermis are: the dendritic pigment producing cells, known as melanocytes, which distribute packages of melanin in melanosomes to surrounding keratinocytes and are responsible for the skin's colour; the Langerhans cells, which are dendritic, antigen-presenting cells, playing an important role in the immune responses of the skin; and the Merkel cells, which have a role as mechanosensory receptors in response to touch (McGrath and Uitto, 2010). Melanocytes, Merkel cells as well as keratinocytes emerge from the outermost of the germ layers, the ectoderm. However, Langerhans cells are the only cells in

the epidermis that are of mesenchymal origin (arising from the mesoderm). The normal human epidermis contains a low percentage (< 1.3%) of lymphocytes, that are usually inconspicuous by immunohistochemical techniques, as well as Toker cells, which have been first described in 1970 in the epidermis of 10% of nipple skin in both sexes, whereas their precise nature and role in normal and diseased skin remain poorly understood (Kanitakis, 2002).

Epidermal appendages

Hair follicles, sebaceous glands, and sweat glands, known as epidermal appendages, are specialised intradermal epithelial structures, which although connected to the skin surface, they are mainly located in the dermis. They are a major source of epithelial cells, thus playing a key role in the re-epithelialization for example in cutaneous wound healing.

Dermo-epidermal junction

A complex membrane synthesised by basal keratinocytes and dermal fibroblasts comprises the so called dermo-epidermal junction (DEJ), which offers the mechanical support needed for the stable adhesion of the epidermis to the dermis. Simultaneously, the DEJ contributes to cell migration, to the exchange of metabolic products between these two compartments, as well as to the epithelial-mesenchymal signalling events (Kanitakis, 2002). It can be divided with the help of light microscopy into two layers: the lamina lucida and lamina densa.

Dermis

The dermis, known as the ‘‘backbone’’ of our skin, provides structural support for its vasculature, appendages, and epidermis and is composed primarily of extracellular matrix. This extracellular matrix consists of several types of proteins, proteoglycans, and glycosaminoglycans, which are largely produced and secreted by fibroblasts. There are two main types of protein fibres, namely collagen and elastic fibres, whereas collagen and in particular Type I is by far the most abundant protein in human skin, accounting for more than 90% of its dry weight (Fisher et al., 2008). Other types of collagen are also contained in human skin, in fact twenty-nine different collagen types have been identified in vertebrate of which at least 12 are expressed in the skin (McGrath and Uitto, 2010). Type III collagen is the second most abundant fibrillar collagen found in the skin with a ratio, when compared to type I, of type I: type III 6:1 (Burgeson et al., 1994). Collagen fibers and their physical properties are responsible for the unique tensile strength and stability of the skin (Uitto, 1993), whereas

elastic fibers comprise not more than 2-4% of the extracellular matrix and are responsible for its elasticity and resilience. Elastic fibers composition includes mainly two proteins, elastin and fibrillin, both of which are produced by resident fibroblasts. As far as the resident cells of the dermis are concerned, fibroblasts constitute its fundamental cells and of all connective tissues, whereas dermal dendrocytes can also be found in the human dermis, representing a heterogeneous population of mesenchymal dendritic cells, recognized mainly thanks to immunohistochemistry (Narvaez et al., 1996). Mast cells are also sparsely distributed in the perivascular and periadnexal dermis (Kanitakis, 2002). Between the dermal collagen, the elastic tissue and the dermal resident cells is the ground substance consisting of glycosaminoglycan/proteoglycan macromolecules.

Subcutaneous tissue/ Hypodermis

The subcutaneous fat tissue, located under the skin, plays a major role in thermoregulation, energy storage, mechanical protection and insulation. In recent years it has been shown that adipose tissue not only counts as a passive lipid storage tissue but that it possesses a central role in lipid and glucose metabolism and, as an endocrine organ, produces numerous hormones and cytokines, for example tumor necrosis factor-alpha (TNF-α), interleukin-6 (IL-6), adiponectin (AdipoQ), leptin (LEP), and plasminogen activator inhibitor-1 (PAI-1) (Hajer et al., 2008). Adipocytes are the main resident cells of the adipose tissue and are arranged in primary and secondary lobules surrounded by other cells, such as macrophages, fibroblasts, endothelial cells and pre-adipocytes.

1.2.2. AS cell "niches" in the skin

The word 'niche' originates from the Latin word '*nidus*', meaning nest and provides a safe and secured microenvironment, where AS cells reside in a quiescent state, until they are activated and start to proliferate, for example in the wound healing process. At the same time niches allow multiple interactions of the contained AS cells, not only within the niche, but also with differentiated cells of neighbour tissues. AS cell niches have been identified throughout the whole human body and most importantly throughout all layers of human skin, namely the epidermis (i.e. interfollicular areas, hair follicle bulge), the dermis (peripilar connective tissue sheaths, hair papilla) and the hypodermis (adipose tissue) (Quatresooz et al., 2012).

1.2.2.1. The epidermal niche

AS cells of the epidermis play a key role in maintaining skin homeostasis, as well as in the skin repairing process by generating new cells to replace either the aged epidermal cells during normal tissue turnover or the damaged cells following injuries (Blanpain et al., 2007). At least three major AS cell niches, which are responsible for replacing the epidermal differentiated cells, have been described to reside within the human epidermis: (i) the basal layer of the interfollicular epithelium/epidermis (IFE), (ii) the sebaceous gland (SG) and (iii) the hair follicle (HF) bulge (Fuchs, 2008; Zouboulis et al., 2008).

1.2.2.1.1. Stem cells of the basal layer of the IFE

As already mentioned, basal cells residing as a single layer on the basal membrane of the epidermis are responsible for the continuous rejuvenation of the skin. As they detach from the basement membrane they withdraw from the cell cycle and enter the process of terminal differentiation, while moving upward to the skin surface, where they finally lose their nuclei and become cornified cells (corneocytes). Corneocytes are continuously shed from the surface of the skin and therefore new differentiated cells must be generated throughout life (Zouboulis et al., 2008). It has been already noticed in the late 80s that the cells of the basal layer of the IFE of adult mouse were unsynchronised, meaning that not all cells were to be found at the same time-point of the cell cycle. This finding was interpreted to mean hat these stem cells were able to divide in an infrequent manner, while their no-stem progeny, named transit amplifying cell, entered the cell cycle and divided a number of times, before committing and becoming a terminally differentiated cell. The hypothesis was that a single stem cell, surrounded by transit amplifying cells lies at the base of a column of differentiated cells, forming an ‘epidermal proliferative unit’ (reviewed by Potten and Morris, 1988; reviewed by Watt and Jensen, 2009). This model implied that there is only a small amount of stem cells located in the basal membrane. However, recent research studies provided evidence, by performing lineage tracing experiments and clonal analysis, that this model might actually not be correct. The new model proposed suggests that basal epidermal cells can divide asymmetrically, thus providing a different point of view on how basal stem cells and committed cells are produced (Lechler and Fuchs, 2005; Clayton et al., 2007; Jones et al., 2007). This new model of the asymmetrical divisions implies that only a single progenitor population, which resides within the basal layer is able to give rise to committed cells. A simplified explanation of this model is to imagine a resident epidermal niche AS cell that

upon stimulation has the ability to follow either one of three different pathways: (i) symmetric division into two cells destined to undergo terminal differentiation, (ii) symmetric division into two cells that remain undifferentiated in the basal layer (self renewal), or (iii) asymetric division into one cell that enters the process of terminal differentiation and one cell that remains undifferentiated (reviewed by Watt and Jensen, 2009) (Fig. 1.2.2.1.1.).

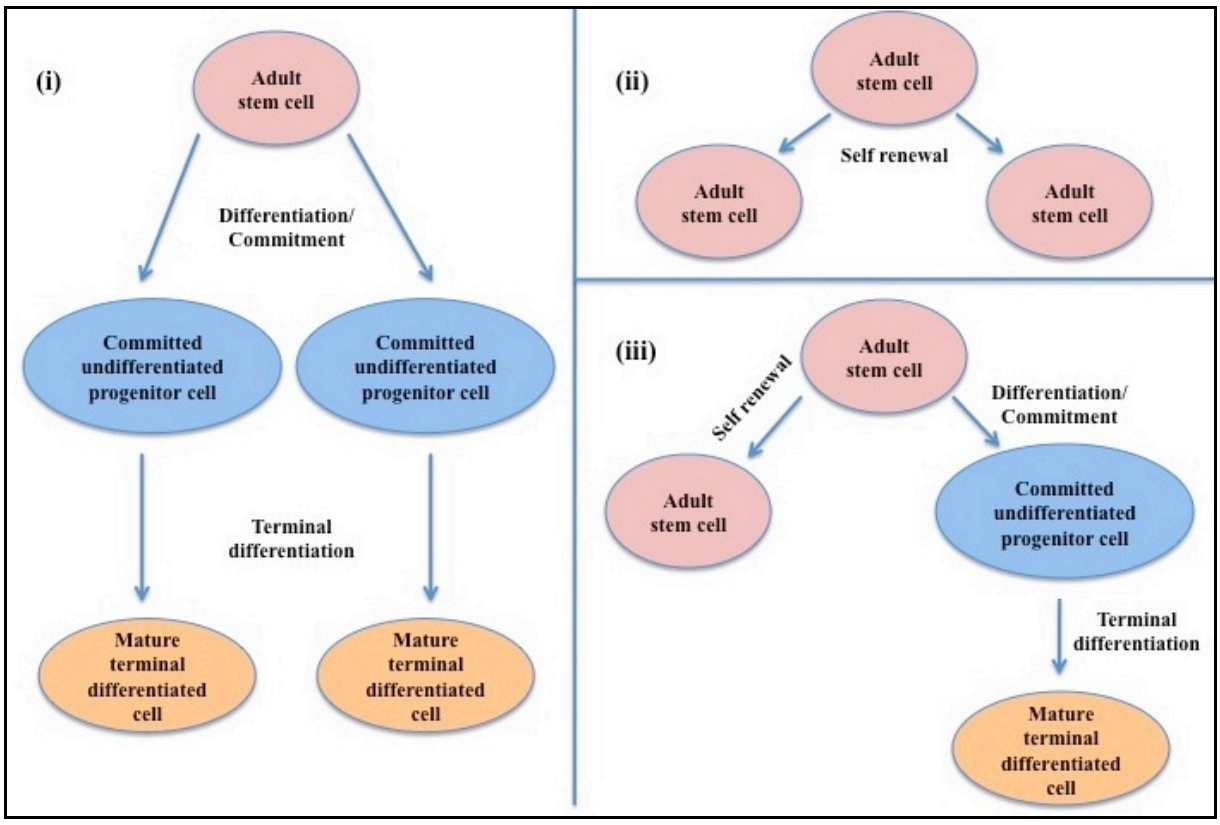

Fig. 1.2.2.1.1. Schematic explanation of the asymetric and symmetric division model. A resident epidermal niche AS cell (pink) upon stimulation (e.g. tissue injury) has the ability to follow either one of three different pathways: (i) symmetric division into two cells destined to undergo terminal differentiation (blue), (ii) symmetric division into two cells that remain undifferentiated in the basal layer (self renewal), or (iii) asymmetric division into one cell that enter the process of terminal differentiation and one that will remain undifferentiated.

Many different pathways have been suggested to play an important role in the regulation, function and proliferation of the AS cells of the IFE, in particular components of the wingless-type (Wnt)/β-catenin, sonic hedgehog (Shh), and transforming growth factor (TGF)-β/bone morphogenetic protein (BMP) pathways (Blanpain and Fuchs, 2006; Yang and Peng, 2010; Wong et al., 2012).

In the last decade, clonal growth assays have managed to give more insight into the AS cells of the IFE by providing a number of markers that enrich for highly clonogenic cells,

including b1 integrins and the epidermal growth factor (EGF) antagonist Lrig1 (Jensen and Watt, 2006; Jones and Watt, 1993; Watt and Jensen, 2009). Specifically, it has been reported that the $\alpha_6\beta_4$ integrin is associated with the basal surface, whereas the $\alpha_2\beta_1$ and $\alpha_3\beta_1$ integrins are associated with the lateral (mainly) and basal (minor) surfaces of epidermal basal cells (De Luca et al., 1990). Furthermore, a study in 2010 revealed several biomarkers being localized uniquely to the basal IFE, namely the CD34 and CD117 and also the biomarkers CK15, CD49f, and CD29 that are all expressed in the IFE and in stem cells of the HF bulge. In addition, in the same study it has been reported that both basal IFE and bulge stem cells do not express CD71 or CD24, suggesting their potential utility as negative selection markers (Jiang et al., 2010).

1.2.2.1.2. Stem cells of the HF

The HF participates throughout life in multiple cycles of regeneration and degeneration. The growth phase of the hair follicle (HF) is known as anagen phase, which can last from 2 up to 7 years, depending among other things on genetically determined factors, the location of the HF etc. The catagen phase follows the anagen phase; it lasts for about 2 to 3 weeks during which apoptosis-driven epithelial regression takes place. The end of the HF cycle is marked by the telogen phase with a duration of about three months, which is a period of relative quiescence and results into the rest of the HF. These events require the presence of fully functional epithelial stem cell populations, which are capable of constructing all epithelial differentiation strata (Zouboulis et al., 2008). Within the HF, the best investigated stem cell compartment lies in the bulge, the lower permanent part of the HF that is established during morphogenesis but does not degenerate during the hair cycle (Cotsarelis et al., 1990; Oshima, et al., 2001). It is now well known that at the start of each new hair cycle, a cluster of stem cells at the base of the bulge becomes activated and starts proliferating. However, grafting and lineage tracing experiments have shown that some bulge stem cells can form not only new HFs but also (sebaceous gland) SGs and epidermis in cases of wound healing. (Blanpain et al., 2004; Claudinot et al., 2005; Fuchs, 2008). That means that, although HF stem cells are multipotent, unless the skin is wounded, they only contribute to HF homeostasis and do not contribute to IFE formation (Ito et al., 2005; Levy et al., 2007, Fuchs, 2008). In addition – at least in murine HF – nestin-positive cells that apparently arise from the epithelial bulge, have been reported to have the capacity to generate non-epithelial cells like neurons or Schwann cells (Hoffman, 2006), indicating a lineage-independent pluripotent character.

There is enough data supporting the observation that the BMP signaling pathway plays a crucial role in follicle stem cell quiescence (Blanpain et al., 2004). The TGF-β signaling pathway also appears to be upregulated in human bulge cells (Tumbar et al., 2004). Furthermore, as anticipated, there is increasing evidence suggesting that the upregulation of transcripts involved in the inhibition of the Wnt pathway is required for the conservation of the quiescent state of HF bulge stem cells (Fuchs and Horsley, 2008).

Markers expressed in the human bulge have also been documented, including CD200, follistatin and frizzled homologue 1 (Ohyama et al., 2006; Jiang et al., 2010). Cytokeratin 15 (CK 15) has also been long known as a useful marker of the bulge region (Lyle et al., 1998). In a further study researchers using single- or multicolour flow cytometry or immunocytochemistry reported that the bulge contained two populations with different localizations, cell sizes, and colony-forming abilities and that K15, CD200, CD34, and CD271 were useful biomarkers for characterizing freshly isolated human follicular epithelial cells in diverse stages of differentiation (Inoue et al., 2009).

1.2.2.1.3. Stem cells of the SG

The SG is located above the bulge and its main role in the skin is to produce fully differentiated sebocytes, which are highly specialized, sebum-producing epithelial cells that release their content by rupture of the cell membrane and cellular degradation (holocrine secretion). Its development is closely related to the differentiation process of the other two epidermal lineages, the HF and the IFE (Zouboulis, 2004). In recent years, a new hypothesis has begun to emerge that a distinct population of stem cells may be present in the SG, other than the stem cell populations of the IFE and the HF bulge, and that this population is actually responsible for the maintenance of the SG. Indeed, lineage tracing experiments conducted in transgenic mice in 2001 proved the presence of long-lived unipotent progenitor cells near or at the base of the SG (Ghazizadeh and Taichman, 2001). Pulse-chase experiments also in mouse skin further suggested the existence of slow-cycling cells in SGs (Braun et al., 2003). Furthermore, in studies using human immortalised sebocytes (SZ95 sebaceous gland cell line) it was shown that every SZ95 sebocyte that underwent clonal growth in culture generated progeny that differentiated into both sebocytes and cells expressing involucrin and cornifin, markers of IFE and HF inner root sheath differentiation, thus providing evidence that a resident pool of progenitor cells exists within the human SG (Lo Celso et al. 2008). The same

results were also observed in a second human sebocyte line, the Seb-E6E7 (Lo Celso et al., 2008).

In 2006, the transcriptional repressor protein of c-Myc, Blimp-1 (also known as PRDM1) was shown to mark a small population of cells at the SG base and therefore has been proposed as a possible marker of the SG stem cell population (Horsley et al., 2006). The Blimp1-positive SG cells were also found to express CK5/CK14. Genetic lineage tracing experiments showed that the Blimp-1-positive SG cells can regenerate the entire SG, including sebocytes (reviewed in Fuchs, 2008). However, contradictory results have been published concerning the fact whether Blimp-1 is actually an appropriate marker for SG stem cells. Blimp-1 expression was examined with standard immunohistochemical methods in samples from embryonic, fetal and adult human skin and in 119 sebaceous lesions comprising all major categories of sebocyte lineage, including hamartomas, cysts and benign and malignant neoplasms. The reported expression pattern failed to reconcile with a function of Blimp-1 as a marker for sebocyte progenitor cells but indicated a major role in terminal differentiation. Within the IFE, its exclusive localization in the granular layer suggested a central function in human skin barrier homeostasis (Sellheyer and Krahl, 2010). Although, Blimp1 is not selectively expressed in SG progenitor cells, but also in terminally differentiating cells in the IFE, SG and HF (Lo Celso et al., 2008), in its absence the SG is primarily affected. In cases of downregulation of Blimp-1 there is overexpression of c-Myc and the SG appears hyperplastic, with enhanced proliferation in the bulge cell compartment (Watt and Jensen, 2009). These contradictory data suggest that it still remains unclear if Blimp-1 would be an efficient marker for SG stem cells, therefore, more experimental data are needed.

Experiments from a variety of mouse models have reported that c-Myc and β-catenin exert opposing effects on SG differentiation. Specifically, activation of c-Myc leads sebocytes to differentiate along the lineages of the IFE and SG, thus generating differentiated sebocytes within the IFE (Braun et al., 2003; Arnold and Watt, 2001). On the other hand, upregulation of β-catenin induces de novo HF morphogenesis and regression of SGs (Lo Celso et al., 2004; Gat et al., 1998). Experiments on the human sebocyte lines SZ95 and Seb-E6E7 have also confirmed c-Myc and β-catenin's opposing effects on sebocyte differentiation, both *in vivo* and *in vitro*. The ability of c-Myc to promote the sebocyte lineage was shown to be independent of its ability to stimulate proliferation via induction of the Indian hedgehog signaling pathway (Lo Celso et al., 2008).

It is clear from the different populations of epidermal stem cells, that of the SG is the least well characterised. Further studies are necessary in order to gain an insight into this stem cell

population, while evidence is still required to establish conclusively that such cells exist in normal human skin.

The differential expression of stem-cell-associated markers, putative features, as well as the involved signaling pathways in human epidermal stem cell regulation are shown in the table, according to their *in situ* location in the epidermis (Table 1).

Table 1. Epidermal stem cell markers and signaling pathways according to their *in situ* location.

In situ location	Signaling pathways	Expression of surface and structural proteins	References
IFE	Shh, TGF-β, BMP, β-catenin/ Wnt, Notch, p63	CD23, CD117, CK15, CD34, CD49f, CD29, CK5, CK14, p63, E-cadherin, integrins (α6β4, α3β1), Lrig1 CD71(-), CD24(-)	Jiang, Zhao et al. 2010, Fuchs 2008; Zouboulis, Adjaye et al. 2008; Jensen and Watt 2006
HF	BMP, TGF-β, β-catenin/Wnt, Shh, Notch, p63, Lef1	CD200, CK15, CK14, CK5, CD49f, CD29, follistatin, CD117, frizzled homologue 1, CD34, CD271, LGR5, LGR6, E-cadherin, p63, integrins (α6β4, α3β1), TCF3, Sox9, Lhx2, NFATc1, Vitamin D receptor CD71(-), CD24(-)	Jiang, Zhao et al. 2010; Ohyama, Terunuma et al. 2006; Inoue, Aoi et al. 2009; Wong, Levi et al. 2012; Zouboulis, Adjaye et al. 2008; Fuchs 2008; Fuchs and Horsley 2006
SG	Shh, c-Myc, PPAR-γ, Wnt, Blimp, Notch	Blimp 1?, CK5, CK14, p63, E-cadherin, integrins (α6β4, α3β1)	Zouboulis, Adjaye et al. 2008; Wong, Levi et al. 2012; Fuchs 2008

1.2.2.2. The dermal niche

In mammalian skin, the existence of AS cells in the dermal compartment of the skin is still poorly understood. The complexity of the structure of the human dermis, as well as its heterogeneous composition of collagens, elastins, glycosaminoglycans and multiple cell types with different embryonic origin, makes the discovery and characterisation of AS dermal populations an intriguing but extremely difficult task. However, many research groups have identified and reported the presence of dermal precursor cell populations. The dermal compartment of the HF consists of the dermal papilla (DP) and dermal sheath (DS), which are both occupied by specialized fibroblasts of mesenchymal origin. Both locations have been considered to be AS cell pools. Multipotent mesenchymal stem cells (MSCs) have also been identified in murine and human dermis and consist a further source of dermal AS cells (Young et al., 2001; Bartsch et al., 2005).

1.2.2.2.1. DP and DS stem cells

During the anagen phase of the HF, connective tissue sheath and the DP are not only massively remodelled but are also greatly expanded (Tobin et al., 2003). This observation led to the assumption that resident mesenchymal precursor cell populations might be present in the dermis, thus providing regenerated cells. Indeed, one dermal cell population that has been recently reported to possess the essential properties of AS cells is that of the DP of the HF. Cells of the DP are not only essential for HF development and function, but are also a reservoir of cells with the potential to differentiate into a range of cell types that are of potential therapeutic importance (Driskell et al., 2011). Differences in Sox2 expression can be used to discriminate DP cells originating from different HF types in early postnatal mouse skin (Driskell et al., 2009). Cells positive for Sox2 are associated with Wnt, BMP, and fibroblast growth factor (FGF) signaling pathways, whereas Sox2- negative cells utilize Shh, insulin growth factor (IGF), Notch, and integrin signaling pathways (Driskell et al., 2009). Additional evidence for the existence of a mesenchymal DS stem cell population is provided by the observation that DS can generate mature mast cells from immature, resident precursor populations (Kumamoto et al., 2003; reviewed by Zouboulis et al., 2008). Both DP and DS stem cell populations have been reported to be able to give rise to mesenchymal cells along the classical mesodermal differentiation pathways, such as adipocytes and chondrocytes – both in vitro and in vivo (Jahoda et al., 2003). In experiments conducted in 2006, the growth and differentiation capacities of putative dermal stem cells in the DS and DP of the HF have been compared to those of multipotent bone marrow mesenchymal stem cells (MSCs). Following exposure to appropriate induction stimuli both cell populations were able to differentiate into various mesenchymal lineages, such as osteoblasts, adipocytes, chondrocytes, and myocytes, expressed neuroprogenitor cell marker, whereas the rate and extent of differentiation were remarkably similar to those of the bone marrow MSCs (Hoogduijn et al., 2006).

Shh signaling is important for early DP development and maturation. It is expressed by the HF epithelium and influences both mesenchyme and epithelium (Yang and Cotsarelis, 2010). BMP, Wnt and FGF signaling pathways seem to also play a crucial role in the regulation of the DP and DS stem cells.

Although the functions of most marker proteins are unknown, they have been widely used to identify DP and DS. Alkaline phosphatase (AP) and CD133 (known also as Prominin-1) are strongly expressed in DP of HF in mouse skin. Versican is reported to be specifically expressed in DP during anagen, whereas α-smooth muscle actin (αSMA) is a marker for DS

in vivo, and a marker for both DP and DS in vitro. In mouse pelage skin, Corin is expressed specifically in the DP (Yang and Cotsarelis, 2010).

Skin-derived precursors (SKPs) in the DP niche

Surprisingly, Toma et al. reported in 2001 the isolation of a unique and distinct cell population from juvenile and adult rodent skin that was able to differentiate *in vitro* in the presence of the mitogens FGF2 and EGF to produce neurons, glia, smooth muscle cells and adipocytes, thus confirming the pluripotency of these cultured precursors from skin. These cells have been identified within the skin dermis and were therefore termed ‘‘skin-derived precursors (SKPs)” (Toma et al., 2001). They are thought to partially originate from the neural crest and have been shown to exit the DP niche in order to participate in cutaneous repair (Toma JG et al., 2005). In comparison with other types of precursors cells, SKPs showed major differences, thus indicating their distinctiveness. Specifically, they were antigenically distinct from MSCs (Toma et al., 2001); they were derived from the dermis and were not able to generate keratinocytes, meaning that they did not belong to the epidermal stem cell niches (Toma et al., 2001); and finally they did not express known markers of melanocytic stem cells or haematopoietic stem cells (Fernandes et al., 2004). However, it has not been clear where SKPs normally reside in the dermis *in vivo*. *In situ* hybridization for transcription factors expressed by SKPs as well as lineage tracing experiments have provided enough evidence to show that the DP comprises one niche for the SKPs and that SKPs comprise at least a fraction of the cells within the follicle DP (Fernandes et al., 2004). However, there are probably other niches of SKPs in the skin that we do not know of, for example SKPs can be isolated also from human foreskin (Toma JG et al., 2005). SKPs have also been isolated from human skin of different ages and origins, further supporting the theory of multipotent stem cell populations with great plasticity in the human DP (Belicchi et al., 2004; Joannides et al., 2004).

Markers expressed by SKPs include a variety of neural crest-associated transcription factors such as Slug, Snail, Twist, Pax3 and Sox9. Moreover, SKPs also express transcription factors associated with the mesenchymal capability of cranial neural crest cells, such as SHOX2 and Dermo-1 (Fernandes et al., 2004; Fernandes et al., 2008).

The key signaling pathways involved in the differentiation of SKP spheres into fibroblast-like cells in vitro have been dissected by microarray analysis recently. ErbB, MAPK, ECM-receptor reaction, Wnt, cell communication, and TGF-β signaling pathways have been reported to be upregulated during this transition (Zhao et al., 2010). Furthermore, the PI3K-

Akt pathway has been shown to hold an important role in the senescence and self-renewal of human SKPs *in vitro* (Liu et al., 2011).

1.2.2.2.2. MSCs of the dermis

Multipotent mesenchymal stem cells (MSCs) have been identified and isolated in various tissues, including human dermis, and represent a further source of dermal AS cells (Young et al., 2001; Bartsch et al., 2005; Chen et al., 2007). Although most of the studies in cutaneous stem cell research have focused on stem cells of the DP of the HF, it is now clear that mesenchymal progenitor cells are also to be found within the fraction of plastic-adherent dermal cells (Young et al., 2001; Bartsch et al., 2005; Chen et al., 2007). Dermal MSCs are generally isolated by repeated passage of adherent dermal cells, followed by analysis of the ability of such cells to differentiate into mesenchymal lineages. Adherent cells that fail to differentiate into mesenchymal lineages are considered to be fibroblasts (Sudo et al., 2007). Sudo et al. analyzed in 2007 the potential of a number of human primary fibroblast-like cell populations to differentiate, showing that most of them could differentiate into at least one mesenchymal lineage to generate osteoblasts, chondrocytes, or adipocytes (Sudo et al., 2007). Furthermore, a murine mesenchymal population devoid of hematopoietic cell markers and capable of forming adipocytes, chondrocytes, osteoclasts, functional smooth muscle cells, and keratinocytes *in vitro* has also been reported. Moreover, this population was able to generate an epidermal layer in a 3-dimensional model of murine skin (Crigler et al., 2007). Even ectodermal and endodermal potential has been attributed to these cells, such as differentiation into hepatocyte-like cells (Chen et al., 2007; Lysy et al., 2007). Most recently, MSCs from human labia minora dermis-derived fibroblasts (hLMDFs) were driven through a 3-stage method to differentiate into insulin-producing cells. Further transplantation of these insulin-producing cells was able to normalize blood glucose levels and rescue glucose homeostasis in streptozotocin-induced diabetic mice (Kim et al., 2012).

Due to the fact that the phenotype of human dermal MSCs is largely similar to that of bone marrow–derived MSCs, the characterisation of these cells is a challenge (Ishii et al., 2005; Chen et al., 2007). However, Chen et al. proposed an approach to identifying phenotypically progenitor cells from adherent culture fibroblasts. The conducted phenotypic analyses showed that the tripotent fibroblasts are nestin(-) and vimentin(+) (Chen et al., 2007). Immunohistochemical staining of human derived MSCs showed that MSC markers CD73, CD90, CD105, as well as CD271 and SSEA-4, are expressed on dermal cells *in situ*.

Specifically, CD271(+) cells showed increased adipogenic, osteogenic, and chondrogenic potential, whereas SSEA-4 (+) cells appeared to have a limited adipogenic differentiation potential (Vaculik et al., 2012).

Recently, three-dimensional analysis of human scalp skin with a confocal microscope clearly demonstrated that perivascular sites may act as a niche of MSCs. Cells at these locations were positive not only for NG2, but also for CD34. Furthermore, CD34-positive cell fractions showed the expected differentiation capacities along the mesenchymal lineages (Yamanishi et al., 2012). These cells have been shown to protect their local matrix microenvironment via tissue-inhibitor-of-metalloproteinase (TIMP) mediated inhibition of matrix metalloproteinase (MMP) pathways, highlighting the importance of the extracellular matrix niche in stem cell function (Lozito and Tuan, 2011; Wong et al., 2012).

The differential expression of stem-cell-associated markers, putative features, differentiation potential, as well as the involved signaling pathways in dermal stem cell regulation and differentiation are presented in the table according to the identified dermal stem populations to-date (Table 2).

Table 2. Dermal stem cell markers, potency and signaling pathways according to different dermal stem cell populations.

Dermal stem cells	Potency	Signaling pathways	Expression of surface and structural proteins	References
DP and DS niche	Osteoblasts, Adipocytes, Chondrocytes, Myocytes	Wnt, Timp, BMP, FGF, Shh, IGF, Notch	CD90, NG2, CD34, CD44, CD54, CD73, CD105, CD133, CD271, Sox-2, AP, aSMA, versican, corin	Hoogduijn, Gorjup et al. 2006; Yang and Cotsarelis 2010; Wong, Levi et al. 2012
SKPs	Neurons, Glia, Smooth-muscle cells, Adipocytes	ErbB, MAPK, ECM-receptor reaction, Wnt, TGF-β, PI3K-Akt	Slug, Snail, Twist, nexin, Wnt5a, Versican, SHOX2, Dermo-1, Sox9, Pax, Nestin, Fibronectin, Vimentin	Fernandes, McKenzie et al. 2004; Toma, McKenzie 2005; Fernandes, Toma et al. 2008; Zouboulis, Adjaye et al. 2008; Zhao, Whitworth et al. 2010; Liu, Liu et al. 2011
MSCs	Adipocytes, Chondrocytes, Osteoblasts, Smooth-muscle cells, Keratinocytes, Hepatocytes, Insulin-producing cells	Wnt, BMP, Notch, FGF	CD73, CD90, CD105, CD271, SSEA-4, CD13, CD29, CD49, CD34, CD44, Stro-1	Crigler, Kazhanie et al. 2007; Chen, Zhao et al . 2007; Lysy, Smets et al. 2007; Vaculik, Schuster et al. 2011; Kim, Yoon et al. 2012
Perivascular scalp MSCs	Osteoblasts, Chondrocytes, Adipocytes	MMP, Timp	NG2, CD34	Yamanishi, Fujiwara et al. 2012
Fibrocytes	Fibroblasts, Myofibroblasts, Adipocytes	TGF-β, PPAR-γ	CD34, CD11b, CD45, CD71, CD80, CD86, Collagen-Type-I, III, Vimentin, HLA-DR	Quan, Cowper et al. 2004; Hong, Belperio et al. 2007

1.2.2.3. The adipose niche

Subcutaneous adipose tissue has been proved to be a precious pool of AS cells for regenerative medicine and represents a highly attractive stem cell source for two major reasons: firstly, the great availability of adipose tissue, as nowadays obesity is a common phenomenon in the developed world, and secondly, the ease of harvest of adipose tissue through routine everyday procedures, for example liposuction surgery. Although multiple different terms have been used to describe the multipotent, plastic-adherent, cell types isolated from adipose tissue, such as adipose-derived stromal cells, human multipotent adipose-derived stem cells, adipose mesenchymal stem cells or preadipocytes, the International Fat Applied Technology Society consented to use the term adipose-derived stem cells (ASCs) (Gimble et al., 2007).

Like MSCs, ASCs exhibit multipotent differentiation capabilities along the mesenchymal lineage, such as adipogenic, chondrogenic, myogenic, neurogenic, osteogenic, and tenogenic differentiation (Guilak et al., 2006; Guilak et al., 2010). The endodermal differentiation of human ASCs, particularly towards the hepatic lineage, has also been established (Seo et al., 2005). Recently, researchers conducted experiments in order to discover the ASC niche using fibrin matrix organ culture systems to sustain adipose tissue (Yang et al., 2010). ASCs were isolated from the interstitium between adipocytes and endothelium, thus providing evidence to support the current hypothesis that ASCs derive from a perivascular niche (Yang et al., 2010).

ASCs express the stromal markers CD9 (tetraspan), CD10, CD29 (integrin β1), CD44, CD73, CD90 (Thy1), and CD166 (ALCAM) (Guilak et al., 2010). Furthermore, they exhibit positive staining for osteopontin, osteonectin, Muc18; receptors for extracellular matrix proteins, e.g. CD54, CD49d (integrin α4), endoglin, CD13; and negative staining for hematopoietic markers, such as CD45 and CD34, and endothelial markers, such as CD31 (Al Battah et al., 2011).

1.3. Dermal fibroblasts: a heterogeneous cell population with a high differentiation potential

1.3.1. General features of fibroblasts

Fibroblasts are large, flat, branching, spindle-shaped cells (Fig. 1.3.1.) that constitute the main structural cells of the dermis and are responsible for the production of glycosaminoglycans,

reticular and elastic fibers, fibronectin, laminin and, most importantly for the major structural ingredient of the dermis, the collagen. Their role in wound healing is critical, as skin would not be able to recover from injury in their absence. Furthermore, apart from producing and organizing the extracellular matrix of the dermis, they also communicate with each other and other cell types, therefore playing a crucial role in regulating skin homeostasis.

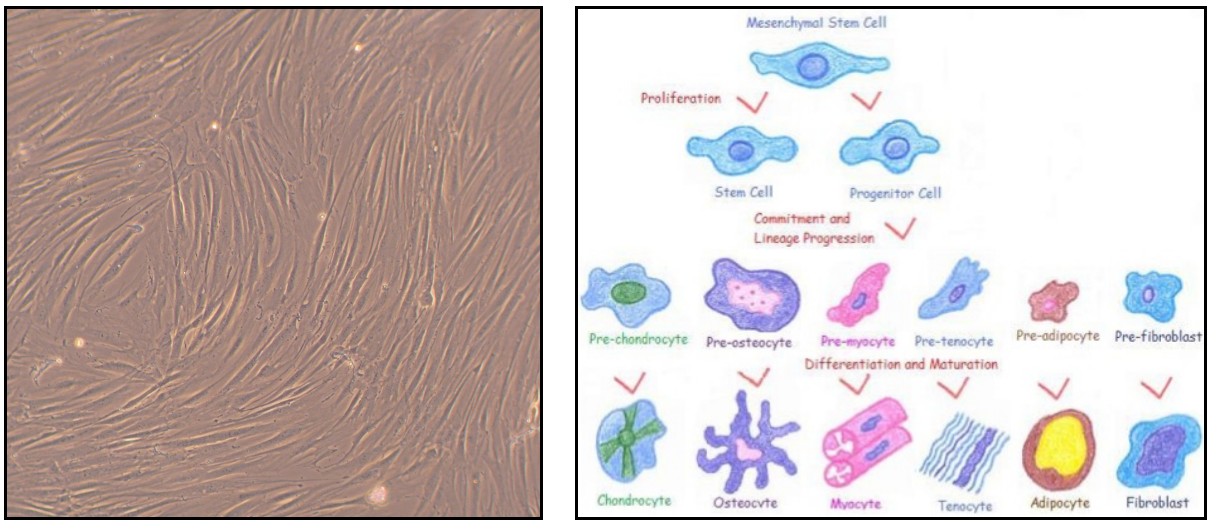

Figure 1.3.1. Morphology of human skin fibroblasts *in vitro* under light microscopy (left) and the mesenchymal cell lineage, where fibroblasts, among other cells, originate from.

Dermal fibroblasts originate from the primitive mesenchyme, which also gives rise to many other different cell types, such as chondrocytes, osteocytes, myocytes, tenocytes and adipocytes (Fig. 1.3.1.). Although fibroblasts are extremely important for the homeostasis of the dermis, there is a significant shortage of information, mostly regarding their differentiation potentials. For a long time fibroblasts have been thought to be nearly terminally differentiated cells and their differentiation capacity was thought to be non-existent. However, in the last decade fibroblasts have gained scientific society's attention and our understanding about these cells has changed immensely.

1.3.2. Dermal fibroblasts' heterogeneity

A number of research groups have proved in recent years that skin fibroblasts comprise a heterogeneous cell population and that they are a dynamic, diverse population of cells. In 2002, Chang et al. by using cDNA microarrays, evaluated the gene expression profiles of fifty primary human fibroblast cultures obtained from 10 different sites in 16 donors *in vitro*. Human fibroblasts exhibited significant topographic differences at the level of gene

expression, and thus this gave evidence that dermal fibroblasts are not the homogenous cell population they were thought to be (Chang et al., 2002). Furthermore, Sorrel and Caplan have reported that normal adult human skin contains at least three distinct subpopulations of fibroblasts, which can be found in unique niches in the dermis, namely papillary, reticular and hair-follicle-associated fibroblasts, each exhibiting distinct features (Sorrell and Caplan, 2004).

1.3.3. Dermal fibroblasts' differentiation potentials

One of the first articles to have implied that fibroblasts may be capable of adipogenic differentiation was published in 1983 by Broad and Ham, who reported that ovine fibroblasts spontaneously underwent adipose differentiation when maintained as a confluent monolayer in a medium containing insulin, dexamethasone and FGF (Broad and Ham, 1983). However, it was not clear whether these cells were of adipocyte lineage and whether they originated from fibroblasts or pre-adipocytes that normally give rise to adipocytes. Since then, many contradictory data have been published concerning the differentiation potential of fibroblasts. Several authors have reported an osteogenic and chondrogenic potential of human dermal fibroblasts (Kresbach et al., 2000; Rutherford et al., 2002; Hee and Nicoll, 2006; Mizuno and Glowacki, 1996; Rutherford et al., 2003). Although adipose differentiation was thought to only be possible for embryonic fibroblasts or the fibroblast-like murine 3T3-L1 cell line (Gregoire, 2001; Gregoire et al., 1998), in 2006 adipocytes were obtained from human orbital fibroblasts (Feldon et al., 2006). More recently, dermal fibroblasts were shown to possess multilineage potential, giving rise to fat-, cartilage- and bone-like cells in experiments where contaminant progenitor cells were excluded, thus giving clear evidence that it is fibroblasts and not contamination with progenitor cells in the examined cell population that possess this differentiation capacity (Junker et al., 2010). The differentiation potential of dermal fibroblasts has been shown to be generally mesodermal. However, there are also reports of transdifferentiation, meaning that fibroblasts were able to cross-differentiate along the endodermal or ectodermal lineage, specifically into neuron- and hepatocyte-like cells (Lysy PA et al., 2007; Bi et al., 2010).

On the other hand, many authors have reported that fibroblasts do not possess such differentiation potential. In 2011, Alt et al. comparatively analysed the antigen and gene profiles, the colony-forming ability and differentiation potential of skin fibroblasts, human ASCs, embryonic lung fibroblasts (WI38) and dermal microvascular endothelial cells. Their

results showed that skin fibroblast consist of a significant number of cells with differentiation potential apart from terminally differentiated fibroblasts, however colony-forming capacity and differentiation potential are specific important properties that discriminate MSCs from fibroblasts (WI38) (Alt et al., 2011). In another study, dermal fibroblasts had an adipogenic and osteoblastic potential, however they exhibited delayed adipogenic differentiation compared with MSCs (Jaager and Neuman, 2011). Moreover, in a comparison of human MSCs and skin fibroblasts by employing cDNA microarray analysis of 9600 genes, human MSCs were found to harbor an expression profile distinct from mature skin fibroblasts, and genes associated with developmental processes and stem cell function were highly expressed in adult MScs but not in dermal fibroblasts. Furthermore, normal skin cells in the same study lacked the ability to differentiate in any of the mesodermal lineage cell types (Brendel et al., 2005).

There is no doubt, that there are still many controversies in the field of human dermal fibroblasts as a cell source for tissue engineering. More experiments need to be conducted in order to establish methods for gaining meaningful amounts of induced cells, such as adipocytes from dermal fibroblasts. Furthermore, little is known about the gene expression profiles that are up- or downregulated during differentiation processes. Moreover, little is known about the possible differences between dermal fibroblasts and their differentiation capacities with respect to different age.

In any case, dermal fibroblasts represent a promising, easily accessible, autologous cell source for tissue repair and regeneration. Understanding the molecular mechanisms underlying the differentiation process of dermal fibroblasts may provide us with new therapeutic targets for diseases where fibroblasts play a key role, such as fibrosis (pulmonary, hepatic etc.).

1.4. Adipose tissue

1.4.1. General features of adipose tissue

Adipose tissue was until recently regarded as a tissue without any specific anatomy and architectural structure. However, current data have shown a strict organization of an organ with discrete structure, a complex vascular and nerve supply net, advanced cytology and cell plasticity (Cinti, 2011). According to its location, it can be generally divided into two compartments: the adipose tissue found in the subcutis and that found surrounding internal organs, known as visceral fat. As already mentioned, adipocytes constitute the main

parenchymal cells and they can be discriminated in two types: white adipocytes and brown adipocytes, which differ not only in their morphology but also in their physiology. Both types arise from mesodermal fibroblast-like adipocytes, known as pre-adipocytes, during a complex process known as adipogenesis (Rosen and Spiegelman, 2000). However, more recent evidence suggests that both brown fat cells and muscle cells seem to derive from the same stem cells (Saely et al., 2012). White adipose tissue (WAT) mainly consists of white adipocytes and stores excess energy in form of triglycerides, whereas brown adipose tissue (BAT) consists mainly of brown adipocytes and is specialized in the dissipation of energy through the production of heat (Saely et al., 2012). Morphologically, white adipocytes are spherical cells, which store a single lipid droplet (mainly consisting of triglycerides) with thin, elongated mitochondria in their cytoplasm. By contrast, brown adipocytes are polygonal cells and contain triglycerides as multiple small vacuoles (Saely et al., 2012). Free fatty acids storage takes place mainly in WAT in the form of triglycerides, which are released in the circulation as free fatty acids and glycerol in cases of tissue high-energy demand.

As far as differences in gene expression are concerned, type 2 iodothyronine deiodinase; the transmembrane glycoprotein Elovl3; the fatty-acid-activated transcription factor peroxisome-proliferator-activated receptor (PPAR); the nuclear coactivator PGC-1 and factors involved in mitochondrial biogenesis and function, as well as homeobox genes HoxA1 and HoxC4 are preferentially expressed in BAT, whereas leptin, the nuclear corepressor RIP140, HoxA4, HoxC8 and matrix protein fibrillin-1 are more abundant in WAT than in BAT (Saely et al., 2012; Gesta et al., 2007).

1.4.2. The process of adipogenesis

The master regulators of adipogenesis are the two principal adipogenic factors, PPARγ and C/EBPα, which control the entire terminal differentiation process. PPARγ is, in particular, the key regulator of adipogenesis. In its absence, precursor cells are not able to express any known aspect of the adipocyte phenotype (Rosen et al., 2002; Farmer, 2006). On the other hand, it has been shown that adipogenesis is possible without the expression of C/EBPα. However, these C/EBPα-deficient cells are insulin resistant (El-Jack et al., 1999).

The most popular cell model, which has been widely used to study the transcriptional events during adipogenesis, is the mouse fibroblast-like preadipocyte cell line 3T3-L1 that differentiates under appropriate induction from determined, fibroblast-like cells into mature adipocytes *in vivo* (Morrison and Farmer, 2000). Known mitogens and hormonal agents that

can induce the differentiation process and initiate adipogenesis in the 3T3-L1 cells include insulin, glucocorticoids, such as dexamethasone (DEX), methyl-isobutyl-xanthine (MIX) and agents that lead to increased cAMP (Morrison and Farmer, 2000). After induction, a complex cascade of transcriptional events takes place (Fig. 1.4.2.) that commences with the upregulation of C/EBPβ and C/EBPδ. Expression of other genes during the early stages of adipogenesis has also been reported, including c-fos, c-jun, junB and c-myc (Cornelius et al., 1994). The C/EBPs then mediate the expression of PPARγ (Clarke et al. 1997) and lead simultaneously to the activation of C/EBPα (Gregoire, 2001), both of which are present later in the differentiation process, mediating most of the end-product genes of adipocytes.

In the adipogenesis cascade, PPARγ activates the promoter of the gene encoding C/EBPα and vice versa, creating a positive-feedback loop (Farmer 2006), thus maintaining their expression despite the decrease of C/EBPβ and C/EBPδ (Shao and Lazar, 1997). In the late and final stages of adipogenesis, PPARγ and C/EBPα induce the upregulation of genes that are involved in major adipose tissue functions, such as insulin sensitivity, lipogenesis and lipolysis, including the glucose transporter GLUT4, the fatty-acid-binding protein 4 (FABP4), the lipoprotein lipase (LPL), the sn-1-acylglycerol-3-phosphate acyltransferase 2 (AGPAT2), perilipin and the secreted factors adiponectin and leptin (Farmer, 2006). Along with C/EBPs and PPARγ, sterol regulatory element binding transcription factor 1 (SREBP-1c) is another regulator known to regulate transcription of LPL and fatty acid synthetase, as well as promoting adipogenesis (Osborne, 2000). Its expression is significantly enhanced in 3T3-L1 preadipocytes in response to insulin (Kim et al., 1998).

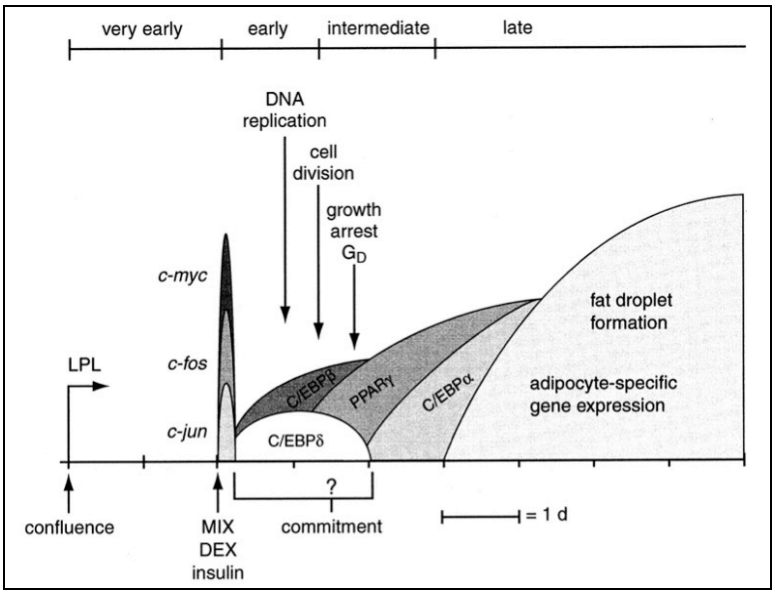

Fig.1.4.2. The progression of preadipocyte differentiation in 3T3-L1 cell line chronologically.

(Ntambi and Young-Cheul, 2000)

In recent years, a constantly increasing number of new transcriptional adipogenic factors as well as regulating mechanisms have been identified. Krox20 is upregulated in the early stages of adipogenesis after exposure of cells to mitogens and it not only promotes expression of C/EBPβ but also cooperates with C/EBPβ to facilitate terminal adipogenesis (Chen et al., 2005; Farmer, 2006). GATA-binding transcription factors GATA-2 and GATA-3, as well as cAMP response element binding protein (CREBP) play also a key role in the molecular control of the preadipocyte-adipocyte transition. In particular, GATA-2 and GATA-3 appear to be downregulated during adipogenesis, whereas CREBP is overexpressed before and during adipogenesis (Gregoire, 2001).

1.4.3. Factors inducing adipogenesis

Many factors have been reported to possess adipogenic properties. Pittenger et al. induced adipogenesis in 1999 in human adult MSCs by treatment with DEX, insulin, 1-methyl-3-isobutylxanthine (IBMX) and indomethacin (Pittenger et al., 1999) and this adipogenic protocol was also used to induce adipogenic differentiation in human fibroblasts in this thesis. The possible molecular mechanisms of these agents that induce the process of adipogenesis are briefly discussed in the following paragraphs.

1.4.3.1. Dexamethasone

DEX is a synthetic glucocorticoid agonist that has been traditionally used to stimulate the glucocorticoid receptor pathway, which is a nuclear hormone receptor in the same superfamily as PPARγ (Rosen and Spiegelman, 2000). Treatment with DEX has been shown to activate the transcription factor C/EBPβ (Wu et al., 1996), which may account for its adipogenic activity. At the same time DEX acts by reducing the expression of pref-1, a negative regulator of adipogenesis (Smas et al., 1999).

1.4.3.2. Insulin

Insulin is known to act through the IGF-1 receptor. It is also well known that both growth hormone and IGF-1 are of major significance in adipogenesis by regulating cell proliferation, differentiation and metabolism of adipocytes (Blueher et al., 2005). In brown preadipocytes it has been shown that progression past preconfluent growth arrest begins with the binding of insulin/IGF-1 to their heterotetrameric tyrosine kinase cell surface receptors. This binding

leads to phosphorylation of insulin receptor-1, which after its activation stimulates the PI3K-Akt pathway to phosphorylate and inhibit FoxO1 and also stimulates the Ras-ERK1/2 MAPK pathways to phosphorylate and activate CREBP. At the same time these two effects down-regulate necdin promoter activity, mRNA levels, and protein expression. This reduction in necdin levels permits the clonal expansion necessary before the terminal differentiation into mature brown adipocytes (Cypess et al., 2011).

1.4.3.3. 1-methyl-3-isobutylxanthine

IBMX is a nonselective cAMP-phosphodiesterase inhibitor that stimulates the cAMP-dependent protein kinase pathway. Studies suggest that IBMX inhibits soluble cyclic nucleotide phosphodiesterases resulting in increased intracellular cAMP levels. Subsequently, cAMP acts through CREBP and promotes differentiation by inducing C/EBP-β. Increased expression of C/EBP-β is required for further PPARγ expression and adipocyte differentiation (Niemela et al., 2008).

1.4.3.4. Indomethacin

Indomethacin is a non-steroidal anti-inflammatory drug that inhibits the function of cyclooxygenase (COX-2), thus inhibiting the production of prostaglandins. It has been shown to promote adipogenesis by increasing C/EBPβ and PPARγ2 expression in a prostaglandin-independent fashion (Styner et al., 2010). Indomethacin has been suggested to belong to PPAR-ligands, like thiazolidinediones and arachidonic acid, which are potent inducers of lipid synthesis in many cell models, such as the sebocyte SZ95 sebaceous gland cell line (Wrobel et al., 2003). Indeed, indomethacin has been found to activate PPARγ and PPARα by binding directly to both, thus directly inducing lipogenesis (Lehmann et al., 1997).

1.5. Clinical background of the study: Therapeutic applications of engineered adipocytes from human dermal fibroblasts

Repair of soft tissue defects after traumatic injury, tumor resection, congenital defects or the ageing process are some of the most common reconstructive and plastic surgical procedures that are performed nowadays. The use of autologous fat tissue grafts as transplants has been a widely used and accepted method, however it is linked to a number of drawbacks, such as the

progressive absorption of the fat grafts, local infections at the site of injection, even topical necrosis of the grafts (Niemela et al., 2008). The potential development of adipocytes from homologue dermal fibroblasts represents a promising, innovative and attractive solution for several clinical challenges, in dermatosurgery as well as in plastic and reconstructive surgery. Injectable autologous adipocytes for small-scale applications in cosmetic surgery, but also as defect-filling after tumor surgery, infections, full-thickness burns, cachexia in HIV-positive or tumor patients are only some of the potential applications of these cells (Tsuji et al., 2009; Welter et al., 2013). Cosmetic applications include augmentation procedures for lips and chin, and rejuvenation procedures to fill out wrinkles of the ageing skin. Breast mammoplasty after mastectomy and breast reconstruction, cases of lipodystrophy or steroid-induced lipoatrophy, as well as depressed scars may also represent therapeutic targets of the adipogenically induced fibroblasts. Applications of engineered fat tissue deriving from homologue skin fibroblasts might also include the treatment of urinary incontinence or vocal cord insufficiency, in which a stable, long-lasting "bulking agent" is needed (Katz et al., 1999; Niemela et al., 2008; Patrick et al., 2001).

Skin fibrosis in systemic sclerosis is associated with loss of subcutaneous adipose tissue but the underlying mechanism is not yet completely understood. Protocols of adipogenic induction of dermal fibroblasts, such as the one I administered in this work, may represent suitable models to examine in depth and gain insight into the molecular mechanisms of scleroderma. Furthermore, in light of the potent anti-fibrotic and lipogenic effects attributed to PPAR-γ recently (Trivedi et al., 2006; Kapoor et al., 2009; Wei et al., 2010), adipogenic treatments or the therapeutic application of the engineered adipocytes topically may represent a future therapeutic approach in cases of scleroderma.

The symptomatic treatment of rare genetic diseases, wherein symptoms resembling aspects of ageing manifest at a very early age, such as the Hutchinson Gilford Progeria syndrome might be improved through application of the adipocytes deriving from homologue dermal fibroblasts.

1.6. Aim of the study

The main aim of this study was to explore the plasticity of human dermal fibroblasts from donors of different ages, specifically their adipogenic potential and elucidate the molecular events that take place during the adipogenic induction of fibroblasts.

In depth, the goals were the following:

- to examine the differentiation potential of human dermal fibroblasts by applying an adipogenic protocol in order to induce adipogenesis;
- to achieve a switch of young and adult skin fibroblasts towards adipocytes and obtain cells, which can accumulate lipids (detection by means of flow cytometry and fluorescence microscopy) and express specific markers of adipocytes (by means of qRT-PCR);
- to reveal the morphology changes taking place in the induced cells via fluorescence and electron microscopy;
- to investigate lineage characteristics of human adult fibroblasts and induced adipocytes from donors of different ages, especially in fibroblasts from 30- and 76-year-old female donors;
- to establish a method of lineage change, which can supply a sufficient amount of differentiated adipocytes from differentiated dermal fibroblasts;
- to map human genes in induced cells and perform a functional grouping analysis of differentially regulated genes in human RNA samples after gene expression analysis using whole human genome oligo microarrays;
- to investigate the differentiation capacity of dermal fibroblasts originating from young donors versus older ones.

«Activity is the only road to knowledge»

George Bernard Shaw

Irish playwright and novelist, 1856-1950

2. MATERIALS AND METHODS

2.1 Materials

2.1.1. Reagents and cell culture media

Salts, buffer reagents, solutions and solvents were purchased from Sigma (Munich, D), Merck (Darmstadt, D), Roth (Karlsruhe, D) and J. T. Baker (Deventer, NL) unless otherwise stated.

Media supplements:

Fetal calf serum (FCS) Cat. Num.: S0145	Biochrom AG (Berlin, D)
Penicillin/Streptomycin (Pen/strep) Cat. Num.: A2213	Biochrom AG (Berlin, D)
ITS (mixture of recombinant human insulin, transferrin and sodium selenite- Cat. Num.: I3146)	Sigma (Munich, D)
Indomethacin-Cat. Num.: I7378	Sigma (Munich, D)
IBMX Cat. Num.: I5879	Sigma (Munich, D)
DEX-Cat. Num.: D4902	Sigma (Munich, D)

Table 3. Different media and their supplementation.

Medium	Media	Serum	Supplements
Adipogenic induction	DMEM high glucose, stable glutamine - PAA (Linz, A) Cat. Num.: E15-883	10% FCS	1µM DEX 200µM indomethacin 10µM (1mg/ml) ITS 0.5 mM IBMX 100U/ml pen/strep
Maintenance	DMEM high glucose, stable glutamine - PAA (Linz, A)	10% FCS	10µM ITS 100U/ml pen/strep
Control	DMEM high glucose, stable glutamine - PAA (Linz, A)	10% FCS	100 U/ml pen/strep
Freezing	40% DMEM high glucose, stable glutamine - PAA (Linz, A)	50% FCS	10% Dimethylsulfoxid (DMSO)

Other Substances:

Trypsin/EDTA (1x) 0.05/0.02% in PBS	PAA (Linz, A)
PBS-Dulbecco (1x) w/o Ca^{2+}, Mg^{2+} (Phosphate-Buffered Saline)	Biochrom AG (Berlin, D)
Trypsin (1:250) 0.25% (w/v)	Biochrom AG (Berlin, D)
Trypan blue solution 0.5% (w/v)	Biochrom AG (Berlin, D)

2.1.2. Cell culture materials

Cell culture flasks 25&75cm²	Nunc (Wiesbaden, D)
6-, 12-, 24-well plates	Nunc (Wiesbaden, D)
Pipette tips (with and without filter)	Biozym (Oldendorf, D)
Cell scraper	Greiner (Frickenhausen, D)
Freezing vials, petri dish, serological pipettes, centrifuge tubes, blue &red cap tubes, FACS tubes	Falcon, Becton Dickinson Labware, Franklin Lakes (NJ, US)
Sterile filters (0.2µm)	B. Braun (Oldendorf, D)
Microscope slides (26x76mm)	Carl Roth Gmbh (Karlsruhe, D)
Cell counting chamber slides (Neubauer slide)	Sigma (Munich, D)

2.1.3. Material for cell biological techniques

Lipid detection

Nile red, DAPI	Sigma (Munich, D)

2.1.4. Materials for RNA & DNA analysis

RNA Quality Control

Agilent RNA 6000 Nano Kit	Agilent Tech. (Waldbronn, D)

RNA isolation

RNeasy Mini Kit	Qiagen (Hilden, D)
RNase-Free DNase Set	Qiagen (Hilden, D)

cDNA synthesis

Ready-To-Go You-Prime First-Strand Beads	GE Healthcare (Waukesha, US)
DEPC-treated water	Invitrogen (Darmstadt, D)
Oligo-dT Primer	GE Healthcare (Waukesha, US)

Two-step quantitative RT-PCR

All primers used were purchased from Qiagen (Hilden, D). QuantiTect Primer Assays® were supplied as a lyophilized mix of forward and reverse primers that were then reconstituted with 1.1ml TE, pH 8.0, to obtain a 10x assay solution. The reconstituted primers were stored as aliquots at -20°C and used within less than 3 months of receipt. Glyceraldehyde 3-phosphate dehydrogenase (GAPDH) was selected as the housekeeping gene based on the literature (Zainuddin et al., 2008), as well as after performing a standard curve of GAPDH expression in serial diluted total RNA and a melting curve analysis. The selected genes that were investigated by means of RT-PCR are presented in Table 4. The exact sequences of the QuantiTect Primer Assays® are not provided by the manufacturer, therefore they are not included in the table.

Table 4. Primer assays for detection of adipogenic gene expression after adipogenic induction.

Gene symbol	NCBI Gene Reference	Amplicon length	Product Number	Ensembl Transcript ID
LEP	NM_000230	105bp	QT00030261	ENST00000308868
LPL	NM_000237	73bp	QT00036771	ENST00000311322
GAPDH	NM_002046	95bp	QT00079247	ENST00000229239
IGFBP2	NM_000597	91bp	QT00066115	ENST00000233809
PPARgamma	NM_005037	113bp	QT00029841	ENST00000309576

QuantiTect SYBR Green PCR Master Mix — Qiagen (Hilden, D)

RNase-Free Water — Qiagen (Hilden, D)

PCR 96-well plates, optical adhesive covers — Bioplastics (Landgraaf, NL)

TE buffer (primer reconstitution) — Qiagen (Hilden, D)

- 10 mM Tris•Cl, 1mM EDTA, pH 8.0

2.1.5. Materials for transmission electron microscopy

Karnovsky fixative solution (Karnovsky, 1965): — AMTS (Lodi, CA, USA)

- 5% glutaraldehyde
- 4% formaldehyde in 0.1M cacodylate buffer
- 50mg $CaCl_2$/100ml final fix

2.1.6. Equipment

Autoclave	Webeco (Bad Schwartau, D)
Centrifuges	Biofuge pico, Heraeus (Osterode, D)
	Biofuge fresco, Heraeus (Osterode, D)
	Uni Vapo 100 H Uni Equip (Martinsried, D)
	Megafuge 1.0 Heraeus (Osterode, D)
	Microcentrifuge 5417R, Eppendorf (Hamburg, D)
	Centrifuge 5810/5810R, Eppendorf (Hamburg, D)
CO_2- incubator	BB16, Heraeus (Osterode, D)
Cellspin cytocentrifuge	Tharmac (Waldsolms, D)
Laminar flow bench	BSB 4A, Gelaire Flow Laboratories (Opera, I)
Magnetic stirrer	MR 2000, Heidolph (Kehlheim, D)
	IKAMAG REG Jahnke & Kunkel (Staufen, D)
Light microscope	IMT-2, Olympus (Berlin, D)
	Zeiss BK37 (Jena, D)
Fluorescence microscope	DM4000 B LED (Leica Microsystems, Bensheim, D)
PCR cycler	Mastercycler Gradient Eppendorf (Hamburg, D)
Camera	Cyber-shot, Sony (Berlin, D)
Mixers	MS1 Minishaker IKA laboratories Jahnke & Kunkel (Staufen, D)
	Thermomixer comfort, Eppendorf (Hamburg, D)
	Vortex IKA VF2, Jahnke & Kunkel (Staufen, D)
pH meter	pH 526, WTW (Weilheim i.OB., D)
Precision balances	Type A200S, Sartorius (Göttingen, D)
RNA concentration calculator	NanoDrop 1000 Spectrophotometer, Thermo Scientific (Wilmington, USA)
RNA quality control	Agilent 2100 bioanalyzer, Agilent Tech. (Waldbronn, D)
FACS	BD FACSCalibur flow cytometer, BD Biosciences (Qume Drive San Jose, CA, USA)
Warming plate	HT200 W, Minitube (Tiefenbach, D)
qReal-time PCR system	ABI PRISM 7000 Sequence detection system, Applied Biosystems (Foster City, CA, USA)
Transmission electron microscope	TEM 10, Zeiss (Jena, D)
Cell culture water bath	Julabo, Th. Karow GmbH (Seelbach, D)

2.2. Methods

2.2.1. Cell culture

2.2.1.1. Cell harvesting

Human dermal fibroblasts

Human skin primary fibroblasts were isolated, after consent of the donors, from the light-protected area of the inner upper arm of women 30 (DFs30)- and 76-years old (DFs76), and from human foreskin (FSFs) coming from young children undergoing surgery. The use of human material was approved by the Ethics Committee of the Charite-Universitaetsmedizin Berlin (application number: EA4/088/09). The skin samples were first gently washed thrice in PBS solution enriched with amphotericin B. Subsequently, fat tissue was removed mechanically and the skin specimens were cut in 4x4 mm squares. Five to 10 skin specimens were placed in a cell culture petri dish (epidermis facing upwards) and digested with 0.25% trypsin solution overnight at 4^{o}C and then for $2^{1/2}$ h at 37^{o}C, in order to separate the epidermis from the dermis. After separation, the dermis specimens were placed on a 100% FCS coated plate and dried for $^{3/4}$ h at 37^{o}C, 8 ml of DMEM medium complemented with 10% FCS and 100 U/ml penicillin/streptomycin was added. Medium change was performed every 2 days. Fibroblasts were allowed to grow out and adhere on the plate ground for about $2^{1/2}$ weeks and then the cells were harvested and transported into 75 cm^2 culture flasks, where their cultivation was continued. Fibroblasts used were between passages 3 and 5. DFs30 and FSFs are referred to in the text also as “young” fibroblasts, whereas DFs76 as “old” ones.

2.2.1.2. Cell cultivation

Cell maintenance took place under laminar flow. Fibroblasts were grown in control medium (Table 3) in 75 cm^2 tissue culture flasks, in a humidified atmosphere with 5% CO_2 at 37^{o}C. Cell culture flasks were equipped with filter caps to allow sufficient gas exchange and the cells were kept out of the incubator to minimize the time of handling procedures. Every 2 days the medium was removed and replaced with warm, fresh produced medium. During cultivation, cells were never left to reach more than 90-100% confluence and were harvested in a semi-confluent state, so that their growth would not be suppressed. All media and solutions used in cell culture were left to reach the appropriate temperature in a 37^{o}C pre-warmed water bath before any handling of the cells. In cases were the medium became acidic

(the pH indicator phenol red in culture medium appeared yellow), the medium was changed earlier.

2.2.1.3. Subculturing of cells

For subculturing, 70-90% confluent fibroblasts in 75 cm^2 culture flasks were rinsed with 10 ml PBS twice and subsequently incubated with 2 ml Trypsin/EDTA solution in the incubator for approximately 5 min. The flask was gently moved back and forth to ensure that the entire fibroblasts monolayer was covered with the solution. The trypsinization continued until the majority of the cells showed a rounded morphology and were no more adherent. At this point, the side of the flask was gently tapped to release the rest of cells from the culture surface. Trypsin is an enzyme, which disrupts peptide bonds and helps the detachment of the cells from the ground of the flask, whereas EDTA is a molecule for complexing metal ions and allows the separation of the cells. Subsequently, 8 ml medium containing 10% FCS was added to the flask. FCS was used in order to stop the proteolytic activity of trypsin. The content of the flask was transferred to a 50 ml tube and centrifuged at 1100 rpm for 5 min. The supernatant was aspirated and the cells were resuspended in 10ml DMEM medium with 10% FCS and 100 U/ml penicillin/streptomycin and counted (2.2.1.4.). The cells were at the end seeded in new 75 cm^2 flasks at a density of 3500 cells/cm^2.

2.2.1.4. Counting of cells and cell viability with Trypan blue

The dye exclusion test with trypan blue is used to determine the number of viable cells present in a cell suspension and also in order to count the total cell number in a cell suspension. The principle is that living cells possess intact cell membranes that cannot be penetrated by certain dyes, such as trypan blue, whereas dead cells do not. The viability of cells can also be assessed through a normal phase contrast microscope by observing the morphology of the cells. Viable fibroblasts appear bright, with projections in their periphery and with no signs of apoptosis. Dead cells are coloured blue with trypan blue.

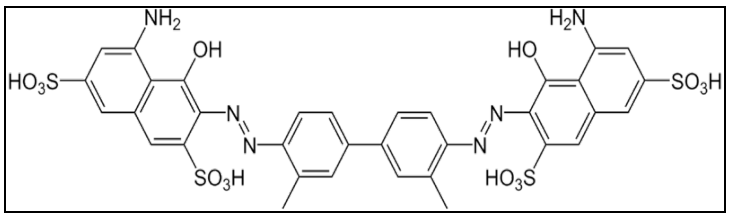

Fig. 2.2.1.4. Chemical structure of Trypan blue ($C_{34}H_{28}N_6O_{14}S_4$)
(Image from http://en.wikipedia.org/wiki/File:Trypan_blue.png)

A counter chamber hemocytometer was used for determining the amount of cells per unit volume of a suspension. The device was originally designed for performing blood cell counts. It consists of a thick glass microscope slide, in which a small chamber lies. This chamber is engraved with a laser-etched grid of perpendicular lines in a way that the area bounded by these lines and the depth of the chamber are known, therefore making it possible to count the cells that are introduced into the chamber and calculate the concentration of cells in the fluid overall.

Protocol: After preparing a cell suspension as already described (2.2.1.3), 20µl of cell suspension was mixed with 20µl of trypan blue suspension (0.4%), vortexed thoroughly and allowed to stand for 5-15 min. Afterwards, the hemocytometer was loaded with a drop of the mixture trypan blue/cell suspension into each of the two counting chambers by carefully touching the edge of the cover slip with the pipette tip and allowing each chamber to fill by capillary action. Then, the slide was viewed through a microscope with 100x magnification and all the cells were counted with a hand-held counter in each of the four corner squares. Viable and non-viable cells were counted separately. Cells on top and left touching middle line were not included. The total cell count was calculated using the following equations:

$$\text{Cells/ml} = \text{average count per square} \times \text{dilution factor} \times 10^4$$

$$\text{Total cell count} = \text{cells/ml} \times \text{total original volume of cell suspension of the sample}$$

To determine the viable cells, the total number of cells and total number of viable cells were counted. Nonviable cells absorbed the dye and were blue, whereas viable cells were impermeable and were not stained. The viability was calculated using the following equation:

$$\text{\% viable cells} = (\text{unstained cells} / \text{total cell count}) \times 100$$

2.2.1.5. Cell freezing

Primary cells in continuous culture are fated for senescence and become more susceptible to microbial contamination. In particular, primary fibroblasts should not be used in experiments if they have been passaged many times. Therefore, it is of vital importance that they are frozen down to be preserved for long-term storage. However, the freezing procedure, especially if performed quickly, can become lethal for the cells due to the damage that ice crystals may cause by alternating electrolytes, dehydration and changes in pH. The best method for preserving cultured cells is storing them in liquid nitrogen in complete medium in the presence of a cryoprotective agent such as dimethylsulfoxide (DMSO). DMSO reduces the freezing point of the medium and also allows a slower cooling rate, the optimal rate of

cooling is 1-3^{o}C per min. The slow cooling rate allows water to move out from the cells before it freezes, therefore the damage from water crystals is significantly reduced. In addition, it is best to use healthy cells that are growing in log phase and are subconfluent and to replace the medium 24 h before freezing.

Protocol: After preparing a cell suspension as already described (2.2.1.3) and after having aspirated the supernatant, the cells were resuspended into a 1 ml freezing medium (Table 3) and the cell suspension was transferred in 1 ml freezing vial. The freezing vials contained approximately 2-4 ml cells per vial and were then placed in a container, which was filled with 200 ml of isopropanol at room temperature. This container was then placed in the -80^{o}C freezer overnight. Isopropanol allows the tubes to freeze slowly, at about 1^{o}C per minute. Approximately 24 h later, the vials were removed from the container and immediately placed in the liquid nitrogen storage tank for long-term storage (-130^{o}C).

2.2.1.6. Cell thawing

It is of great importance to thaw cells properly in order to maintain a high percentage of viable cells. Cryoprotectants, such as DMSO that are used in the freezing medium during the freezing procedure are toxic above 4^{o}C, therefore it is vital to perform the thawing of the cells as quickly as possible.

Protocol: After removing the freezing vial from the liquid nitrogen storage, while wearing the appropriate equipment, the vial was placed in a 37^{o}C water bath for approximately 1-2 min, with constant agitation until its content was thawed. The vial was then sterilized with 70% alcohol and the content was diluted in a 10-fold volume of warm culture medium and centrifuged at 1000 rpm for 5 min. The supernatant was discarded, the cell pellet resuspended in 20 ml culture medium and then distributed in two 75 cm^2 flasks. Further cell cultivation was performed as already described (see 2.2.1.2.).

2.2.1.7. Adipogenic differentiation protocol

Adipogenic differentiation was performed in monolayer culture as previously described by Pittenger et al. for MSCs (Pittenger et al., 1999). Subconfluent dermal fibroblasts in 75 cm^2 were harvested as previously described and a cell suspension was created (see 2.2.1.3.). The cells were counted with trypan blue and subsequently seeded in 6- and 24-well-plates. For 24-well plates and 6-well plates a density of 5x10^4 cells per well and 2x10^5 cells per well was selected respectively. The cells were left to stand with control medium (Table 3) for

approximately 48 h, in order to reach 100% confluency. The medium volume-to-surface area used was between 0.2-0.5 ml/cm^2. Specifically, 2ml/well for 6-well plates and 500μl/well for 24-well plates. Postconfluent cells were then treated for 72 h with the adipogenic induction medium (Table 3). The day of the first treatment with the adipogenic medium corresponded to differentiation day 1. Afterwards, on day 4, the adipogenic medium was replaced with the so called maintenance medium (Table 3) for another 72 h. On day 7 the cycle was repeated three times with the same time intervals. Afterwards, fibroblasts were cultured for an additional week only in maintenance medium. Control fibroblasts were cultured in normal cell growth medium containing 10% FCS and 100 U/ml penicillin/streptomycin (Table 3). On the last day of the adipogenic differentiation, which was day 23, the detection of lipid accumulation was confirmed after Nile red staining with fluorescence microscopy and flow cytometry. In addition, RNA samples were collected for cDNA microarrays and quantitative real time PCR, in order to perform gene expression analysis. Transmission electron microscopy was also performed, after fixation with Karnovsky solution to explore in detail the morphological changes in the induced cells. A complete differentiation time schedule describing the medium changes during the adipogenic experiment is presented in Table 5.

Dexamethasone, IBMX and insulin solutions were stored at -20ºC; fresh media were prepared before each treatment; medium changes were performed gently in order to avoid disruption of the newly formed lipid droplets in the cytoplasm of fibroblasts; plates were kept in a humidified atmosphere with 5% CO_2 at 37^{o}C. The experiment was performed thrice and each time the negative control and treatment wells were in triplicates.

Table 5. Adipogenic differentiation time schedule.

Day	Induced cells	Negative control
1	Adipogenesis induction medium	Control medium
4	Maintenance medium	Control medium
7	Adipogenesis induction medium	Control medium
10	Maintenance medium	Control medium
13	Adipogenesis induction medium	Control medium
16	Maintenance medium	Control medium
19	Maintenance medium	Control medium
23	**Nile red staining for fluorescence microscopy and FACS** **Transmission electron microscopy** **RNA isolation for qRT-PCR and cDNA microarray analysis**	

2.2.2. Cell biological methods

2.2.2.1. Nile red staining assay

Lipid accumulation was assessed by means of the Nile red fluorescence assay. Nile red, also known as 9-diethylamino-5H-benzo-alpha-phenoxazine-5-one is an excellent vital stain for the detection of intracellular lipid droplets by fluorescence microscopy and flow cytometry (Greenspan et al., 1985). As a lipophilic substance, Nile red dissolves in a wide range of organic solvents, but negligibly in water.

Fluorescence is the property of an atom or a molecule to absorb light at a particular wavelength (excitation) and to subsequently emit light of longer wavelength after a brief interval (emission), which is named the fluorescence lifetime. The emission and excitation wavelengths of fluorescence dyes have been reported to differ. In the case of Nile red, when the cells are viewed for gold-yellow fluorescence (excitation: 450-500 nm; emission > 528nm), neutral lipids such as triglycerides are detected and when the cells are viewed for red fluorescence (excitation: 515-560 nm; emission > 590 nm), polar lipids indicative of phospholipid containing organelles are seen (Greenspan, Mayer et al., 1985). However, it has also been reported that the best selectivity for cytoplasmic lipid accumulation is obtained with yellow-gold fluorescence (528 nm) rather than for red fluorescence (>610 nm), since with the latter condition a diffuse staining of the entire cell is observed, while with the former, a more selective staining of lipid droplets is obtained (Greenspan and Fowler, 1985).

Protocol: Stock solution of Nile red was prepared with a concentration 1mg/ml in acetone and was stored in +4^{o}C protected from light. For Nile red staining a working solution with 1ml stock solution: 100 ml PBS was prepared. On day 23 of the induction experiment the cells were stained with Nile red and the accumulation of intracellular lipid droplets was assessed by fluorescence microscopy and flow cytometry. The process followed for cell harvesting and Nile red staining differed depending on which fluorescence method was selected; these are described in detail below.

2.2.2.2. Detection of lipids by means of Nile red flow cytometry

General principles of flow cytometry

Flow cytometry is a technique for measuring the physical and chemical characteristics of cells as the cells pass in a fluid stream through a measuring point surrounded by an array of detectors. The flow cytometer performs this analysis by capturing the light that emerges from

cells after they pass through a laser beam. The most important feature of this method is that it enables quick measurements to be made on individual cells, thus giving a detailed analysis of each single cell in a cell population. Cellular characteristics, such as size, complexity and phenotype of the examined cells can be specified in detail by this method.

The major components of a normal flow cytometer include: the fluid system, which directs the cell stream through the laser beam, the lasers, which are the source for scatter and fluorescence, the collection optics and filters, which detect light signals coming from particles and the electronics and peripheral computer, which convert the detector signals into data suitable for further analysis. For accurate analysis, it is of great importance that cells are analysed one at a time. This is achieved by introducing the sample as a sheath fluid or saline solution into the flow cytometer and by utilizing the phenomenon of hydrodynamic focusing, which compresses the fluid stream to a diameter of one cell.

Forward scatter or FSC is the amount of light being scattered in the forward direction when the cell passes through the laser beam. In practise, FSC reflects the diameter of a cell, thus providing information of the size of the cells. Smaller cells produce a small amount of FSC and larger cells a greater amount of FSC. On a flow cytometry histogram, FSC represents usually the x axis, where smaller cells appear on the left and larger cells on the right of the plot. On the other hand, the side scatter or SSC represents the light that is scattered at larger angles when a cell travels through the laser beam. It is mostly caused by granularity and structural complexity inside a cell and thus reflects the cellular structure. On a flow cytometry plot, SCC usually represents the y axis, where complex cells appear on the upper end of the axis, whereas cells with low internal complexity appear on the lower end. The combination of FSC and SSC produces a two-dimensional scatter plot and this multiparametric analysis is of great importance for investigating cell populations.

One very important parameter of flow cytometry is that, except for the useful measurements that can be made using light scattering measurements alone, it can also be used to quantify particle-associated fluorescence. The fluorescence signal can be detected after special staining of the examined cells through a series of optical mirrors and filters that are positioned along the same path as the SSC. Fluorescent stains, also known as fluorochromes, can vary according to which organelle they are designed to label and include nucleic acid stains, stains conjugated antibodies, stains conjugated proteins, stains conjugated enzyme substrates, indicator stains for ions -Ca^{2+}, Na^{+}, K^{+}, stains for cytoskeletal proteins and stains for functional organelles. Nile red belongs to the fluorochromes that stain intracellular lipids

and has been proven to be a reliable fluorescence stain for flow cytometry (Greenspan et al., 1985).

In the present work, a BD FACSCalibur with dual laser with 4-color parameters was used. The features of this analyzer are as follows (Fig. 2.2.2.2.):

- laser specifications:15 mW 488 nm, air-cooled argon-ion laser; red diode laser, 635 nm
- fluorescence detectors and filters: high performance, high dynamic range photo-multipliers with bandpass filters : 530 nm (FITC), 585 nm (PE/PI), 661 nm (APC) and >650 nm (PerCP) with base unit, >670 nm (PerCP) with FL4 option
- sample flow rate: 3 selectable flow rates of 60 mL/min, 35 mL/min and 12 mL/min. Particle velocity in flow cell approximately 6 m/sec
- electronics: Mac operating system with CellQuestPro software for acquisition. Further analysis of the data was conducted with the Cyflogic software.

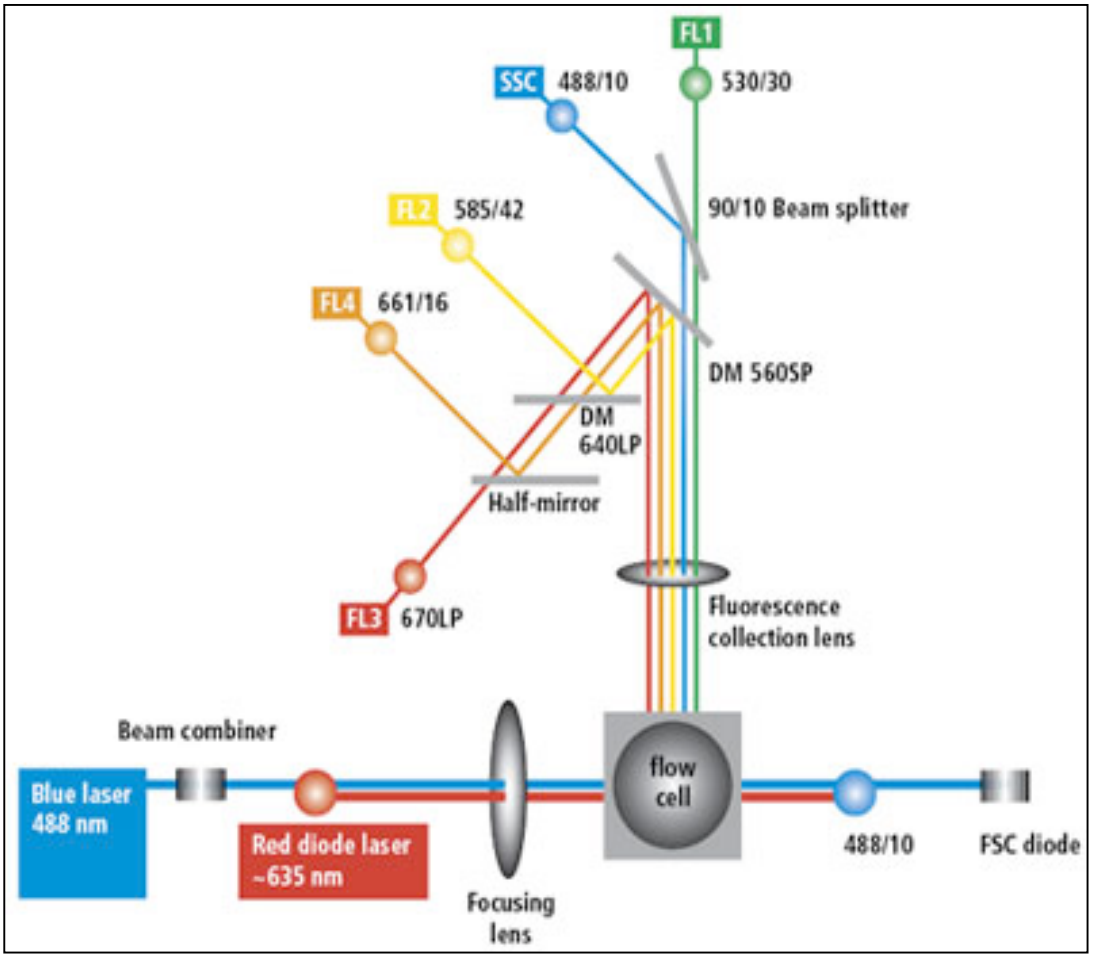

Fig. 2.2.2.2. BD FACSCalibur Optical Path Configuration
(Image from: www.bdbiosciences.com)

Protocol: To assess the extent of adipocytic differentiation of fibroblasts, the cytosolic triglyceride content was determined after Nile red staining by means of flow cytometry. Dermal fibroblasts were seeded in 6-well plates and treated according to the adipogenic protocol (see 2.2.1.7.). On day 23 the cells were washed with PBS twice and then harvested by adding trypsin-EDTA, as already described (see 2.2.1.3.). The harvested cells were counted and 1ml single-cell suspensions of 10^5-10^6 cells/ml in PBS were prepared and placed in polystyrene (Falcon) tubes. 50µL of the working solution of Nile red was added to each 1mL cell suspension and the mix was gently vortexed and incubated for 10 minutes at 37^0C in darkness. Cells were subjected to flow cytometric analysis with 10000 events collected for each sample, each measurement point was repeated in 3 parallel replicates. The optical system used in the FACSCalibur collects yellow and orange light (560–640 nm corresponding to neutral lipids) in the FL2 channel and red light (>650 nm corresponding to polar lipids) in the FL3 channel. Therefore, both polar and neutral lipid amounts were determined. Non-stained cells were used as an autofluorescence background and were excluded during analysis of the samples. Samples of induced cells of different ages were normalized against the non-induced negative control cells of the same age. Lipid accumulation is presented as the percentage of positively stained cells in the induced cell population versus the positively stained cells in the non-induced negative control cells. The results are also presented as overlay histograms in the FL2 and FL3 channel for neutral and polar lipids, respectively. Data analysis and overlays were produced using the free flow cytometry data analysis software Cyflogic® version 1.2.1.

2.2.2.3. Detection of lipids via fluorescence microscopy

Assessment of cytosolic lipid accumulation was also performed after Nile red staining by means of fluorescence microscopy. To obtain a better insight into the localization of the lipid droplets, a counter staining with the blue-emitting fluorochrome 4,6-diamidino-2-phenylindole, also widely known as DAPI that is used to label the nuclei of the cells was performed. DAPI possess an excitation wavelength of 358nm and an emission wavelength of 461 nm.

Solutions used:

DAPI stock solution: 1 mg/ml of DAPI powder in H_2O, stored at -20°C, light protected

DAPI working solution: 1 ml from stock solution in 10 ml of PBS

Nile red stock solution: 1 mg/ml Nile red in DMSO

Nile red working solution: 100 µl from stock solution in 10 ml PBS

Protocol: Fibroblasts were seeded in 24-well plates and treated according to the adipogenic protocol that has already been described (see 2.2.1.7.). On day 23 the cells were washed with PBS twice and then harvested by adding trypsin-EDTA (see 2.2.1.3.). A cell suspension in PBS was prepared and cytospins with a total cell number of $3x10^4$ cells/cytospin were generated with a cellspin cytocentrifuge. The cytospins were then directly incubated with the Nile red working solution at 37°C for 10 min, quickly washed with PBS and incubated for another 5 min at room temperature with DAPI working solution and subsequently directly observed under a DM4000 B LED fluorescence microscope (Leica Microsystems, Bensheim, D). For DAPI detection the ultraviolet illumination filter was used, whereas for Nile red detection, the FITC filter. Subsequently overlay photos were generated.

2.2.2.4. Transmission electron microscopy

General principles of transmission electron microscopy

The transmission electron microscope operates on the same basic principles as the light microscope, however it uses as "light source" electrons instead of light, thus making it possible to achieve a resolution a thousand times better than with a light microscope, reaching a maximum potential magnification of 1 nanometer.

A transmission electron microscope contains four parts: electron source, electromagnetic lens system, sample holder, and imaging system. The beam of electrons is generated by a cathode and is subsequently vacuumed up by a high voltage (50-150 kV) at the anode. The higher the voltage is, the shorter are the electron waves and the higher is the resolution. The accelerated electron beam travels through a drill-hole at the bottom of the anode and from there it follows a way analogous to that of a ray of light in a conventional light microscope through multiple electromagnetic lenses. The electromagnetic lens system consists of electronic coils generating an electromagnetic field. The electron beam is first focused by a condenser and then passes through the examined sample, where it is partially scattered and the density of this deflection reflects the electron density of the sample. The greater the mass of the atoms comprising the sample, the greater is the degree of deflection.

Since biological samples mainly consist of atoms with low atomic numbers (C, H, N, O), their contrast ability is very weak. Therefore, it is essential to ‘‘stain’’ them with special contrast-enhancing heavy metals, such as molybdenum, uranium, or tungsten to overcome this obstacle.

At the end, scattered electrons are collected by the imaging system and an image is produced that is subsequently enlarged by an additional lens-system. This image can be presented on a fluorescent screen or can be documented on black and white photographic material with the degree of darkness corresponding to the electron density of the samples.

Sample preparation: Fibroblasts were harvested after the treatment and were fixed for 1 h with Karnovsky's fixative. Subsequently, the fixed cells were sent to the Institute of Anatomy, Musculoskeletal Research Group, Ludwig-Maximilian-University Munich, Chairman: Prof. Dr. med. Mehdi Shakibaei, where the further analysis was conducted.

Briefly, after the cells had been fixed, the cell pellet was mechanically dissolved with a cell scraper and centrifuged in sterile tubes. Next, the cell pellet was post-fixed in 1% OsO_4 solution, rinsed with 0.1 M phosphate buffer and dehydrated in an ascending alcohol series (10% to 96% ethanol). The samples were then embedded in Epon and cut on a Reichert-Jung Ultracut E (Heidelberg, D) in ultrathin sections. The sections were then contrasted with 2% uranyl acetate/lead citrate and subsequently images were taken with a transmission electron microscope TEM 10, Zeiss (Jena, D).

2.2.3. Molecular biological methods

2.2.3.1. RNA isolation, purification and DNase treatment

RNA isolation and purification was performed with the RNeasy Mini Kit Qiagen (Hilden, D). With this method, the isolation of pure RNA is achieved through the combination of a silica-based selective binding membrane with a high speed microspinner. The specialized high-salt buffers used during this procedure allow all RNA molecules up to 100 µg and longer than 200 bases to be isolated. The abundant amount of the isolated RNA at the end of the protocol is comprised mostly of mRNA, whereas other RNA subtypes are selectively excluded, since they are in their majority not longer than 200 bases. Since RNA is an extremely unstable product that can be easily degraded by the presence of ribonucleases (RNases), strict precautions were taken throughout the whole procedure such as gloves, special material used only for RNA isolation, separate RNase-free pipettes and filter pipette tips. Work with RNA was always done on ice and following the manufacturer's instructions (Rneasy Mini Handbook ®, Qiagen, Hilden, D).

Solutions and Buffers: 14.3 M β-mercaptoethanol, 70% ethanol, trypsin, PBS, DEPC (diethylpyrocarbonate) water RLT buffer (ready to use), RW1 buffer (ready to use), RPE

buffer (ready to use), lysis buffer (10 µl β-mercaptoethanol/ml RLT buffer), RDD buffer (ready to use), DNase I in 550 µl RNase-free water

Protocol: At day 23 of the adipogenic experiment, cells were lysed, after the medium was aspirated, in 6-well plates with 2 ml lysis buffer/well (10 µl β-mercaptoethanol/ml RLT buffer). This buffer contains a high concentration of denaturating guanidine-thiocyanate, which destroys RNases, thus making the purification of intact RNA possible and at the same time disrupts all cell walls and plasma membranes in order to release all RNA contained in the sample. Homogenization was achieved by centrifugation (14000 rpm) for 2 min and by passing the lysates multiple times through a blunt 20-gauge needle fitted to an RNase-free syringe. Lysates were then transferred into centrifuge tubes and either stored in -80^{o}C for later processing or were immediately used for further RNA isolation. Afterwards, 70% ethanol (2 ml) was added and mixed by pipetting to each lysate separately and the samples were then applied to an RNeasy Mini spin column. This column is supplied with a silica-based membrane, where total RNA can bind, and the columns were centrifuged for 15 sec at 10.000 rpm in order to wash away possible contaminants. At this point an on-column DNase digestion with the RNase-free DNase Set (Qiagen, Hilden, D) was performed in order to eliminate genomic DNA contamination. 350 µl of RW1 buffer was added to each spin column and centrifuged for 15 sec at 10000 rpm. The flow-through was discarded. 10 µl of the DNase I stock solution was added to 70 µl of RDD buffer and the mixture was gently centrifuged, directly applied to each spin column membrane and the samples were then incubated for 15 min at room temperature. To wash out the DNase mix, 350 µl of the RW1 buffer was added to the spin columns, which were then centrifuged for 15 sec at 10000 rpm and the flow-through was discarded. 500 µl RPE buffer was then added to each spin column twice and after each addition the samples were centrifuged for 15 sec and 2 min respectively at 10000 rpm. After the second centrifugation, the RNeasy spin column was carefully removed from the collection tube and placed in a new 1.5 ml collection tube for the final step, the RNA elution. 30 µl RNase-free water was directly added to the membrane, the spin column was centrifuged for 1 min at 10.000 rpm and this step was repeated once more with 25 µl of RNase-free water. At the end of this procedure a total of 50 µl of pure RNA was generated.

2.2.3.2. Measurement of RNA concentration

The measurement of the RNA concentration of the samples that were generated after the procedure described in the 2.2.3.1 section was performed with the Thermo Scientific

Nanodrop 1000 Spectrophotometer (Wilmington, USA) and the analysis of the data with the software ND-1000 v3.5.2, according to the manufacturer's instructions (NanoDrop 1000, User's Manual).

The principle of this technology is based on UV absorption, where the absorbance of nucleic acids is measured at 260 and 280 nm. For the conversion of the calculated absorbance in concentration units, the Beer-Lambert equation is used, which is as follows:

$$c = (A * e) / b$$

(c: nucleic acid concentration in ng/microliter; A: absorbance in absorbance units; E: wavelength-dependent extinction coefficient in ng-cm/microliter; b: path length in cm)

The generally accepted extinction coefficients for RNA are 40 ng-cm/µl. The NanoDrop 1000 Spectrophotometer uses path lengths of 1.0 mm and 0.2 mm. The measurement of a sample requires that the spectrophotometer is first "blanked", meaning that a spectrum is taken from a reference material and stored in the memory of the spectrophotometer, which uses it as an array of light intensities by wavelength.

At the same time Nanodrop 1000 Spectrophotometer has also the capacity to assess the purity of the calculated RNA sample. RNA has its absorption maximum at 260 nm and the ratio of the absorbance at 260 and 280 nm is used to assess the RNA purity of an RNA preparation. Pure RNA has an A260/A280 of 2.1. However, in order to achieve high quality control of the samples used in this thesis, an additional RNA quality control was performed with the Agilent 2100 Bioanalyzer (2.2.3.3.).

Protocol: At first, the parts of the spectrophotometer (lower-sensor pedestal and upper-lid pedestal) were carefully washed with distilled H_2O in order to remove any possible contaminants. 1.5µL H_2O was carefully pipetted onto the sensor and measured. Then, 1.5µL of TE buffer was placed on the sensor and the system was blanked. For each sample, 1.5µL was calculated and each sample was measured in triplicates. After each measurement, the sensor was carefully wiped to prevent sample carryover between samples. The data were saved and exported in an Excel file for further analysis.

2.2.3.3. Quality control of RNA

The Agilent 2100 Bioanalyzer was used in order to assess the quality of the isolated RNA. This method is based on a lab-on-a-chip technology to perform capillary electrophoresis by using a fluorescent dye that binds to RNA and thus analyzes both RNA concentration and

integrity. This analysis is based on traditional gel electrophoresis principles. There are two kinds of chips in the market for the analysis of RNA, the NanoChip for the analysis of low amounts of RNA (25 ng/μl – 500 ng/μl) and the PicoChip for lower levels of RNA (50 pg/μl to 5000 pg/μl). In this thesis the RNA 6000 Nano Kit was selected.

Method principle: The NanoChip consists of sample wells, gel wells and a well for an external standard, the ladder. Among the wells, micro-channels create a network that communicates with all wells. At the beginning, these micro-channels are filled with a mixture of a sieving polymer (Gel Matrix) with a fluorescence dye (Dye Concentrate) and subsequently each well is loaded with a sample and the special ladder-well with the preselected marker. Once the wells and channels are filled, the chip is an integrated electrical circuit. Similar to the traditional electrophoresis, charged molecules, such as the RNA, are electrophoretically driven by a voltage gradient. The mixture of the Gel Matrix with the Dye Concentrate plays the role of the traditional agarose gel and the molecules are separated by size, with smaller fragments travelling faster than bigger ones. The fluorescence Dye Concentrate binds with the RNA strands and makes possible the detection of these biomolecules. The data appear in images known as electropherograms or peaks.

As mentioned before, in every chip there is a separate well for an external standard, the RNA Nano 6000 ladder, which must be present in every single run. This ladder contains six RNA fragments ranging from 0.2 to 6 kb at a total concentration of 150 ng/μl and is used as a reference point for data analysis. The software automatically compares the unknown samples to the ladder fragments in order to determine the concentration of the unknown samples and to identify the ribosomal RNA peaks. In general, the electropherogram of eukaryotic RNA appears to have two distinct ribosomal peaks corresponding to 18S and 28S, respectively. Normally, the 28S RNA peak is twice as high as the 18S RNA peak and this is a sign of a good RNA sample quality. The ratio 28S/18S is widely used as a reliable marker for RNA integrity and in theory, ratios over 2 are indicative for a high quality RNA sample. However, Agilent has introduced a more accurate software algorithm for calculating RNA degradation, known as RNA Integrity Number (RIN). RIN is based on a numbering system from 1 to 10, with 1 being the most degraded and 10 being the most intact RNA sample. According to the manufacturer's instructions, freshly harvested cultured cells or freshly harvested tissue from a laboratory animal should possess a RIN higher that 7.5-8, otherwise there was a problem with the way the RNA extraction procedure was performed. For highly demanding assays like microarray analyses, RIN values higher than 8 are required for tissue cultured cells (Genome Center Maastricht, 2007).

Reagents used:

Agilent RNA 6000 Ladder

RNA Nano Dye Concentrate

Agilent RNA 6000 Nano Marker

Agilent RNA 6000 Nano Gel Matrix

Protocol: The RNA Nano 6000 reagents were put into a light-protected area for 30 min before starting, at room temperature. According to the manufacturer's instructions, all electrodes on the bioanalyzer were carefully decontaminated before and after each chip run, with the RNaseZap or RNase-free DI water providedby the manufacturer. The Gel Matrix was prepared by filtering 550 µL in the supplied filter column and centrifugation at 4000 rpm for 10 min. 1 µl of the Dye Concentrate was then added to 65 µL Gel Matrix, vortexed thoroughly and spun at 13,000 g for 10 min. The fresh gel-dye mixture was prepared before each run and used within the same day. Afterwards, the chip was put for preparation into the special chip priming station. 9 µL of gel-dye mix were introduced into the marked well and distributed by means of a plunger. Another 9 µL gel-dye mix was introduced into the remaining marked wells and subsequently 5 µL of the Nano Marker into all sample wells and the ladder well. 1 µL ladder was put into the well marked with a ladder and at the end 1 µL RNA sample was put into each sample well. In empty wells, 1 µL of distilled water was added to maintain volume. The loaded chip was then put on the vortexing station for 1 min at 240 rpm and afterwards was carefully put into the bioanalyzer, where the integrity of the samples was assessed.

2.2.3.4. cDNA synthesis

RNA was transcribed into full-length first-strand cDNA using the Ready-To-Go You-Prime First-Strand Beads from GE Healthcare. These beads consist of buffer, dATP, dCTP, dGTP, dTTP, murine reverse transcriptase (FPLCpureTM), RNAguardTM (porcine) and RNase/DNase-free BSA and are able to utilize Moloney Murine Leukemia Virus (M-MuLV) reverse transcriptase to generate first-strand cDNA. The first-strand reaction was primed with oligo-dT primers.

Protocol: 5 µg of the RNA sample were reconstituted in DEPC water to a total volume of 30 µl in an RNase-free tube. The mixture was then heated up at 65^0C for 10 min and then quickly put on ice for an additional time of 2 min. Afterwards, the mixture was transferred into the tube containing the two first-strand reaction beads, where 2 µl of oligo-dT primers and 1.8 µl

of DEPC water were further added to a final volume of 33 µl. The solution was left to sit at a room temperature for about a minute and was then gently mixed by pipetting and briefly centrifuged. At the end, the mixture was incubated for 60 min at 37^0C and the 33 µl final volume of cDNA that were generated were diluted in 67 µl DEPC water. The cDNA samples were stored in -20^0C and were used within three months from the production date.

2.2.3.5. Quantitative real time polymerase chain reaction (qRT-PCR)

qRT-PCR is a highly sensitive method that enables detection, exponential amplification and quantification of a specific sequence of nucleic acids in real time by using fluorescent technology. cDNA, RNA or double-strand DNA can all be used as substrates and their quantification is achieved by determination of the cycle when the PCR product is detected for the first time. In the conventional PCR, this is not the case and the detection of the product is an endpoint detection, meaning that the PCR products cannot be accurately quantified. In this thesis, all qRT-PCR reactions were performed on an ABI Prism 7000 sequence detector system and subsequently analysed using the ABI Prism 7000 SDS software version 1.2 (Applied Biosystems, Foster City, CA, USA).

Method principle: At the beginning of amplification, the reaction mixture contains the cDNA sample, the specific primers, and the fluorescence dye, specifically SYBR® Green I which binds all double-stranded DNA molecules, emitting a fluorescent signal of a defined wavelength after binding. There are three major steps that take place during a qPCR reaction and each step is repeated over 40 cycles:

- Denaturation is the first step where cDNA is denatured at a temperature 90^oC (~94^oC), leading to the separation of the two strands.
- Annealing allows the binding of the specific primers that are complementary to a sequence on each strand. The primer sites are often about 100 bases apart. The appropriate temperature for this step is based on the calculated melting temperature (Tm) of the primers (5°C below the Tm of the primer). In the conducted experiments of this thesis the Tm of the primers used was 60°C, therefore the selected temperature for the annealing step was 55°C.
- Extension or elongation is the last step, it occurs at 72°C, where the activity of the DNA polymerase is optimal, and primer extension occurs at rates of up to 100 bases per second. During elongation, more and more SYBR Green dye molecules bind to the newly synthesized double–stranded DNA, and since the reaction is monitored continuously, an increase in fluorescence is viewed in real-time. At the beginning of the next heating cycle,

the dye molecules are being released again and therefore the fluorescence signal falls. Signal intensity increases with increasing cycle number due to the accumulation of PCR product.

Protocol: The reagents used were: QuantiTect SYBR Green PCR Master Mix, 10x QuantiTect Primer Assay, template cDNA and RNase free water. All reagents were kept on ice during the entire procedure. At first, the reaction mix was prepared according to the manufacturer's instructions, the exact component concentrations are shown in detail in Table 6. The cDNA template was not added in the reaction tube but was introduced separately, into each well of the 96 well plate, after addition of the reaction mix. The plate was briefly centrifuged and placed in the real-time cycler. The cycling conditions of the cycler are shown in Table 7. The additional initial PCR activation step of 15 min at 95°C was essential in order to activate the HotStarTaq DNA Polymerase, which was already included in the QuantiTect SYBR Green PCR Master Mix. Data analysis was performed by calculating the fold changes using the ΔΔC(T) method as already described (Livak and Schmittgen, 2001). Induced fibroblast values were compared to each control sample after normalisation against the calibrator value. Specific genes were analyzed by qRT-PCR at two different timepoints of the adipogenic treatment, on the 8th and on the 23rd day of the adipogenic induction.

Table 6. Reaction mix setup for qRT-PCR

Component	Volume (in µl)
2x QuantiTect SYBR Green PCR Master Mix	12.5
10x QuantiTect Primer Assay	2.5
RNase-free water	8
Template cDNA	2
Total volume	*25*

Table 7. Cycling conditions for qRT-PCR

Step	Time	Temperature (°C)
PCR activation step	15 min	95
3-step cycling		
Denaturation	15 sec	94
Annealing	30 sec	55
Extension	30 sec	72
Number of cycles	*40*	

2.2.3.6. cDNA microarray

Gene expression analysis of the RNA samples of human fibroblasts originating from 30- and 76-year-old donors was conducted by using the Agilent Whole Human Genome Oligo Microarrays (one-color; ca. 41,000 human genes and transcripts) and was performed by Miltenyi Biotec (Bergisch-Gladbach, D). The RNA samples that were subjected to microarray analysis are presented in Table 8.

Table 8. List of RNA samples used for microarray analysis.

RNA sample description	RNA sample ID
DFs30 untreated control cells	DFs30 K
DFs30 induced cells	DFs30 B
DFs76 untreated control cells	DFs76 K
DFs76 induced cells	DFs76 B

Processing: For the linear T7-based amplification step, 1 µg of each total RNA sample was used. To produce Cy3-labeled cRNA, the RNA samples were amplified and labeled using the Agilent Quick Amp Labeling Kit. Yields of cRNA and the dye-incorporation rate were measured with the ND-1000 Spectrophotometer. The hybridization procedure was performed according to the Agilent 60-mer oligo microarray processing protocol using the Agilent Gene Expression Hybridization Kit. Briefly, 1.65 µg Cy3-labeled fragmented cRNA in hybridization buffer was hybridized overnight (17 h, 65°C) to Agilent Whole Human Genome Oligo Microarrays 4x44K using Agilent's hybridization chamber and oven. Finally, the microarrays were washed once with the Agilent Gene Expression Wash Buffer 1 for 1min at room temperature followed by a second wash with preheated Agilent Gene Expression Wash Buffer 2 (37°C) for 1 min. The last washing step was performed with acetonitrile. Fluorescence signals were detected using Agilent's Microarray Scanner System. The Agilent Feature Extraction Software was used to read out and process the microarray image files. Further functional grouping analysis of differentially regulated genes was conducted by the Bioinformatics Services of Miltenyi Biotec (Bergisch-Gladbach, D).

Differentially expressed genes were further filtered according to Gene Ontology (GO) terms or mapped to KEGG pathways using DAVID (http://david.abcc.ncifcrf.gov) (Huang et al., 2009).

2.2.4. Statistical analysis

Values represent the mean values ± standard deviation (SD) of at least three experiments. Statistical significance was calculated by the Student's t-test. Mean differences were considered to be significant as follows: $p < 0.001$ ***; $p < 0.01$ **; $p < 0.05$ *. Data and graphs were produced with MS Excel 2008.

«Big results require big ambitions»

Heraclitus of Ephesus

pre-Socratic Greek philosopher, ca. 535 BC- ca. 475 BC

3. RESULTS

3.1. Lipid accumulation detection in induced FSFs, DFs30 and DFs76

Adipogenic differentiation was evaluated by using Nile red staining on the last day of the adipogenesis induction procedure (Table 5). After induction, dermal fibroblasts from donors of different ages, namely FSFs, DFs30 and DFs76, displayed intracellular lipid droplets, which could be visualised by Nile red staining using fluorescence microscopy. This observation was indicative of the achieved transdifferentiation of dermal fibroblasts towards adipocytes (Figs. 3.1.1.-3.1.9.). Both neutral (gold-yellow fluorescence, excitation: 450-500 nm; emission> 528 nm) and polar (red fluorescence, excitation: 515-560 nm; emission > 590 nm) intracellular lipid accumulation were assessed. Control cells that received no treatment showed minimal or complete absence of Nile red staining.

FSFs

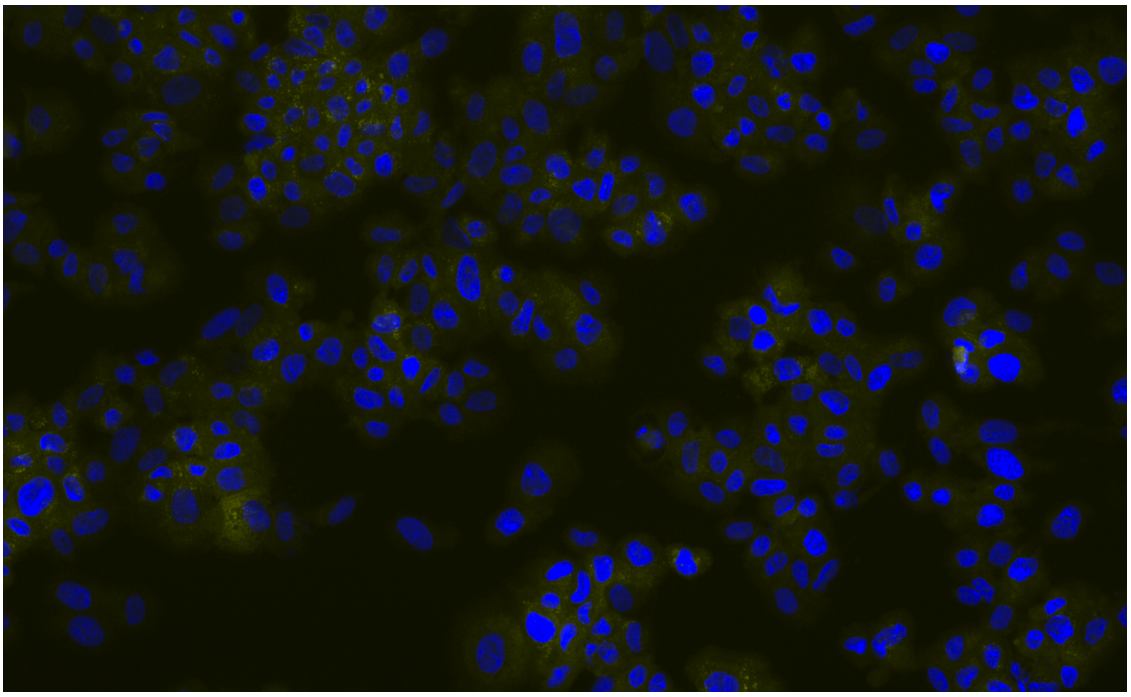

Figure 3.1.1. Content of neutral lipids in untreated foreskin fibroblasts on the 23rd day of culture (negative control) observed by fluorescence microscopy after Nile red staining. No lipid accumulation was observed.

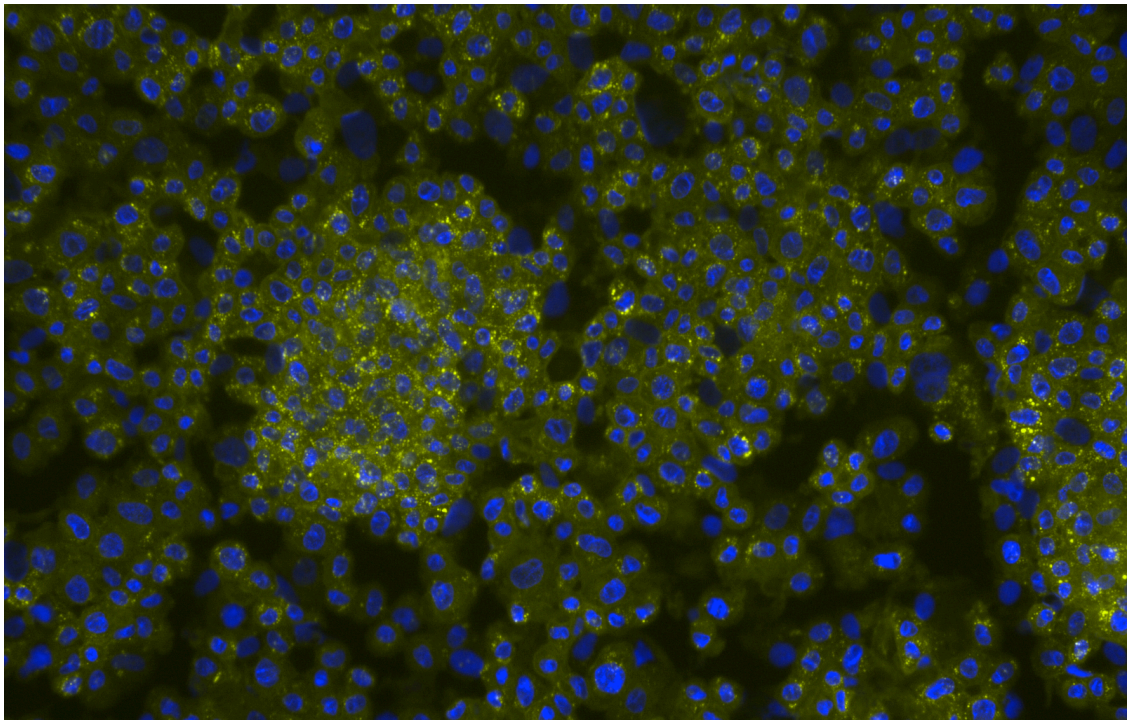

Figure 3.1.2. Content of neutral lipids in induced foreskin fibroblasts on the 23rd day of the adipogenic treatment observed by fluorescence microscopy after Nile red staining. Neutral lipid accumulation was detected in the cultured cells.

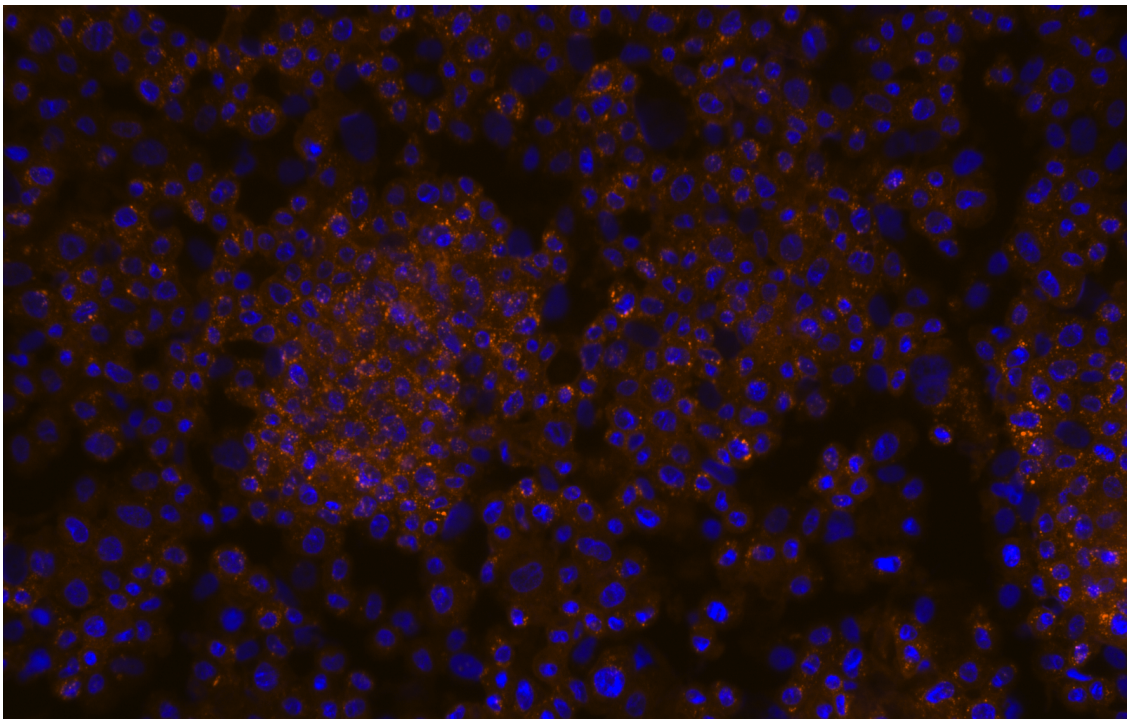

Figure 3.1.3. Content of polar lipids in induced foreskin fibroblasts on the 23rd day of the adipogenic treatment observed by fluorescence microscopy after Nile red staining. Polar lipid accumulation was detected in the cultured cells.

DFs30

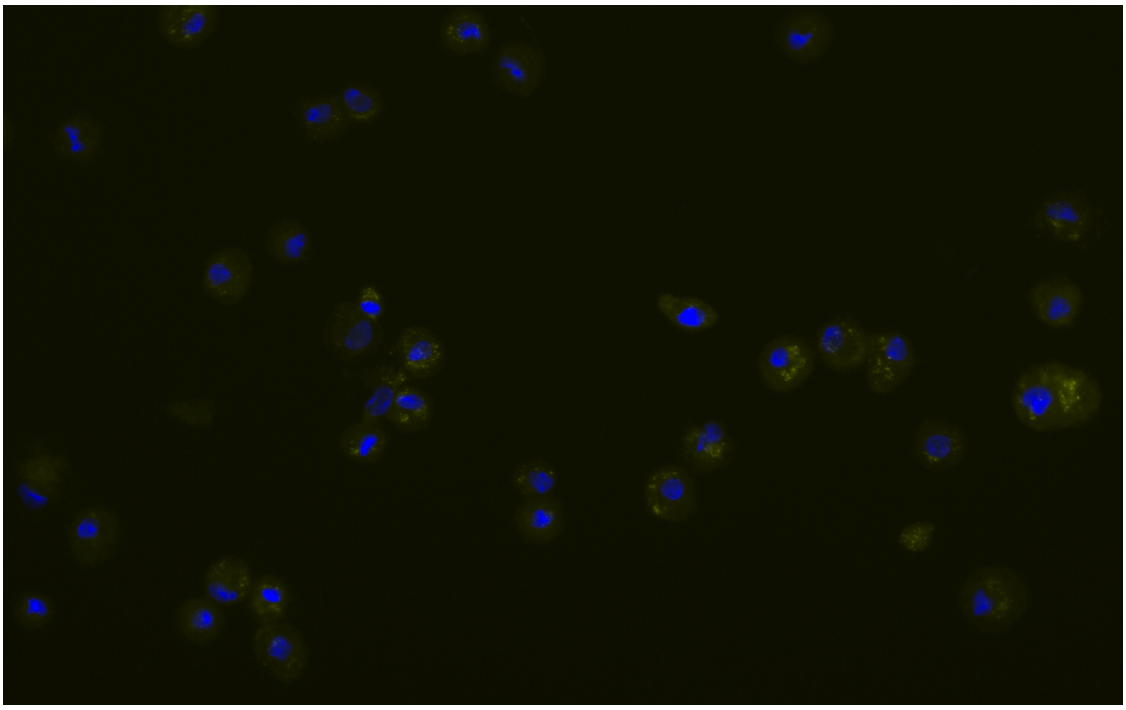

Figure 3.1.4. Content of neutral lipids in untreated DFs30 on the 23rd day (negative control) observed by fluorescence microscopy after Nile red staining. Minimal cytoplasmic lipid accumulation was detected.

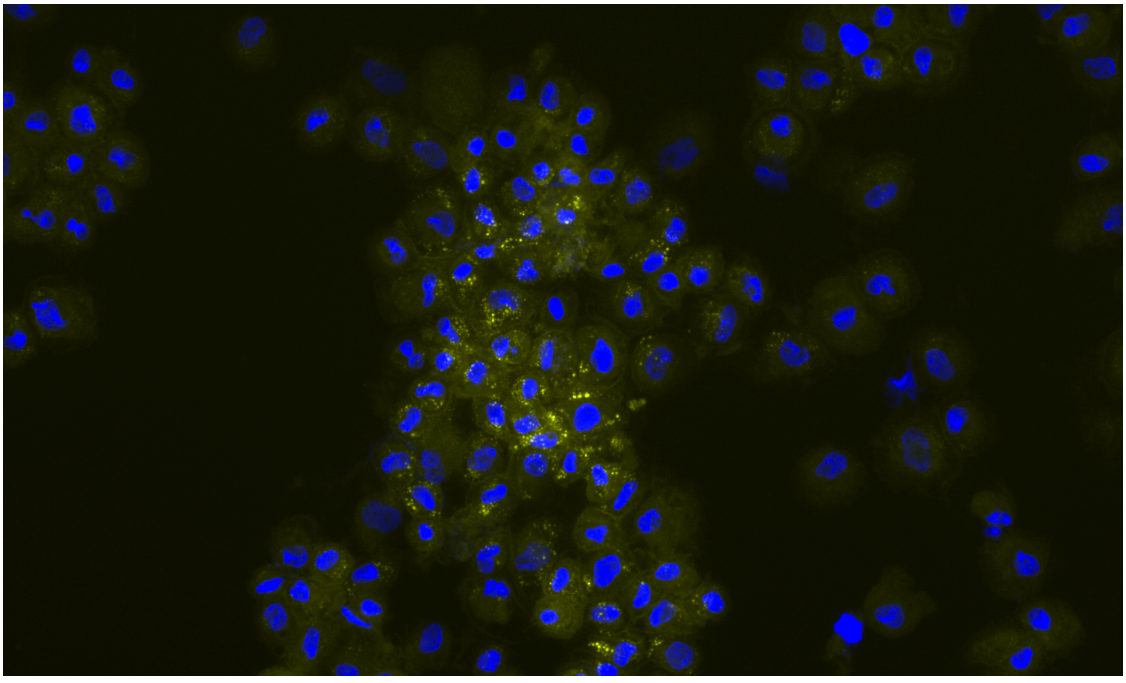

Figure 3.1.5. Content of neutral lipids in induced DFs30 on the 23rd day observed by fluorescence microscopy after Nile red staining. Enhanced cytoplasmic neutral lipid accumulation was detected in comparison to the control.

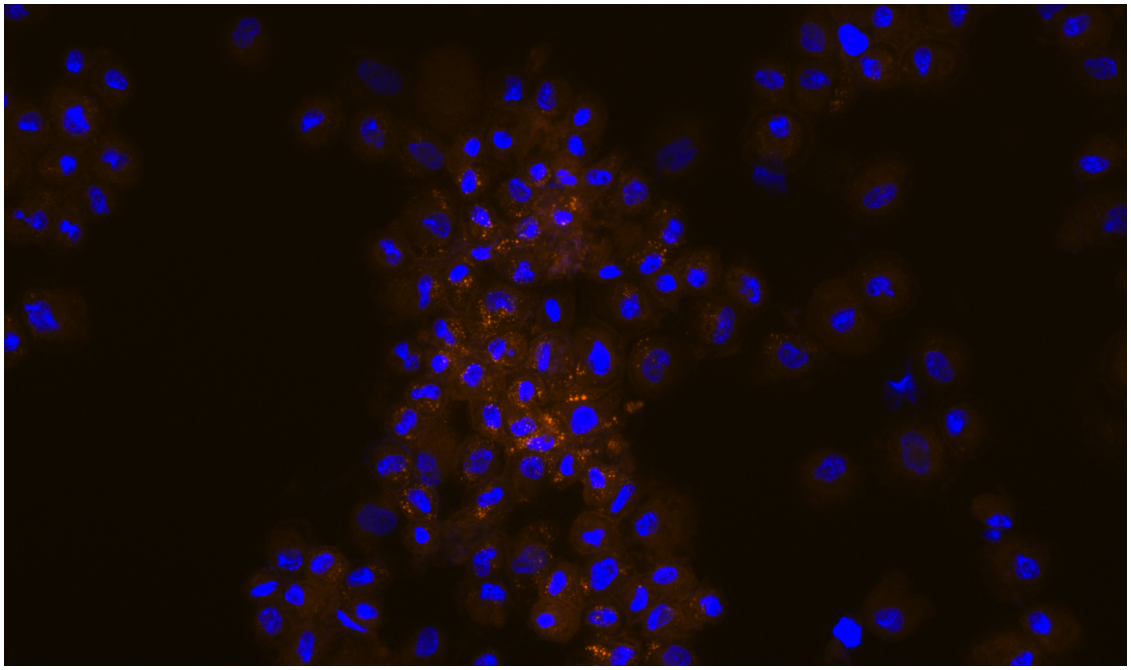

Figure 3.1.6. Content of polar lipids in induced DFs30 on the 23rd day observed by fluorescence microscopy after Nile red staining. Enhanced cytoplasmic polar lipid accumulation was also detected in comparison to the control.

DFs76

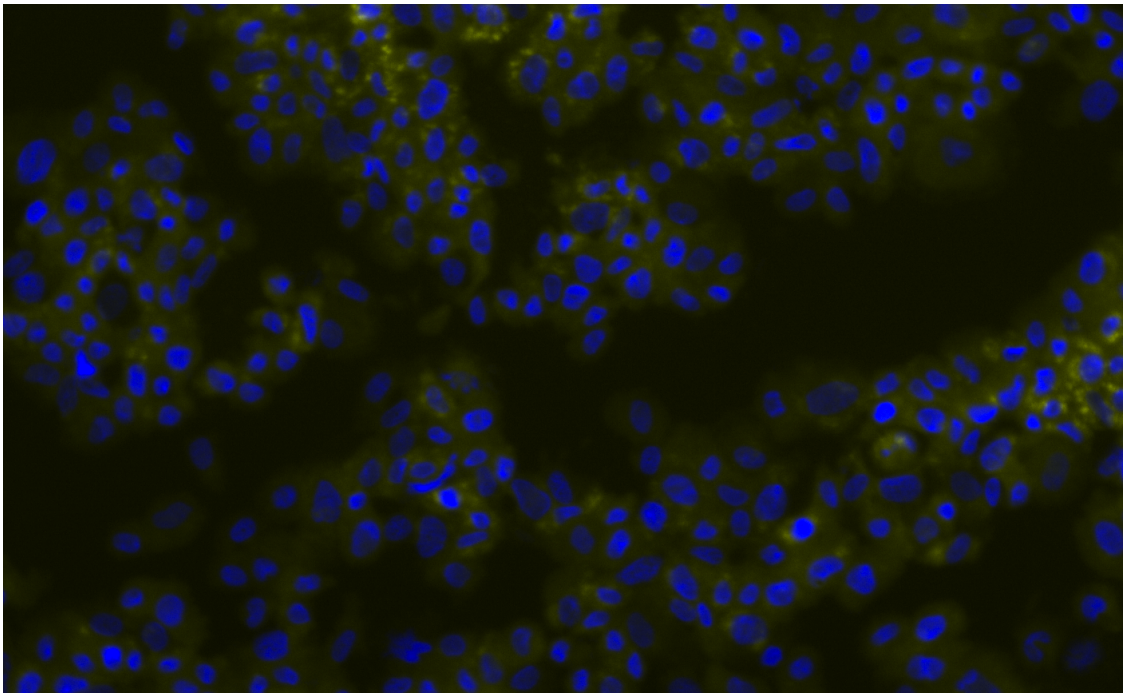

Figure 3.1.7. Content of neutral lipids in untreated DFs76 on the 23rd day (negative control) observed by fluorescence microscopy after Nile red staining. Minimal cytoplasmic lipid accumulation was detected.

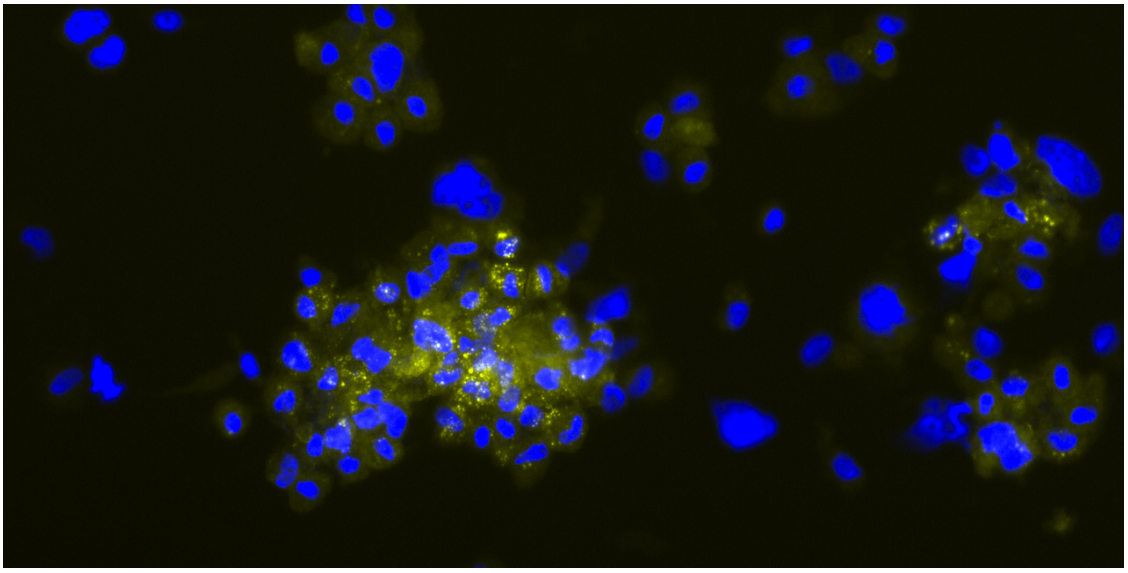

Figure 3.1.8. Content of neutral lipids in induced DFs76 on the 23rd day of the adipogenic induction observed by fluorescence microscopy after Nile red staining. Increased cytoplasmic neutral lipid accumulation was detected compared with the negative control.

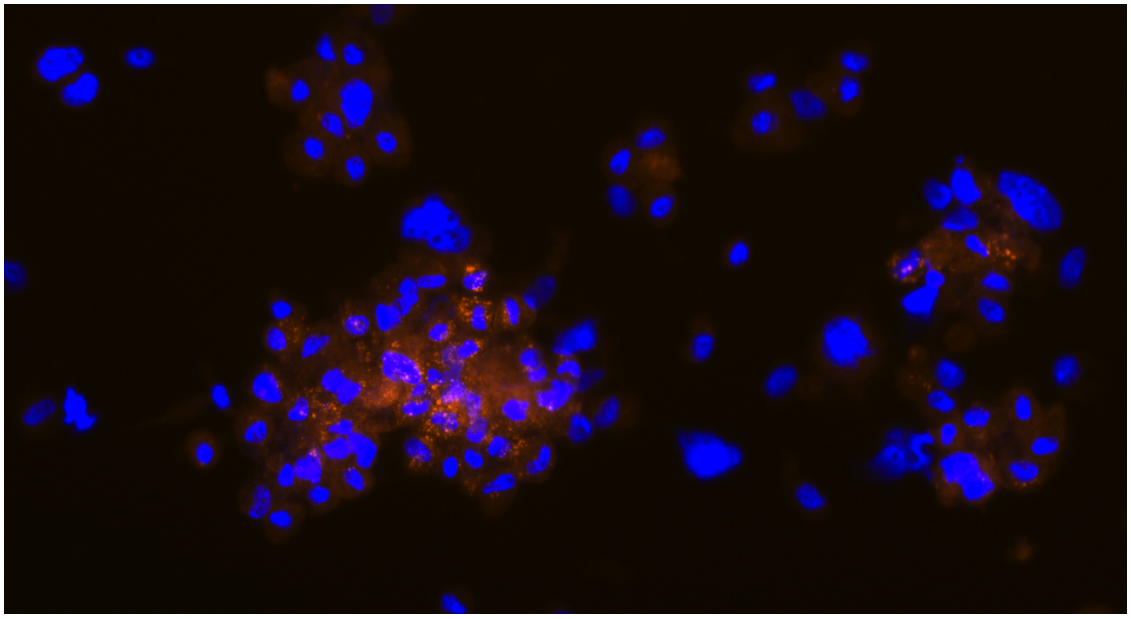

Figure 3.1.9. Content of polar lipids in induced DFs76 on the 23rd day of the adipogenic induction observed by fluorescence microscopy after Nile red staining. Increased cytoplasmic polar lipid accumulation was detected compared with the negative control.

3.2. Cytoplasmic lipid accumulation capacity differs among fibroblasts from donors of different ages

After adipogenic induction of young (FSFs and DFs30) and old fibroblasts (DFs76), an increase of both neutral and polar lipids was observed by flow cytometry after Nile red staining among fibroblasts from donors of different ages. However, old fibroblasts showed a restricted capacity for lipid production, whereas younger fibroblasts produced higher amounts of lipids.

3.2.1. FSFs exhibit increased lipid content after adipogenic induction

A significant increase of both neutral ($p<0.05$) (Fig. 3.2.1.1.) and polar lipids ($p<0.001$) (Fig. 3.2.1.2) was observed in FSFs, cultured for 23 days according to the adipogenic protocol. The neutral lipid content was increased 16% in comparison to the control cells, whereas polar lipids showed an increase of 19% compared to control cells.

(A)

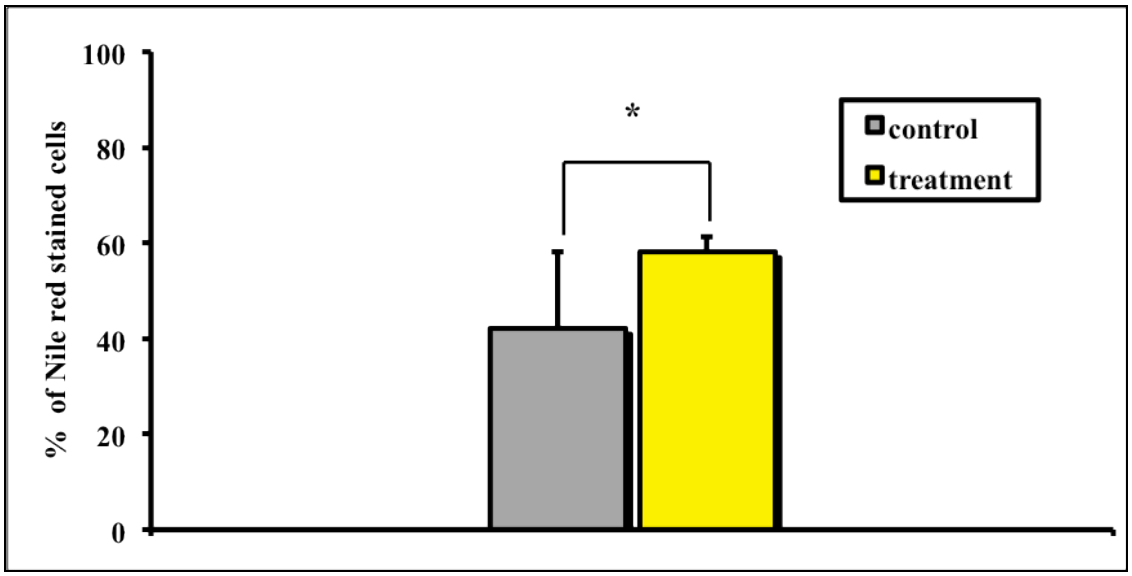

(B)

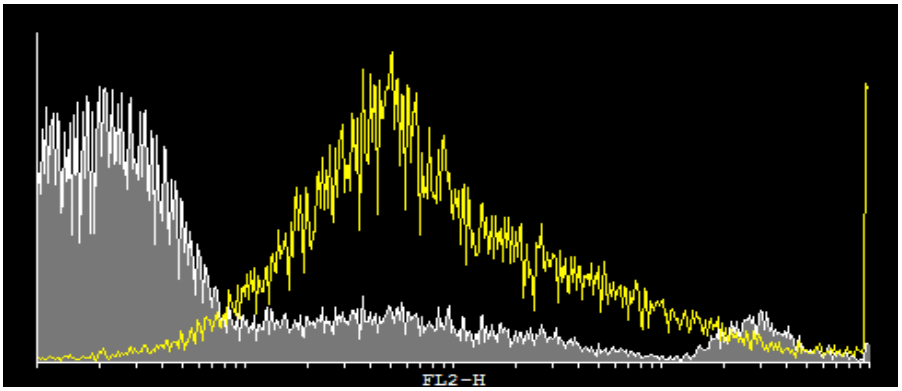

Fig. 3.2.1.1. Increase of neutral lipid content in FSFs after adipogenic induction detected by flow cytometry after Nile red staining. FSFs were seeded in 6-well plates at a density of $2x10^5$ cells/well and were subsequently treated over a period of 23 days according to the adipogenic protocol. On day 23, neutral lipid accumulation was measured by flow cytometry after Nile red staining in the FL2 channel (560–640 nm) in a FACSCalibur. **A.** The left column (grey) represents the amount of positively stained (neutral lipid-containing) control cells and the right column (yellow) the positively stained (neutral lipid-containing) induced cells. Values represent the mean of six measurements from three independent experiments ± SD (* $p<0.05$). **B.** The histogram shows an overlay of control cells versus treated cells on the 23rd day of the adipogenic induction. The grey-shaded peak represents the control positively stained cells, whereas the yellow peak line the induced positively stained cells.

(A)

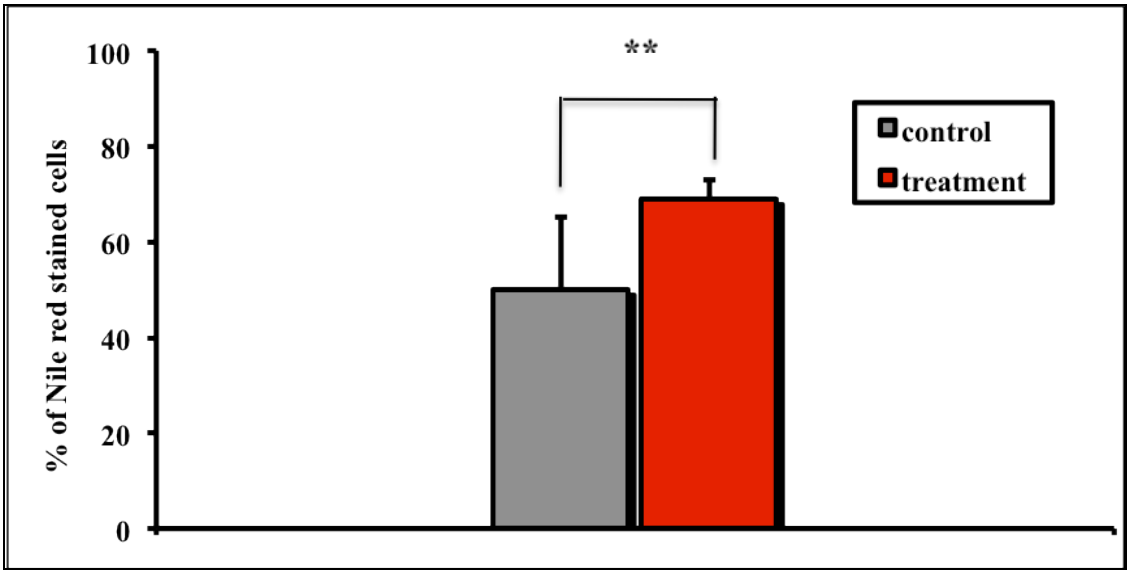

(B)

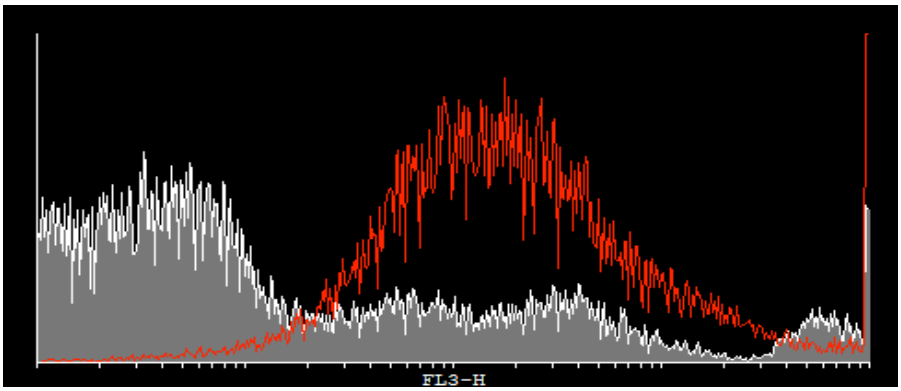

Fig. 3.2.1.2. Increase of polar lipid content in FSFs after adipogenic induction detected by flow cytometry after Nile red staining. FSFs were seeded in 6-well plates at a density of $2x10^5$ cells/well and were subsequently treated over a period of 23 days according to the adipogenic protocol. On day 23, polar lipid accumulation was measured by flow cytometry after Nile red staining in the FL3 channel (>650 nm) in a FACSCalibur. **A.** The left column (grey) represents the amount of positively

stained (polar lipid-containing) control cells and the right column (red) the positively stained (polar lipid-containing) induced cells. Values represent the mean of six measurements from three independent experiments ± SD (** $p<0.01$). **B.** The histogram shows an overlay of control cells versus treated cells on the 23rd day of the adipogenic induction. The grey-shaded peak represents the positively stained control cells, whereas the red peak line the induced positively stained cells.

3.2.2. DFs30 exhibit the strongest lipid accumulation among fibroblasts from donors of different ages

The most abundant and significant increase ($p<0.001$) of neutral (Fig. 3.2.2.1.) as well as polar lipids (Fig. 3.2.2.2.) among fibroblasts of different ages was observed in DFs30 on the 23rd day of the adipogenic induction. Polar lipid accumulation was, as in the FSFs, slightly stronger than that of neutral lipids. Neutral lipid content was enhanced 50% in comparison to the control cells, whereas polar lipids showed an increase of 52% compared to control cells.

(A)

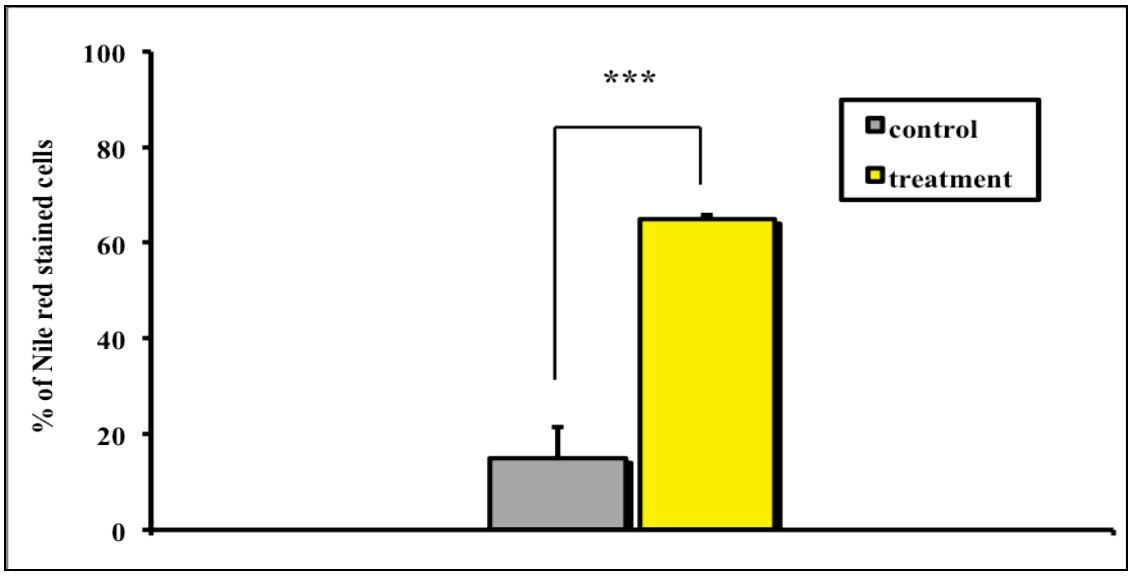

(B)

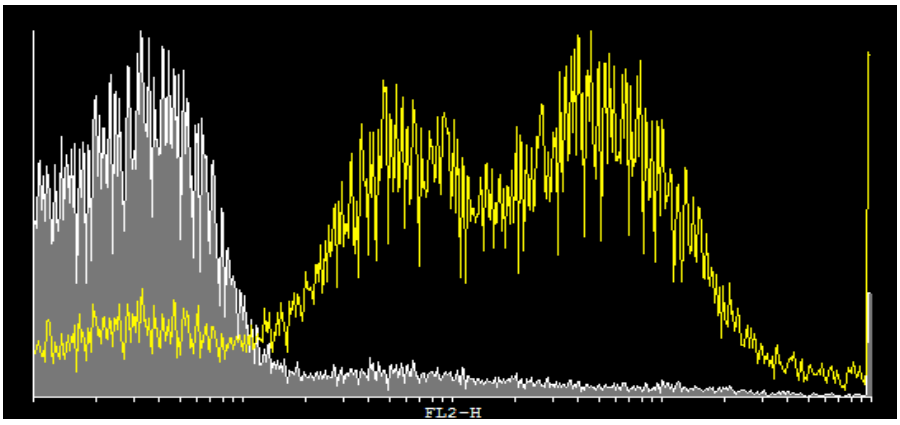

Fig. 3.2.2.1. Increase of neutral lipid content in DFs30 after adipogenic induction detected by flow cytometry after Nile red staining. DFs30 were seeded in 6-well plates at a density of $2x10^5$ cells/well and subsequently treated over a period of 23 days according to the adipogenic protocol. On day 23, neutral lipid accumulation was measured by flow cytometry after Nile red staining in the FL2 channel (560–640 nm) in a FACSCalibur. **A.** The left column (grey) represents the amount of positively stained (neutral lipid-containing) control cells and the right column (yellow) the positively stained (neutral lipid-containing) induced cells. Values represent the mean of six measurements from three independent experiments ± SD (* $p<0.05$). **B.** The histogram shows an overlay of control cells versus treated cells on the 23rd day of the adipogenic induction. The grey-shaded peak represents the positively stained control cells, whereas the yellow peak line the induced positively stained cells.

(A)

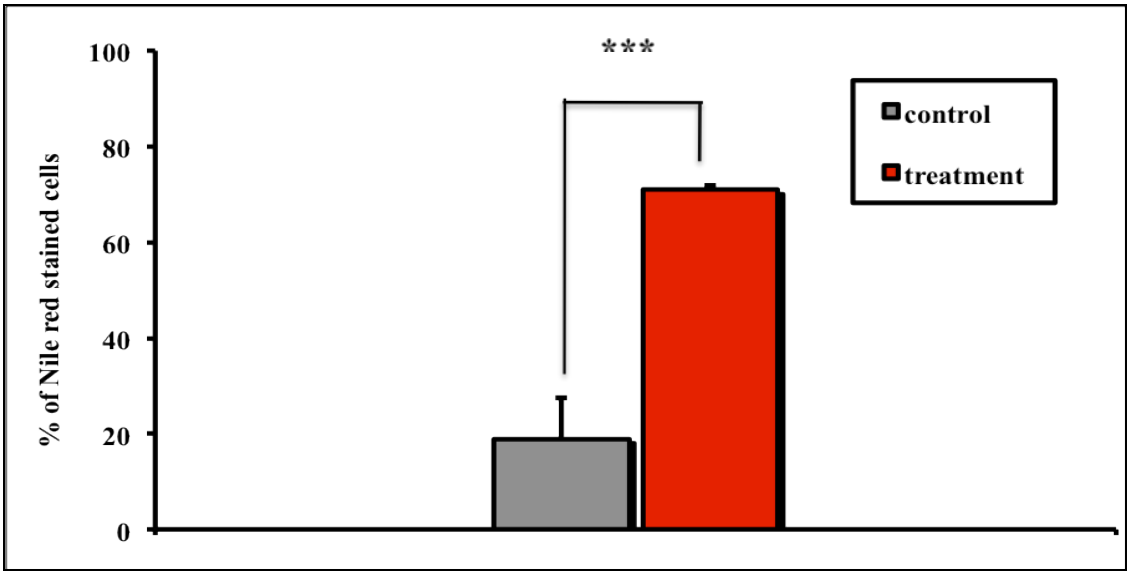

(B)

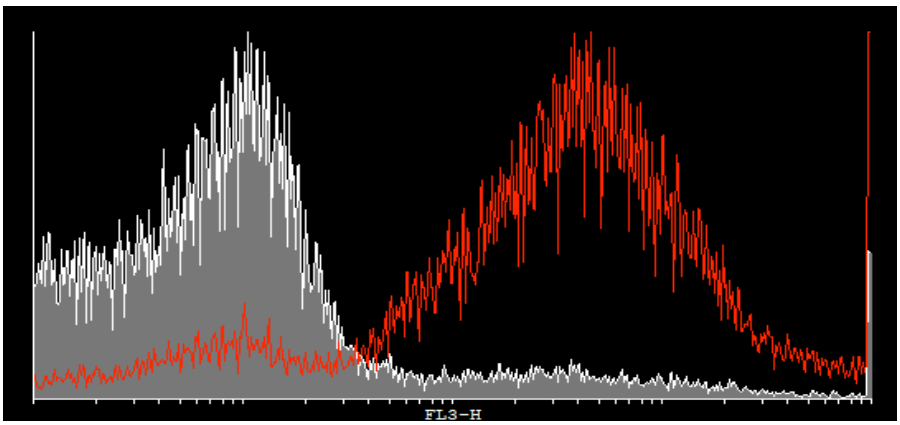

Fig. 3.2.2.2. Increase of polar lipid content in DFs30 after adipogenic induction detected by flow cytometry after Nile red staining. DFs30 were seeded in 6-well plates at a density of $2x10^5$ cells/well and subsequently treated over a period of 23 days according to the adipogenic protocol. On day 23, polar lipid accumulation was measured by flow cytometry after Nile red staining in the FL3 channel

(>650 nm) in a FACSCalibur. **A.** The left column (grey) represents the amount of positively stained (polar lipid-containing) control cells and the right column (red) the positively stained (polar lipid-containing) induced cells. Values represent the mean of six measurements from three independent experiments ± SD (** $p<0.01$). **B.** The histogram shows an overlay of control cells versus treated cells on the 23rd day of the adipogenic induction. The grey-shaded peak represents the positively stained control cells, whereas the red peak line the induced positively stained cells.

3.2.3. DFs76 accumulate minimal amounts of both neutral and polar lipids

Dermal fibroblast from older donors (DFs76) showed a markedly lower lipid accumulation in contrast to younger fibroblasts (FSFs and DFs30). Neutral lipid content was increased 5% in induced cells in comparison to control cells (non-significant result) (Fig. 3.2.3.1.). Polar lipid accumulation was also increased 5% in induced cells when compared to the control cells but this result was marginally significant ($p<0.05$) (Fig. 3.2.3.2.).

(A)

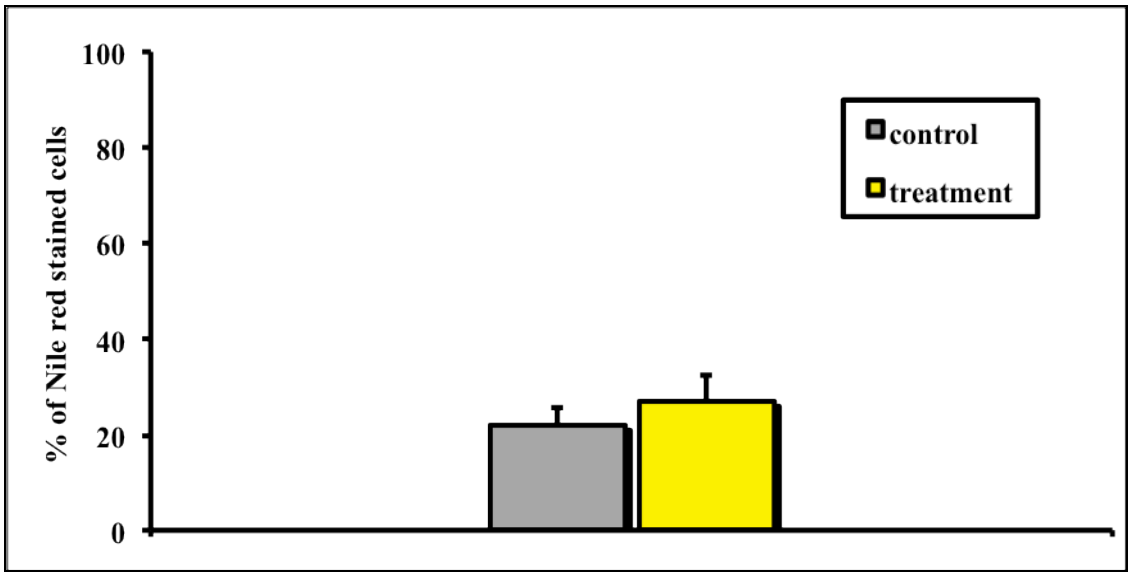

(B)

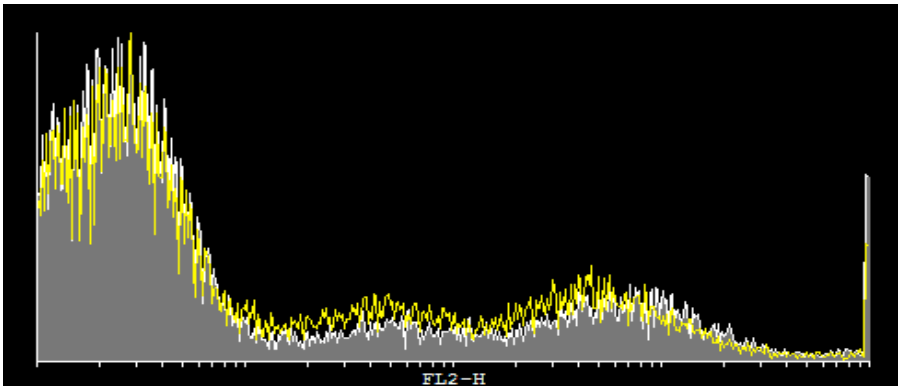

Fig. 3.2.3.1. Non-significant minimal increase of neutral lipid content in DFs76 after adipogenic induction detected by flow cytometry after Nile red staining. DFs76 were seeded in 6-well plates at a density of $2x10^5$ cells/well and subsequently treated over a period of 23 days according to the adipogenic protocol. On day 23, neutral lipid accumulation was measured by flow cytometry after Nile red staining in the FL2 channel (560–640 nm) in a FACSCalibur. **A.** The left column (grey) represents the amount of positively stained (neutral lipid-containing) control cells and the right column (yellow) the positively stained (neutral lipid-containing) induced cells. Values represent the mean of six measurements from three independent experiments ± SD (* $p<0.05$). **B.** The histogram shows an overlay of control cells versus treated cells on the 23rd day of the adipogenic induction. The grey-shaded peak represents the positively stained control cells, whereas the yellow peak line the induced positively stained cells.

(A)

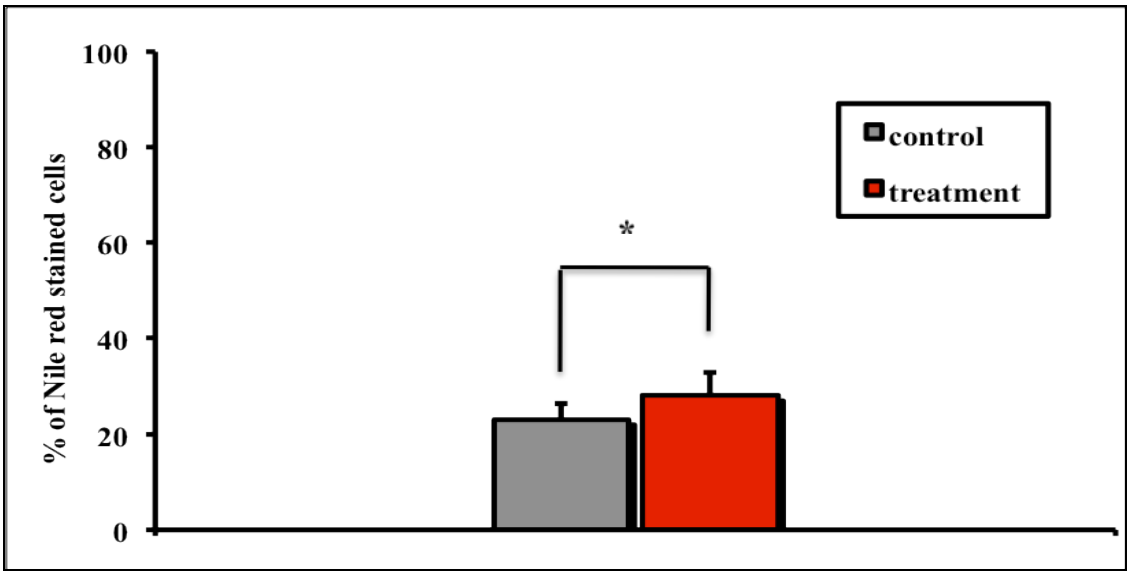

(B)

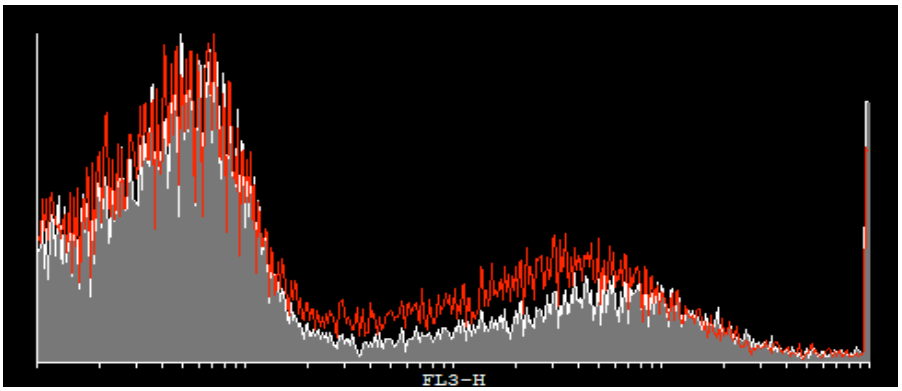

Fig. 3.2.3.2. Minimal increase of polar lipid content in DFs76 after adipogenic induction detected by flow cytometry after Nile red staining. DFs76 were seeded in 6-well plates at a density of $2x10^5$ cells/well and subsequently treated over a period of 23 days according to the adipogenic protocol. On day 23, polar lipid accumulation was measured by flow cytometry after Nile red staining in the FL3

channel (>650 nm) in a FACSCalibur. **A.** The left column (grey) represents the amount of positively stained (polar lipid-containing) control cells and the right column (red) the positively stained (polar lipid-containing) induced cells. Values represent the mean of six measurements from three independent experiments ± SD (** $p<0.01$). **B.** The histogram shows an overlay of control cells versus treated cells on the 23rd day of the adipogenic induction. The grey-shaded peak represents the positively stained control cells, whereas the red peak line the induced positively stained cells.

3.3. Fibroblasts from donors of different ages exhibit different morphological changes

Morphological changes in the induced fibroblasts on the 23rd day of the adipogenic induction were detected by light microscopy. In order to examine the cell changes that have been detected by light microscopy in more detail, transmission electron microscopy analysis was performed. Increased lipid accumulation with simultaneous formation of large cytoplasmic lipid vacuoles has been identified in the cytoplasm of all induced cell. However, the morphology of the induced DFs76 showed damaged cytoplasmic membranes in certain cells, whereas membranes in FSFs and DFs30 were intact. This observation was further supported by the lipid data obtained by flow cytometry, where only a decent lipid accumulation could be detected in the DFs76 (5%), whereas FSFs and DFs30 showed a large increase of intracellular neutral lipid accumulation (19% and 50% respectively).

3.3.1. Morphological changes of FSFs

The typical spindle-shaped, flat, fibroblast morphology was identified in control cells (Fig. 3.3.1.1. A). However, FSF morphology was markedly altered after adipogenic differentiation; induced cells presented a more round-shaped cytoplasm (arrows) after 23 days of adipogenic treatment (Fig. 3.3.1.1. B).

(A) **(B)**

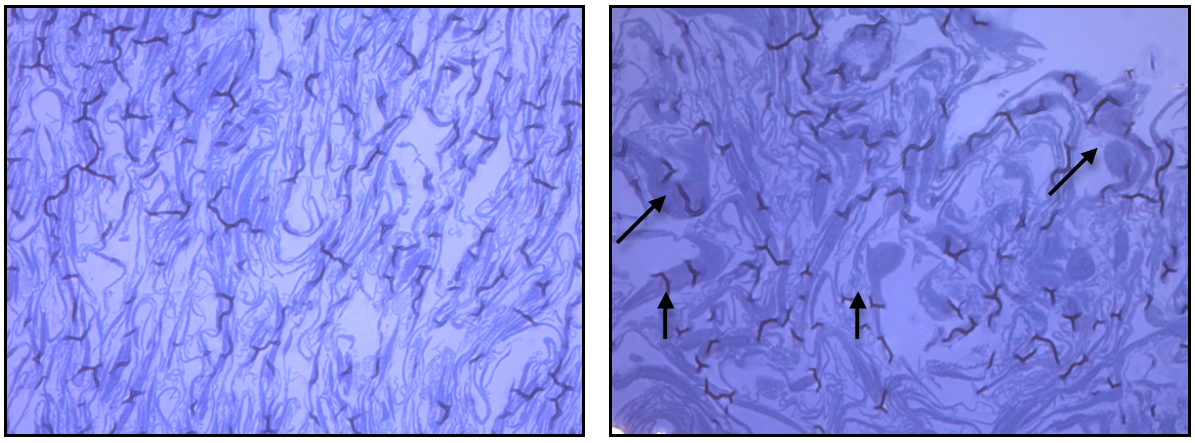

Fig. 3.3.1.1. FSF morphological changes after adipogenic induction. Light microscopy of (A) untreated control FSFs and (B) induced FSFs according to the adipogenic protocol on the 23rd day of treatment. Control cells show no changes in their fibroblast morphology, whereas induced cells have acquired an adipocyte-like morphology. Black arrows point out the round-shaped morphology of the induced cells. Magnification: (A); (B) x100.

Control FSFs presented normal intercellular contents in the transmission electron microscopy analysis (Fig. 3.3.1.2.). Cell nuclei (N) appear slender and elongated, nuclear chromatin was evenly distributed within the nuclei and cell organelles, such as the endoplasmic reticulum (black arrows), Golgi apparatus and mitochondria, were present and well organised and developed. These findings are consistent with a high activity, synthesis and vitality of the cells. No lipid vacuoles were present in the cytoplasm of the control cells.

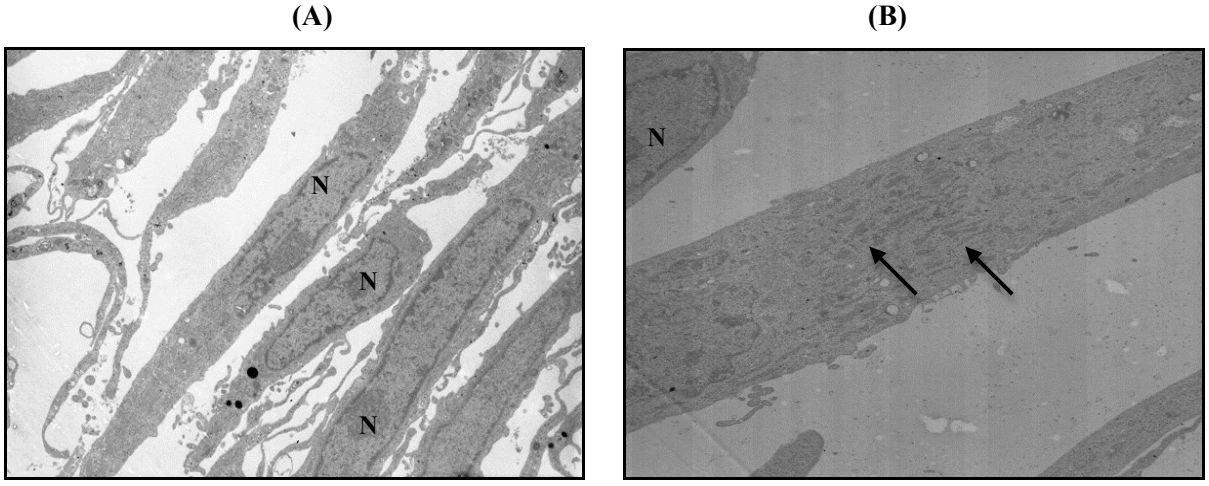

Fig. 3.3.1.2. Transmission electron microscopy of control FSFs on the 23rd day of culture. A. Control cells show typical spindle-shaped fibroblast morphology with elongated nuclei (N), evenly distributed nuclear chromatin and **B.** vital, well developed organelles, such as the endoplasmic reticulum (black arrows). No cytoplasmic lipid accumulation is detected. Magnification: (A) x5000; (B): x10000.

In contrast, cells that received adipogenic stimulation over a period of 23 days formed lipid inclusions in the cytoplasm, indicating the adipogenic capacity of these cells. Transmission electron microscopy revealed signs of ongoing adipogenesis such as cell rounding and lipid droplet accumulation (Fig. 3.3.1.3.). A certain amount of cells were identified to contain multiple, discrete lipid droplets as well as large lipid vacuoles (black arrows). Cell nuclei (N) appeared normal, with chromatin evenly distributed within them and with no signs of apoptosis, such as condensed and marginalized chromatin. Cell organelles such as

mitochondria (white arrows) could be well identified and cell membranes appeared intact with no signs of damage, therefore indicating vital, highly active cells (Fig. 3.3.1.3.).

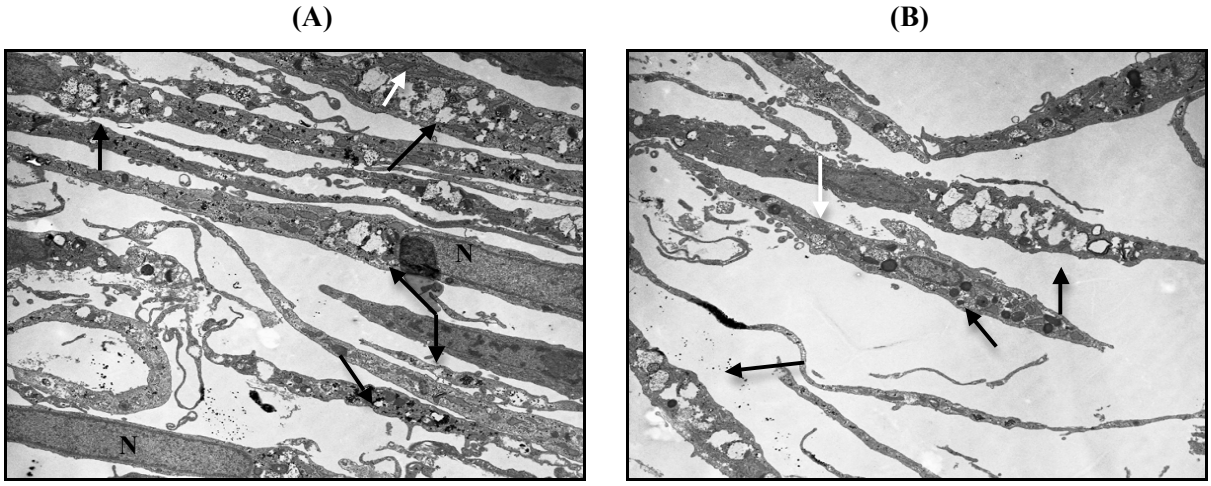

Fig. 3.3.1.3. Transmission electron microscopy of induced FSFs on the 23rd day of the adipogenic treatment. Cells contain multiple, discrete lipid droplets as well as large lipid vacuoles (black arrows). Nuclei (N) and cell organelles such as mitochondria (white arrows) have typical appearance, which is indicative of cell vitality and cell membranes are intact with no signs of damage. The cytoplasm of most induced cells appears to have acquired a more round-shaped morphology in comparison to control cells. Magnification: (A); (B): x5000.

3.3.2. Morphological changes in DFs30

DFs30 control cells showed the normal spindle-shaped fibroblast morphology in light microscopy (Fig. 3.3.2.1. A). Induced DFs30 exhibited the most abundant morphological changes among all induced fibroblasts and this finding was consistent with the lipid measurements in flow cytometry analysis. On the 23rd day of adipogenic induction, DFs30 had acquired a completely different morphology in comparison to control, with large vacuoles filled with lipid droplets being abundant in their cytoplasm. DFs30 morphology was shown to be very similar to that of adipocytes and these changes were seen in the majority of the monolayer cultures under adipogenic stimulation. Black arrows indicate large lipid vacuoles and lipid accumulation in the induced cells (Fig. 3.3.2.1. B).

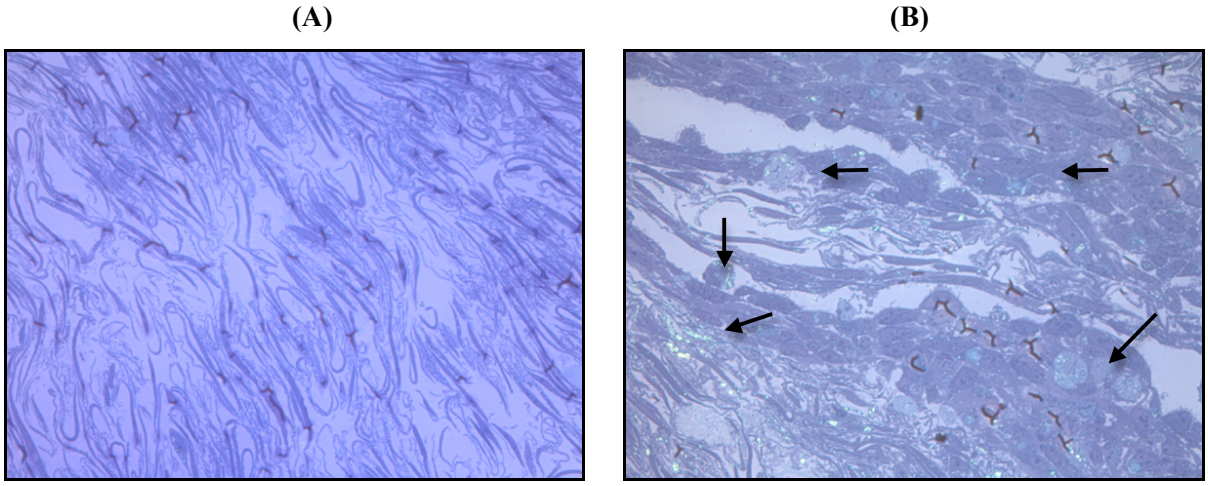

Fig. 3.3.2.1. Cell morphological changes in DFs30 after adipogenic induction. Light microscopy of (A) control DFs30 and (B) induced DFs30 on the 23rd day of maintenance according to the adipogenic treatment. Control cells exhibit their typical fibroblast morphology, whereas induced cells have clearly acquired an adipocyte-like morphology. Black arrows indicate the round-shaped induced cells containing large vacuoles filled with lipids in their cytoplasm. Magnification: (A); (B) x100.

Transmission electron microscopy analysis confirmed the light microscopy findings. Control DFs30 presented normal intercellular contents (Fig. 3.3.2.2.). Cell nuclei (N) appeared elongated, nuclear chromatin was evenly distributed and cell organelles such as endoplasmic reticulum and mitochondria (black arrows) were well organised and developed, a finding that is consistent with a high activity, synthesis and vitality of the cells. No lipid accumulation was detected in the cytoplasm of the control cells (Fig. 3.3.2.2.).

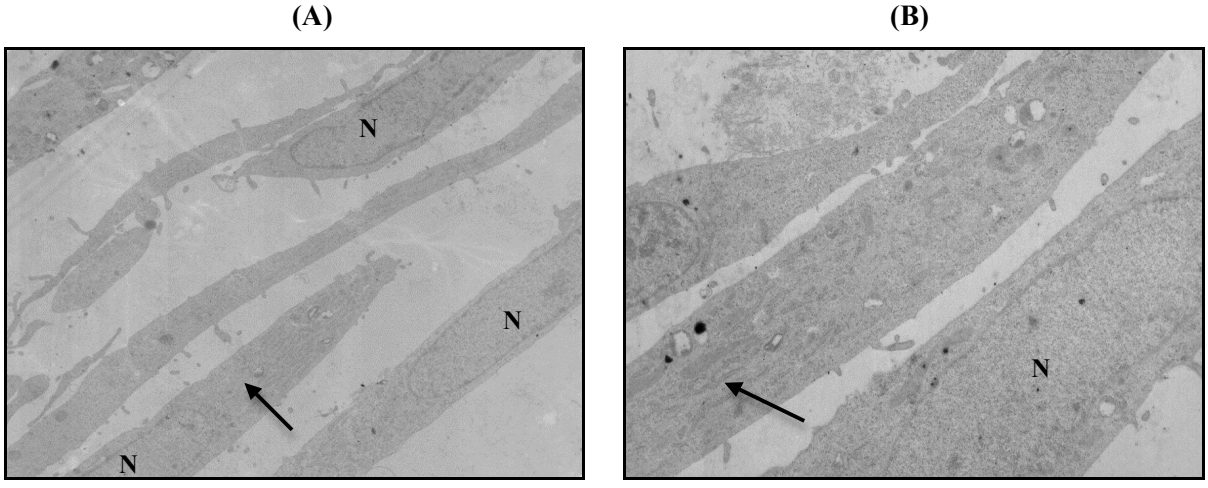

Fig. 3.3.2.2. Transmission electron microscopy of control DFs30 on the 23rd day of culture. A. Control cells show typical fibroblast morphology with elongated nuclei (N), evenly distributed nuclear chromatin and **B.** vital, well developed organelles, such as endoplasmic reticulum and mitochondria (black arrows). No cytoplasmic lipid accumulation is detected. Magnification: (A) x5000; (B): x10000.

Of all types of induced fibroblasts, induced DFs30 showed the strongest intracellular lipid accumulation in their cytoplasm (Fig. 3.3.2.3.). A large number of cells appeared to contain multiple, discrete lipid droplets as well as large lipid vacuoles (black arrows). Total vacuolation of cell cytoplasm was also observed in a number of cells (black arrowhead). Cell nuclei (N) and cell organelles such as endoplasmic reticulum and mitochondria (white arrows) appeared normal and no morphological signs of apoptosis were present. Cell membranes appeared intact with no signs of damage, indicating vital, highly active cells (Fig. 3.3.2.3.)

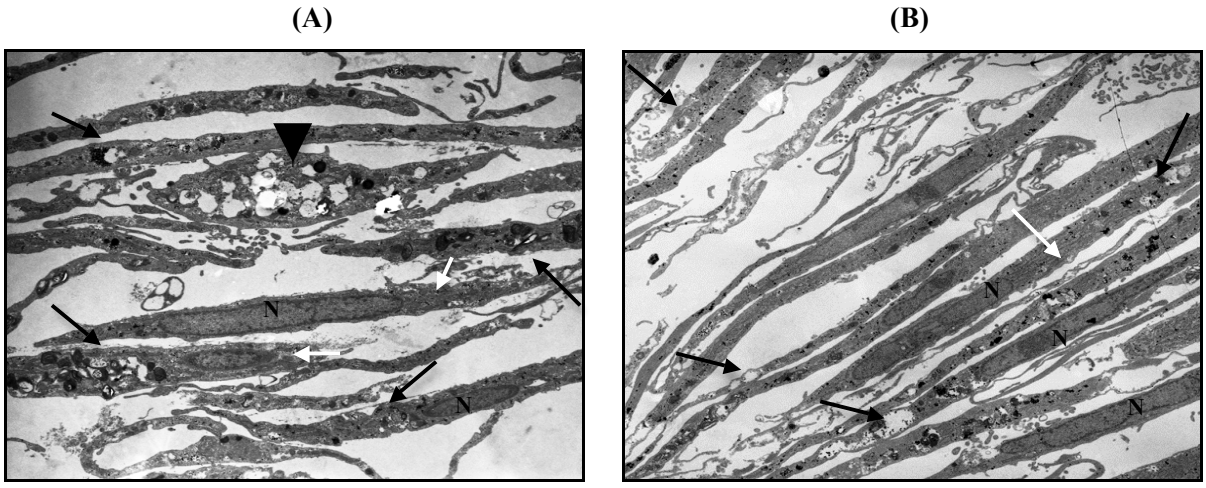

Fig. 3.3.2.3. Transmission electron microscopy of induced DFs30 on the 23rd day of the adipogenic treatment. Cells contain multiple, discrete lipid droplets as well as large lipid vacuoles (black arrows). Nuclei (N) and cell organelles such as mitochondria (white arrows) have a typical appearance, which is indicative of cell vitality and cell membranes are intact with no signs of damage. Total vacuolation of cell cytoplasm was also observed (black arrowhead). Magnification: (A); (B): x5000.

3.3.3. Morphological changes in DFs76

DFs76 control cells exhibited a normal spindle-shaped fibroblast morphology (Fig. 3.3.3.1. A). Induced DFs76 exhibited no marked morphological changes, at least in light microscopy analysis and only single induced cells could be identified that accumulated lipids in their cytoplasm (black arrow) (Fig. 3.3.3.1. B).

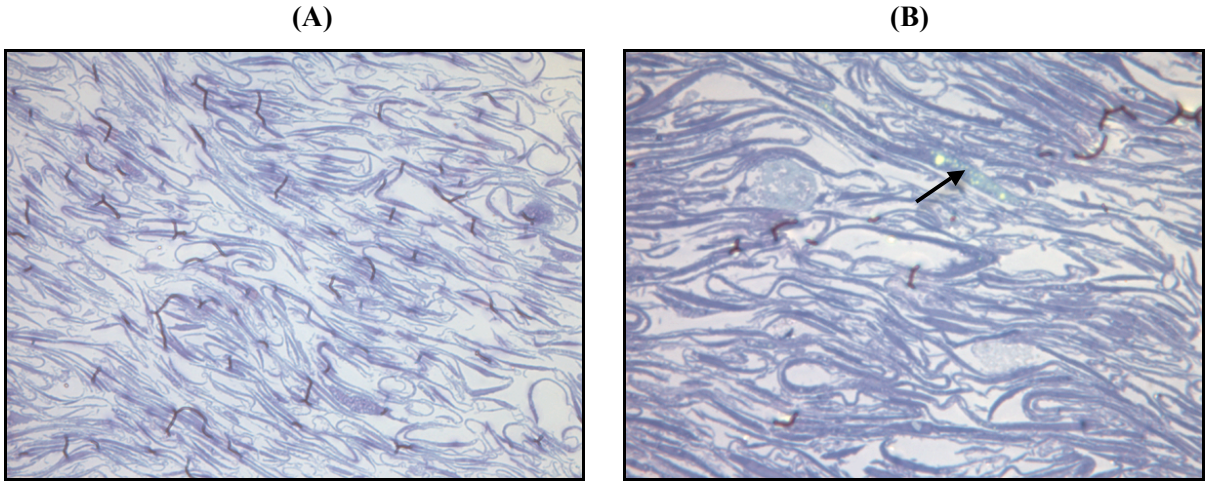

Fig. 3.3.3.1. Cell morphological changes in DFs76 after adipogenic induction. Light microscopy of (A) control DFs76 and (B) induced DFs76 according to the adipogenic protocol on the 23rd day of treatment. Control cells have a distinctive fibroblast morphology. Morphology of induced cells does not appear to be markedly affected in comparison to control cells, however single cells that contain lipid droplets in their cytoplasm can be identified (black arrow). Magnification: (A) x100; (B) x200.

Control DFs76 also presented typical fibroblast morphology in transmission electron microscopy studies (Fig. 3.3.3.2.). Cell nuclei (N), nuclear chromatin and cell organelles such as endoplasmic reticulum and mitochondria (black arrows) were well organised and no lipid accumulation was detected in the cytoplasm of the control cells (Fig. 3.3.3.2.).

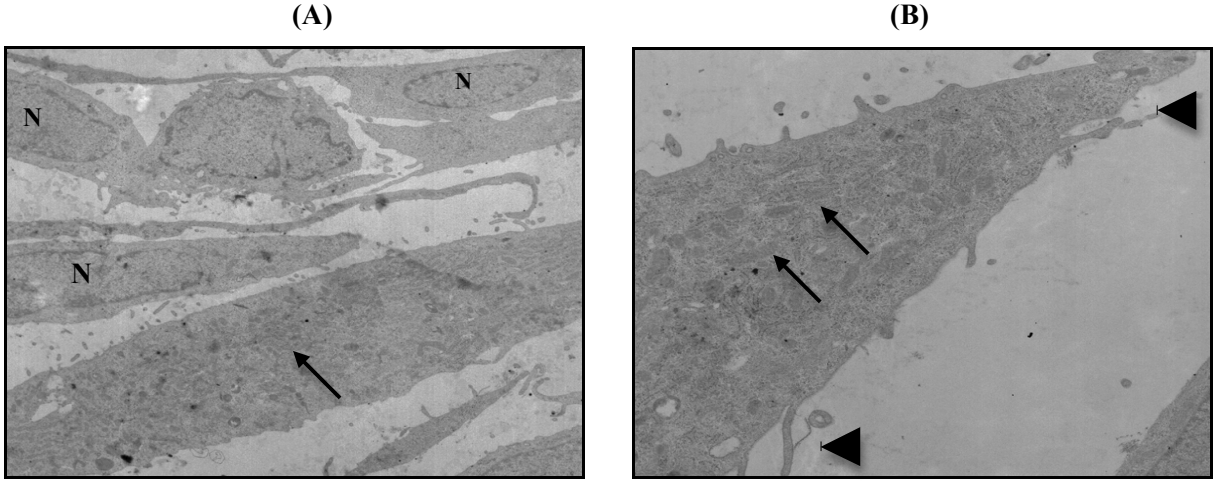

Fig. 3.3.3.2. Transmission electron microscopy of untreated control DFs76 on the 23rd day of treatment. Control cells show typical fibroblast morphology. Nuclei (N), nuclear chromatin and cell organelles, such as endoplasmic reticulum and mitochondria are well developed (black arrows). Numerous pseudopods can be identified (black arrowheads). No cytoplasmic lipid accumulation is detected. Magnification: (A) x5000; (B): x10000.

Surprisingly, the transmission electron microscopy analysis revealed that induced DFs76 are actually capable of producing and accumulating intracellular lipids and in many cells their cytoplasm was found to be occupied by large lipid vacuoles (Fig. 3.3.3.3.). However, most of these cells presented damaged membranes (black arrows) and complete loss of their cytoplasmic structure (Fig 3.3.3.3.). Unexpectedly, cell nuclei (N) exhibited no signs of apoptosis, such as condensed or marginalized chromatin (Fig. 3.3.3.3.). The fact that cell membranes were found to be damaged may explain the finding of flow cytometry, which showed that fibroblasts from old donors were not able to produce lipids.

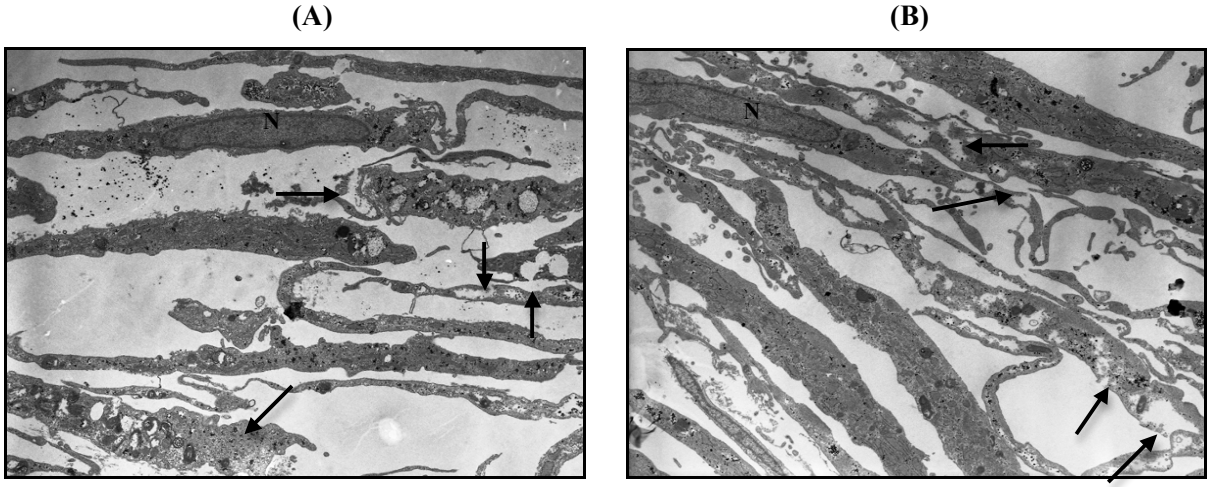

Fig. 3.3.3.3. Transmission electron microscopy of induced DFs76 on the 23rd day of the adipogenic treatment. Cells contain multiple lipid droplets as well as large lipid vacuoles. However, most of the induced DFs76 presented damaged membranes (black arrows) and complete loss of their cytoplasmic structure (Fig 3.3.3.3.). Cell nuclei (N) exhibited no signs of apoptosis, such as condensed or marginalized chromatin**.** Magnification: (A); (B): x5000.

3.4. Evaluation of the adipocyte lineage potential of dermal fibroblasts by means of gene expression analysis

Human dermal fibroblasts from different ages (30- and 76-year old donors) were induced towards an adipogenic phenotype. Subsequently, the gene expression profiles of these cells was compared to the profiles of control cells of the same age in order to identify differential gene expression by employing whole human genome oligo microarrays (Agilent Technologies). The effect of the adipogenic treatment on major signaling pathways of cell differentiation and adipogenesis was also evaluated. Moreover, in order to examine whether the induced cells expressed adipocyte-specific genes, their transcriptional phenotype was compared to the gene expression profiles of human adipocytes (Urs et al., 2004) and human

bone marrow-derived MSCs after adipogenic induction, as described in the literature (Sekiya et al., 2003). Furthermore, selected gene expression of key regulatory genes of adipogenesis and adipocytes was evaluated by qRT-PCR analysis.

3.4.1. RNA samples used for microarray analysis exhibited RIN values between 8.8 and 10

Quality control of the RNA samples used for the microarray analysis (DFs30K, DFs30B, DFs76K, DFs76B) via the Agilent 2100 Bioanalyzer platform (Agilent Technologies) showed high RNA quality with RIN values between 8.8 and 10 (Fig. 3.4.1.).

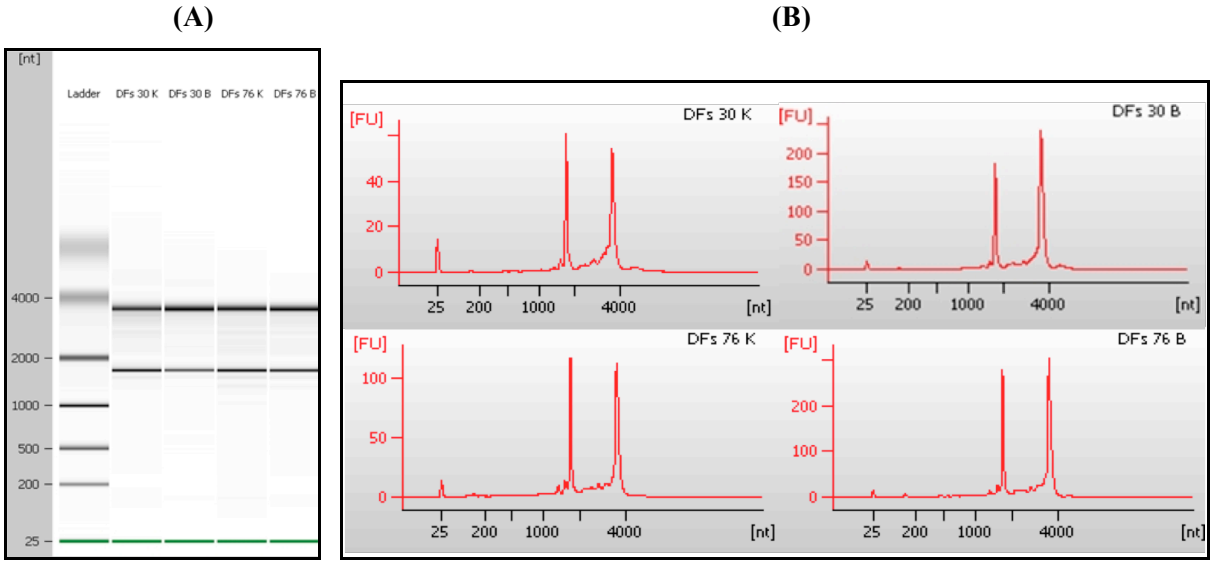

Fig. 3.4.1. Gel image (A) and electropherograms (B) of RNA quality check of total RNA samples. **(A)** The RNA molecular weight ladder is shown in the first lane, where the lowest migrating green band represents an internal standard. (B) The two peaks represent ribosomal RNA: left 18S and right 28S RNA. All RNA samples had RIN values between 8.8 and 10. Nt: nucleotides, FU: fluorescence.

3.4.2. Gene expression analysis of the adipogenic induced DFs30

3.4.2.1. Differentially regulated genes in induced DFs30 compared with control DFs30

Microarray analysis showed 9,308 differentially regulated genes, among them 4,722 significantly upregulated and 4,586 significantly downregulated ones, in induced DFs30 compared with control DFs30 (Fig. 3.4.2.1.).

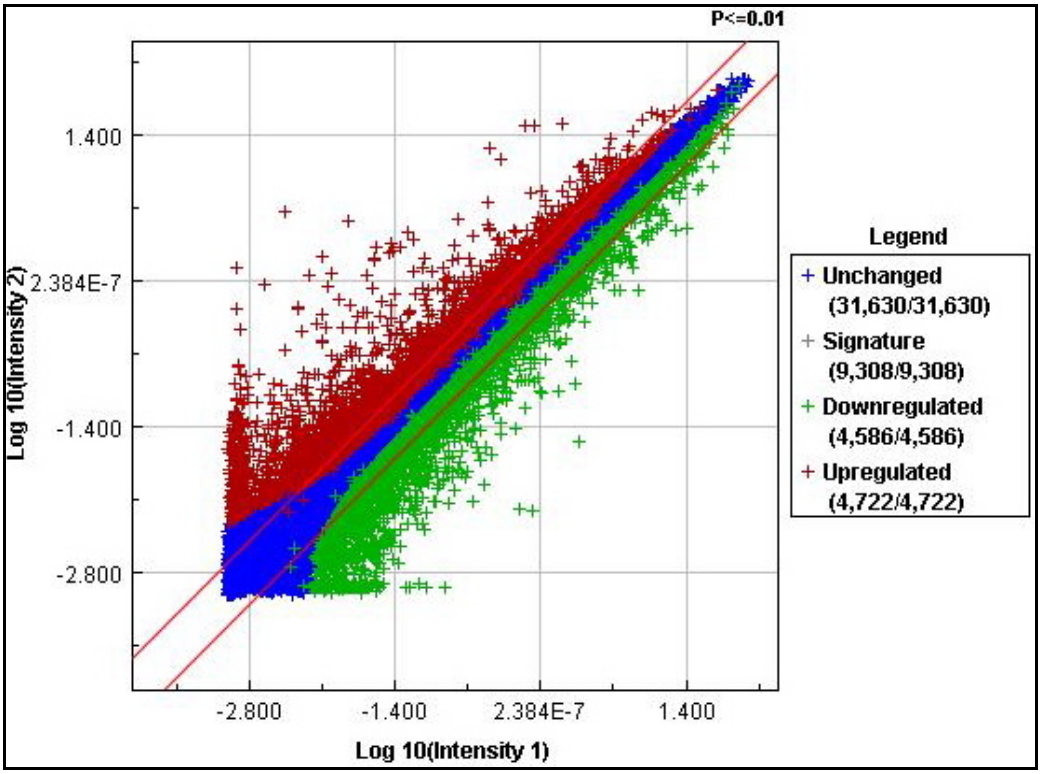

Figure 3.4.2.1. Scatter plot of signal intensities of all spots of induced DFs30 versus control DFs30 cells. The signal intensities of each feature represented by a dot are shown in double logarithmic scale. X-axis: control-log signal intensity; y-axis: sample-log signal intensity. Red diagonal lines define the areas of 2-fold differential signal intensities. Blue cross: unchanged genes. Red cross: significantly upregulated genes (p-value <0.01). Green cross: significantly downregulated genes (p-value <0.01). Grey cross (legend): summary of significantly up- and downregulated signatures.

3.4.2.2. Genes involved in cell differentiation and in lipid metabolism were significantly upregulated in induced DFs30

In the functional grouping analysis, significantly regulated genes were annotated with information from various databases in order to find common features among the genes sharing similar expression characteristics. The annotations used were derived from Gene Ontology (GO), which provides information on molecular function. Among the 4,722 significantly upregulated genes in the induced DFs30, 222 key genes were implicated in cell differentiation and 115 key genes in lipid metabolism (Fig. 3.4.2.2.). A large number of genes that regulate development (340), receptor signaling (328), cellular transportation (250), response to toxins (204), protein modification (193), cytoskeleton (184), cell cycle (158) and metabolism (155) were also found to be upregulated.

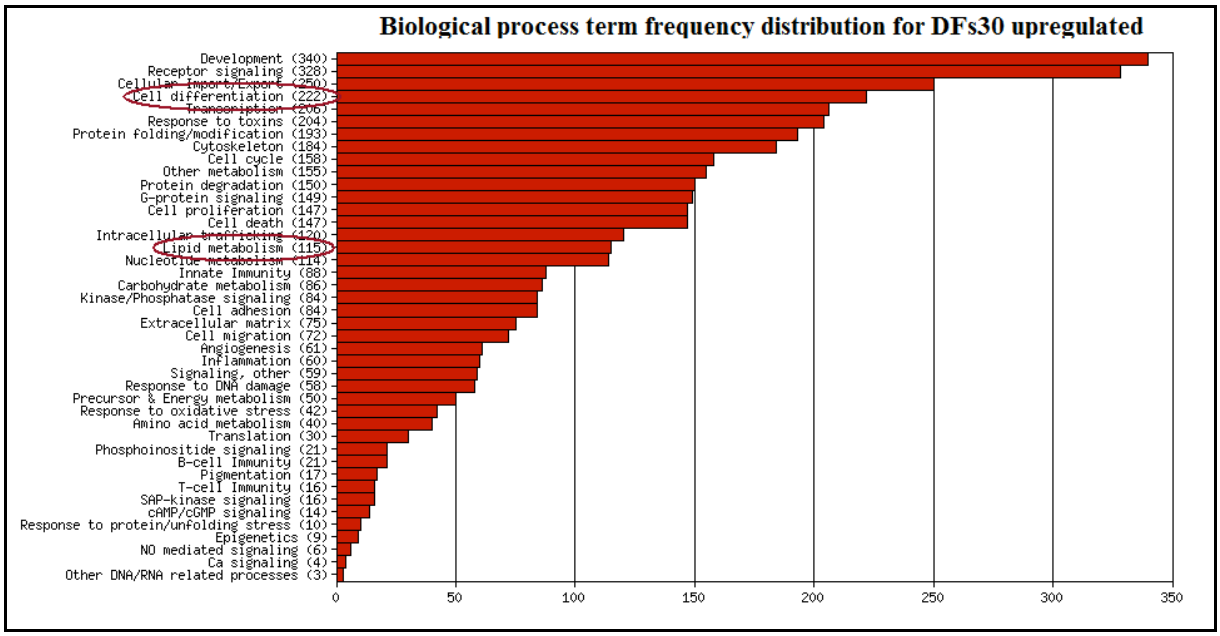

Fig. 3.4.2.2. Functional grouping analysis of at least two-fold upregulated genes. Frequency of upregulated genes in induced DFs30 compared with control DFs30 in categories describing "biological processes". 222 genes implicated in cell differentiation and 115 genes implicated in lipid metabolism were found to be significantly upregulated (red circles).

Master regulating adipogenic transcription factors were significantly upregulated in adipogenic induced DFs30, such as the PPARγ, PPARγ co-activator-1α, c-Fos and FoxO1. However, none of the subunits of the major adipogenic regulators C/EBPs could be identified. Furthermore, genes with a key role in lipid metabolism, such as lipogenesis [LPL, stearoyl-CoA desaturase (SCD)] were overexpressed. Moreover, secreted proteins regulating cell metabolism during adipogenesis were also upregulated (apolipoproteins B and D, retinol binding protein). Leptin, leptin receptor, low-density lipoprotein receptor and phospholipase family genes that are expressed in mature adipocytes were upregulated, too. Genes important in lipid metabolism that showed a significant upregulation in the induced DFs30 are shown in Table 9. Statistical significance was reached for every gene with p-values <0.05.

Table 9. Selection of significantly upregulated genes (more than two-fold) implicated in lipid metabolism in adipogenic induced DFs30 compared with control DFs30 and their fold changes.

Gene symbol	Gene description	Fold changes	Gene symbol	Gene description	Fold changes
ABCD2	ATP-binding cassette, D2	6.7	INSIG1	insulin induced gene 1	2.2
ACOT7	acyl-CoA thioesterase 7	2.8	LDLR	low density lipoprotein receptor	3.2
ACSBG1	acyl-CoA synth bubblegum 1	3.1	LEP	leptin	56
ACSL1	acyl-CoA synth long-chain 1	3.1	LEPR	leptin receptor	3.2
ACSM5	acyl-CoA synth medium-chain 5	21.6	LPL	lipoprotein lipase	8.2
ADH4	alcohol dehydrogenase 4	4	LRP8	apolipoprotein e receptor	4
AJ710526	sorbin and SH3 domain1	4.8	MCAT	ACP acyltransferase	3
ALOX12	arachidonate 12-lipoxygenase	6.1	MLXIPL	MLX interacting protein-like	5.6
ALOX15B	arachidonate 15-lipoxygenase,B	17	NPHP3	nephronophthisis 3	2.1
ALOX5AP	arachidonate 5-lipoxyg-activ.prot.	4	OLAH	oleoyl-ACP hydrolase	6.9
APOB	apolipoprotein B	24.2	P2RX7	purinergic receptor P2X,7	2.7
APOB48R	apolipoprotein B48 receptor	5	PCSK9	propr. convertase subtilisin/kexin9	6.5
APOD	apolipoprotein D	8.2	PIGL	phosphatidylinosit glycan anchor biosynth.	2.1
ARV1	ARV1 homolog	5.2	PIK3R1	phosphoinositide-3-kinase, 1	4.7
ASAH2	N-acylsphingosine amidohydrolase	3.6	PLA2G2A	phospholipase A2, group IIA	4.2
B3GNT5	b-1,3-N-acetylglucosaminyltransf.5	27.9	PLA2G5	phospholipase A2, group V	2.2
CAV1	caveolin 1	2.3	PLB1	phospholipase B1	5.6
CAV3	caveolin 3	2.7	PLCL2	phospholipase C-like 2	2.3
CPNE3	copine III	2.1	PLCXD1	spec. phospholip. C, X dom1	3.6
CPNE7	copine VII	2.9	PLCXD3	spec. phospholip. C, X dom 3	4.7
CRYL1	crystalline, lambda 1	2.9	PLP1	proteolipid protein 1	11
CYP19A1	cytochrome P450, family 19, A1	23.7	PLTP	phospholipid transfer protein	2.7
CYP1A1	cytochrome P450, family 1,A1	3.1	PPARγ	peroxis.prolif-activated recept.γ	25.6
CYP27A1	cytochrome P450, family 27, A1	2.2	PPARγC1A	PPARG coactivator 1 alpha	8.9
CYP39A1	cytochrome P450, family 39,A1	3.9	PRKAA2	protein kinase, AMP-activated, α2	2.1
CYP7A1	cytochrome P450, family 7, A1	11.7	PTEN	phosphatase and tensin homolog	2.1
CYP7B1	cytochrome P450, family 7, B1	2.9	PTGDS	prostaglandin D2 synthase	2.8
DGAT2	diacylglycerol O-acyltransferase2	5	PTGS1	prostaglandin-endoperoxide synthase 1	10.5
DHCR24	24-dehydrocholesterol reductase	9.4	RBL1	retinoblastoma-like 1	6.1
EBPL	emopamil binding protein-like	2.6	RBP4	retinol binding protein 4	12.5
ELOVL3	elongation of very long chain fatty acids	4.8	SCD5	stearoyl-CoA desaturase 5	2.6
ELOVL6	ELOVL family member 6	2.4	SEC14L2	SEC14-like 2	2.4
ENPP2	ectonucl. pyrophosph/phosphodiest2	4.4	SERPINA3	serpin peptidase inhibitor, clade A 3	4.2
ENST00000319406	lysocardiolipin acyltransferase 1	4.5	SIRT1	sirtuin 1	2.1
ETNK2	ethanolamine kinase 2	2.4	SORBS1	sorbin and SH3 domain containing 1	24.2
FABP5	fatty acid binding protein 5	7.9	SQLE	squalene epoxidase	2.2
GAL	galanin prepropeptide	7	SRD5A3	steroid 5 alpha-reductase 3	2.6
GDPD4	glycerophosphodiest. phosphodiest.4	15.5	ST8SIA5	ST8 -sialyltransferase 5	3.1
GGT5	gamma-glutamyltransferase 5	3.4	STAR	steroidogenic acute regulatory protein	5.1
GM2A	GM2 ganglioside activator	3.1	SULT1B1	sulfotransferase family, 1B, member 1	28.7
HADH	hydroxyacyl-CoA dehydrogenase	2.9	SULT1E1	sulfotransferase family 1E, member 1	14.7
HADHA	hydroxyacyl-CoA dehydrogenase	2.1	TBXAS1	thromboxane A synthase 1	13.2
HNF1A	HNF1 homeobox A	7.7	UGT2B17	UDP glucuronosyltransferase 2, B17	2.1
HSD11B1	hydroxysteroid (11b) dehydrogenase 1	2.2	UGT2B7	UDP glucuronosyltransferase 2, B7	4.4
HSD11B2	hydroxysteroid (11b) dehydrogenase 2	4.5			

3.4.2.3. Major signaling pathways of cell differentiation and adipogenesis were significantly regulated in adipogenic induced DFs30 compared with control DFs30

In addition, various resources for information on involvement in biological signaling pathways were employed. Major pathways that play a crucial role in the cell differentiation process and adipogenesis, such as the insulin receptor, TGF-β, Wnt, Notch, hedgehog, phosphoinositide, FGF, Notch, BMP and steroid receptor signaling pathways were found to be significantly regulated (Table 10). Key regulatory genes exhibited expression differences in the DFs30 adipogenic induced fibroblasts when compared to control cells and an analytical presentation of the fold changes in key genes for each pathway is shown in Table 10. The highest fold change (100) in DFs30 induced cells compared with control fibroblasts was observed in the phosphoinositide signaling pathway and in the gene coding the endothelin receptor type B (EDNRB), whereas the lowest (-100) in the gene wingless-type family member 4 (WNT4; FGF and Wnt signaling pathways) and the gene fibroblast growth factor 18 (FGF18; FGF pathway).

Table 10. Differential regulation of signaling pathways in adipogenic induced DFs30 compared with control DFs30. In each pathway significantly regulated genes are presented with the corresponding fold changes (more than two-fold). Grey font: downregulated genes; Black font: upregulated genes.

Gene symbol	Gene description	Fold changes	Gene symbol	Gene description	Fold changes
	Insulin receptor signaling			**TGFbeta signaling**	
GAB1	GRB2-associated binding prot. 1	-2.3	ACVR2A	activin A receptor, type IIA	-2.1
IGF1R	insulin-like growth factor 1 recept.	-3.8	BAMBI	BMP membr.-bound inhib.	-5
IGF2	insulin-like growth factor 2	-2.3	BMPER	BMP bind. endothelial regul.	-2.3
IL1B	interleukin 1, beta	-7.8	CCL2	chemokine ligand 2	-2.3
PTPRE	prot. tyrosine phosphatase, recept. E	-6.8	FOXD1	forkhead box D1	-3
ENPP1	ectonucl.pyrophosph./phosphodiest.1	4.6	GDF10	growth different. factor 10	-16.4
FOXO1	forkhead box O1	5	GDF6	growth different. factor 6	-2.4
IGF1	insulin-like growth factor 1	2.4	HPGD	hydroxyprostagl. Dehydrog.15	-5.5
IGFBP3	insulin-like growth fact.2 bind.prot.3	2	ITGA8	integrin, alpha 8	-6.2
PHIP	pleckstrin homology interacting prot.	7.4	PDGFA	platelet-derived growth factor a	-2.5
PI3KR1	phosphoinositide-3-kinase, reg. unit1	4.7	PTPRK	prot. tyrosine phosph.recept.K	-2.4
SORBS1	sorbin and SH3 domain containing 1	24.2	SMAD1	SMAD family member 1	-2.1
	Wnt pathway		SMAD2	SMAD family member 2	-3.4
CDH1	cadherin 1, type 1, E-cadherin	-2.3	TGFβ3	transforming growth factor β3	-2
EP300	E1A binding protein p300	-3.1	THBS1	thrombospondin 1	-2.4
FZD7	frizzled homolog 7 (Drosophila)	-2.8	ASPN	asporin	2.5
TCF7L2	lymphoid enhancer-binding factor 1	-2.7	BMP4	bone morphogenetic protein 4	2.6
WNT2	wingless-type family member 2	-27.1	FNTA	farnesyltransferase, a	2.5

WNT3	wingless-type family member 3	-2.2
WNT4	wingless-type family member 4	-100
BARX1	BARX homeobox 1	6.6
DKK1	dickkopf homolog 1	8.6
FRZB	frizzled-related protein	2.6
HNF1A	HNF1 homeobox A	7.7
RSPO1	R-spondin homolog	2
RUNX2	runt-related transcription factor 2	7
SOX17	sex determining region Y-box 17	14
WISP1	WNT1 inducible signal. Path. prot.1	2
WNT16	wingless-type family member 16	9.3
	Phosphoinositide signaling	
AGT	angiotensinogen	-2.9
DRD1	dopamine receptor D1	-16
HTR2A	5-hydroxytryptamine receptor 2A	-2.2
IGF1R	insulin-like growth factor 1 recept.	-3.8
AURKA	aurora kinase A	3.1
BUB1B	budd. uninhibit. by benzimid.1b	2.6
EDNRA	endothelin receptor type A	2.5
EDNRB	endothelin receptor type B	100
HMGB2	high-mobility group box 2	2
IGF1	insulin-like growth factor 1	2.5
LTB4R	leukotriene B4 receptor	2.2
NDC80	kinetochore complex component	2
NPR3	atrionatriuretic peptide receptor C	3.1
P2RY6	pyrimidinergic receptor P2Y6	4.8
SPAG5	sperm associated antigen 5	4.1
TGM2	transglutaminase 2	3
TOP2A	topoisomerase (DNA) II alpha	3.5
UBE2C	ubiquitin-conjugating enzyme E2C	4.5
	BMP signaling	
ACVR2A	activin A receptor, type IIA	-2.1
BMPER	BMP binding endothelial regulator	-2.3
FOXD1	forkhead box D1	-3
FST	follistatin	-2.1
GDF6	growth differentiation factor 6	-2.4
MSX2	msh homeobox 2	-2.1
SMAD1	SMAD family member 1	-2.1
ZNF8	zinc finger protein 8	-2.1
ACVRL1	activin A receptor type II-like 1	2.4
BMP4	bone morphogenetic protein 4	2.6
CHRDL1	chordin-like 1	62.3
GPC3	glypican 3	16
HIPK2	homeodomain interact. prot.kinase 2	3.7
HOXA13	homeobox A13	4.6
ID1	inhibitor of DNA binding 1	5.3
NOG	noggin	2.4
ZFYVE16	zinc finger, FYVE domain 16	9.1
FOS	FBJ mur. Osteos. viral oncog.	2.6
GDF5	growth differentiation factor 5	5.9
GPC3	glypican 3	16
HIPK2	homeodom.interact.prot.kin.2	3.7
HOXA13	homeobox A13	4.6
ID1	inhibitor of DNA binding 1	5.3
ING2	inhibitor of growth family 2	2.8
NOG	noggin	2.4
PEG10	paternally expressed 10	6
TTK	TTK protein kinase	2.2
	Notch signaling	
DTX4	deltex homolog 4	-3.8
FOXC1	forkhead box C1	-3.1
HES1	hairy and enhancer of split 1	-3
NRG1	neuregulin 1	-12.5
TP63	tumor protein p63	-5.2
CFD	complement factor D (adipsin)	4.5
DLL1	delta-like 1	2.5
DNER	delta/notch-like EGF repeat	14.8
HEY1	hairy/enhancer-of-split	2.7
	FGF signaling	
CTGF	connective tissue growth factor	-3.7
FGF18	fibroblast growth factor 18	-100
FGF2	fibroblast growth factor 2	-2.5
FGF9	fibroblast growth factor 9	-30.4
FGFR2	fibroblast growth factor receptor 2	-2.7
NDST1	N-deacetylase/N-sulfotransferase 1	-2.3
THBS1	thrombospondin 1	-2.1
WNT4	wingless-type family, member 4	-100
FGF12	fibroblast growth factor 12	5.3
FGFR1	fibroblast growth factor receptor 1	3.4
RUNX2	runt-related transcription factor 2	7
	Steroid receptor signaling	
DNAJA1	DnaJ (Hsp40) homolog, A1	-2.2
FHL2	four and a half LIM domains 2	-4.6
MED13	mediator complex subunit 13	-2.1
MLL2	mixed-lineage leukemia 2	-2.2
AR	androgen receptor	15.9
IGF1	insulin-like growth factor 1	2.5
KLF9	Kruppel-like factor 9	2.2
PGR	progesterone receptor	7.7
PIAS2	prot. inhibitor of activ. STAT2	2.1
PPARγC1A	PPARγ, coactivator 1 a	8.9
	Hedgehog signaling pathway	
CREBBP	CREB binding protein	-2
GLI1	GLI family zinc finger 1	-5.6
CCNB1	cyclin B1	2.8
CDC2	cyclin-dependent kinase 1	2.1

PPAR signaling pathway

The essential transcription factor of adipogenesis, the peroxisome proliferator-activated receptor γ (PPARγ) was found to be significantly upregulated in our induced DFs30. Furthermore, a considerable amount of target genes of the PPARγ signaling pathway, such as the LPL, CAP, ACS, were identified to be significantly upregulated. Isoforms of the FABP ligands also exhibited a differential expression (Fig. 3.4.2.3.).

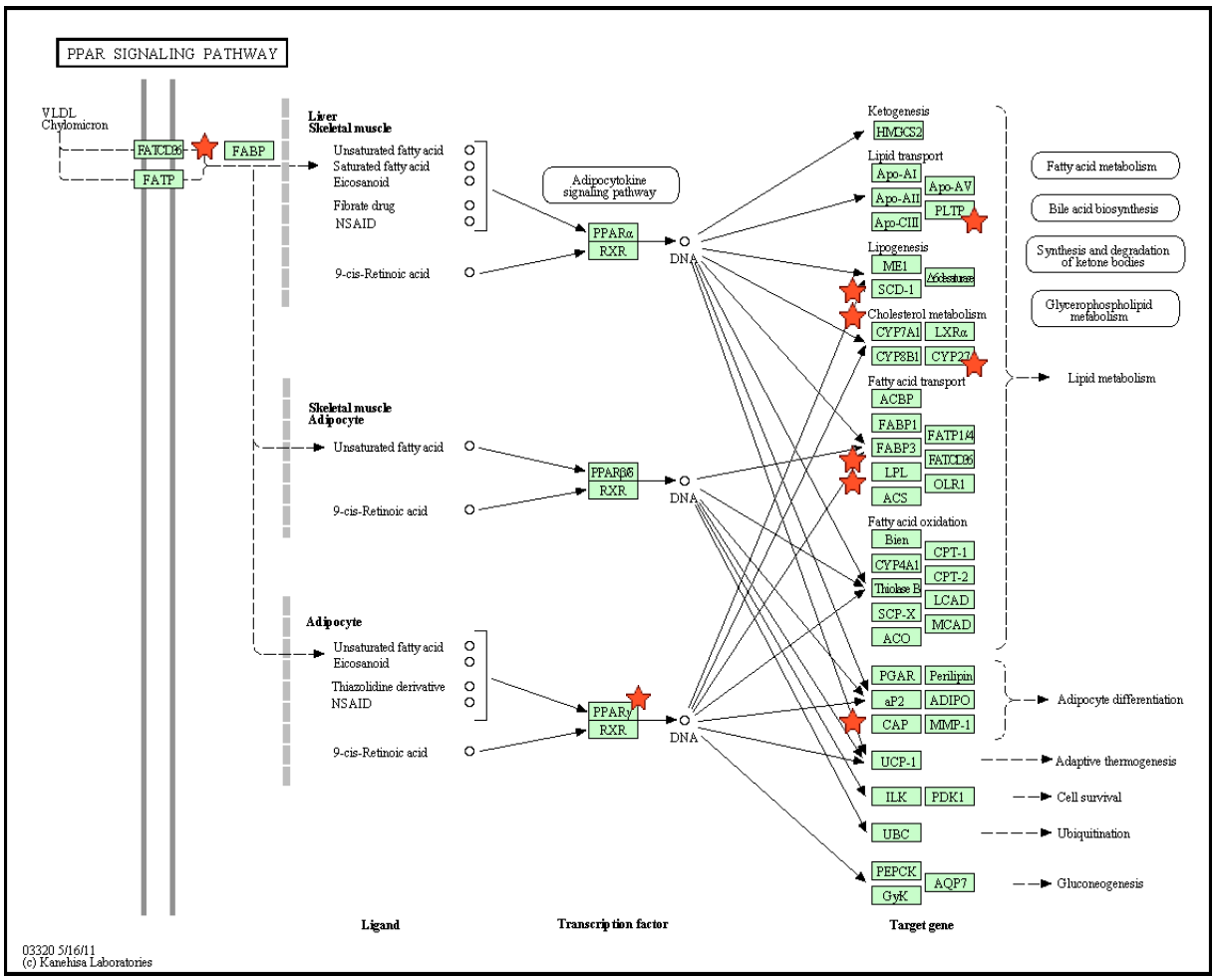

Fig. 3.4.2.3. The KEGG-pathway shows genes that are upregulated (red asterisk) in the PPAR signaling pathway in the adipogenic induced DFs30.

3.4.2.4. Comparison of the transcription profiles of adipogenic induced DFs30 versus human adipocytes and adipocytes deriving from differentiated MSCs

In order to examine whether our induced cells expressed adipocyte-specific genes, their transcriptional phenotype was compared with that of normal human adipocytes (Table 11a) deriving from the subcutaneous abdominal fat from healthy women, as this has been

described in the literature (Urs et al., 2004). A second comparison was conducted with the gene expression profile of adipocytes deriving after adipogenic induction of human bone marrow-derived MSCs (Table 11b) as described by Sekiya et al., in 2003 (Sekiya et al., 2003).

Adipogenic induced DFs30 vs. human adipocytes (Table 11a)

Urs et al. (2004) performed a study on gene expression profiling in human adipocytes using microarray technology and they provided novel markers for the characterisation of human adipocytes. In total, 77 genes involved in metabolism/transport, transcription factors and binding proteins, signaling molecules and cellular matrix proteins were reported to be overexpressed in human adipocytes. Our results were compared one-to-one to the reported genes (Table 11a). 19 genes out of the 77 were found to be significantly regulated in the adipogenic induced DFs30, approximately 25% of the adipocyte markers reported by Urs et al. (2004). Among them, only 4 genes (AGT, PTPN21, CAP2, ECM2) showed a negative regulation, which was not in accordance with the data of Urs et al. (2004). However, the overexpression of these genes was reported as non-significant by the authors. Furthermore, in several cases we found a significant upregulation not of those genes that Urs et al. (2004) have reported as adipocyte markers, but of other members of the same superfamily. For example, phospholipase CD1 was overexpressed in human adipocytes but not in the induced DFs30. However, several other members of the superfamily of phospholipases (PLCL2, PLCXD1, PLCXD3) were significantly upregulated and therefore were included in Table 11a (in bold). In addition to apolipoprotein B that was overexpressed both in human adipocytes and the induced DFs30, we also found a significant upregulation of further apolipoproteins in our cells (APOD, APOB48R- in bold). The majority of genes sharing the same overexpression in human adipocytes and induced DFs30 belonged to the group of genes involved in metabolism and transport. Major transcription factors of adipogenesis were upregulated in the induced DFs30, such as PPARγ and IGFBP2, however we could not identify an upregulation of the factor C/EBPD. IGF2BP1 and IGF1 (in bold) were also upregulated in the induced DFs30 but not in human adipocytes. The transcription activator of the c-fos promoter was not regulated in induced DFs30, in contrast to human adipocytes, however c-FOS was significantly upregulated in induced DFs30 (in bold). Glutathione peroxidase 3, which was overexpressed in both adipocytes and induced DFs30, was 100-fold upregulated in the DFs30. Table 11a provides an overview of the comparison of the transcription profile of human adipocytes versus the adipogenic induced DFs30 and DFs76.

Table 11a. Transcriptional profile of induced DFs30/DFs76 vs. human adipocytes. All genes included, except for those in bold, were reported as markers of human adipocytes (Urs et al., 2004). Genes in bold represent genes that were significantly upregulated in the induced DFs30 and not in human adipocytes, but are either members of the same superfamily as the reported genes or are known to play a role in adipogenesis. Fold changes refer to untreated control fibroblasts of the corresponding age group and for every gene a p-value<0.05 was considered statistically significant. NE stands for no expression, where no significant regulation was observed.

Gene Symbol	Gene description	Expression in induced DFs30	Expression in induced DFs76
	Metabolism and transport	(fold changes to control cells)	
FABP4	Fatty acid binding protein 4	NE	NE
FABP5	Fatty acid binding protein 5	7.9	NE
FABP7	Fatty acid binding protein 7	NE	NE
LBP	Lipopolysaccharide binding protein	NE	NE
LPL	Lipoprotein lipase	8.2	12.2
LYPLA1	Lysophospholipase 1	NE	NE
FACL2	Fatty acid CoA ligase	NE	NE
APM1	Adipose most abundant transcript 1	NE	NE
PLIN	Perilipin	NE	NE
SCD	Stearoyl CoA desaturase	2.6	2.3
ADFP	Adipose differentiation-related protein	NE	NE
AGT	Angiotensinogen	-2.9	NE
VN	Vitronectin	NE	NE
UCP4	Uncoupling protein 4	NE	NE
PLCD1	Phospholipase C D1	NE	NE
PLCL2	**Phospholipase C-like 2**	**2.3**	**NE**
PLCXD1	**Specific phospholipase C, X1**	**3.6**	**NE**
PLCXD3	**Specific phospholipase C, X3**	**4.7**	**NE**
GPD1	Glycerol 3 phosphate dehydrogenase 1	2.2	-4.3
ALDH6A1	Aldehyde dehydrogenase 6	2.1	NE
ALDH1A2	Aldehyde dehydrogenase	NE	NE
ACOX3	Acyl CoA oxidase 3	NE	NE
LIPC	Lipase, hepatic	NE	NE
LIPE	Lipase, hormone sensitive	NE	NE
PFKFB3	6-Phosphofructo-2-kinase 3	NE	3.1
PFKFB4	**6-Phosphofructo-2-kinase 4**	**2.1**	**NE**
APOB	Apolipoprotein B	24.2	NE
APOD	**Apolipoprotein D**	**8.2**	**7.7**
APOB48R	**Apolipoprotein B receptor**	**5.0**	**NE**
DGAT1	Diacylglycerol O-acyltransferase 1	5.0	NE
LRP8	LDL receptor 8	4.0	NE
DGKG	Diacylglycerol kinase γ	NE	NE
ATP8A2	ATPase, aminophospholipid transporter	NE	NE
ATP2B2	ATPase-Ca2 transporting plasma membrane	NE	NE
CTSG	Cathepsin G	11.0	NE
HSD11B2	Hydroxysteroid (11-B) dehydrogenase 2	4.5	NE
HSD11B1	**Hydroxysteroid (11-B) dehydrogenase 1**	**2.2**	**NE**
GPX3	Glutathione peroxidase 3	100.0	NE
MASP1	Mannan-binding lectin serine protease 1	NE	-2
CHST1	Carbohydrate sulfotransferase 1	NE	NE

CHST2	**Carbohydrate sulfotransferase 2**	**2.4**	**2.2**
CHST4	**Carbohydrate sulfotransferase 4**	**23.1**	**4.4**
CHST6	**Carbohydrate sulfotransferase 6**	**2.1**	**NE**
CHST7	**Carbohydrate sulfotransferase 7**	**2.1**	**2.2**
GLUL	Glutamine synthase	32.8	3.8
CYB5	Cytochrome b-5	NE	3.6
MGST1	Microsomal glutathione S-transferase	NE	NE
AMT	Aminomethyltransferase	NE	NE
USP8	Ubiquitin specific protease 2	NE	NE
CRYAB	Crystalline, αB	NE	NE
TAP1	Transporter 1, ATP binding cassette	NE	NE
KCNH2	K voltage-gated channel subfamily 11	NE	NE
FXYD1	FXYD domain containing ion transport regulator 1	NE	NE
PLEK	Pleckstrin	NE	NE
SPTBN4	Spectrin	NE	NE
ABCE1	ATP-binding cassette, subfamily E	NE	NE
	Transcription factors and binding proteins		
TFCP2	Transcription factor CP2	NE	NE
PPARγ	PPAR γ	25.6	4.8
PPARγC1A	**PPARγ coactivator 1a**	**8.9**	**6.8**
RXRA	Retinoid X receptor A	NE	NE
RXRB	Retinoid X receptor B	NE	NE
TNFAIP2	Tumor necrosis factor-α interacting protein 2	NE	4.9
REQ	Requiem	NE	NE
E2F5	E2F transcription factor 5	NE	NE
E2F1	E2F transcription factor 1	NE	NE
E2F2	**E2F transcription factor 2**	**2.1**	**NE**
C/EBPD	C/EBPδ	NE	3.2
IGFBP2	Insulin-like growth factor binding protein 2	4.9	3.9
IGFBP3	**Insulin-like growth factor binding protein 3**	**-3.5**	**NE**
IGF2BP1	**Insulin-like growth factor 2 binding protein12**	**2.2**	**NE**
IGF1	**Insulin-like growth factor 1**	**2.5**	**NE**
IGFBP7	**Insulin-like growth factor binding protein 7**	**NE**	**3.4**
CROC4	Transcription activator of the c-fos promoter	NE	NE
FOS	**FBJ osteosarcoma oncogene**	**2.6**	**8.2**
GDF8	Growth differentiation factor 8	NE	NE
ZNF336	Zinc finger protein 336	NE	NE
STAT5B	Signal transducer and activator of transcription 5B	NE	NE
SMARCB1	SWI/SNF complex	NE	NE
	Signaling molecules		
PTPRS	Protein tyrosine phosphatase receptor S	NE	NE
PTPRZ1	Protein tyrosine phosphatase receptor Z1	NE	NE
PTPN21	Protein tyrosine phosphatase N21	-2.2	NE
INSR	Insulin like receptor	NE	NE
ADORA2B	Adenosine receptor 2B	NE	NE
AGTRL1	Angiotensin receptor L1	NE	NE
ATIP1	AT2 receptor interacting protein 1	NE	NE
SCAP1	Src family associated phosphoprotein 1	NE	NE
IL22R	Interleukin 22 receptor	3.0	NE
IL22	**Interleukin 22**	**30.7**	**NE**
3-PAP	3-phosphatase adapter protein	NE	NE
MAP4K3	Mitogen-activated protein kinase kinase 3	NE	NE

CAP2	Adenylyl cyclase associated protein 2	-2.5	NE
	Cellular matrix and cytoskeleton		
COL1A2	Collagen type 1A2	NE	3.5
MMP7	Matrix metalloprotein 7	NE	18.54
ECM2	Extracellular matrix protein 2	-2.6	NE
DPT	Dermatopontin	NE	3

Adipogenic induced DFs30 vs. adipocytes from differentiated human MSCs

Sekiya et al. (2003) assayed gene expression during and at the end-point of adipogenesis of human MSCs and reported increases in expression of 65 genes, which were proposed as markers of adipogenesis. Our results were compared one-to-one with the reported genes (Table 11b). 43 out of the 65 proposed genes were regulated in the induced DFs30, approximately 66% of the reported markers of adipocytes deriving from adipogenic differentiated MSCs. Among them, 7 genes (CHI3L1, PCK1, IBSP, CXCL1, NPTX1, TGF-β, IGF2) showed a negative regulation, which is not consistent with the data of Sekiya et al (2003). Although NPTX1 showed an opposite regulation than expected, NPTX2 was found significantly upregulated and exhibited the most abundant upregulation among all differentially expressed genes (100 fold). NPTX2 was not differentially expressed in the work of Sekiya et al. (2003).

In certain cases we found a significant upregulation not of the gene that Sekiya et al. (2003) have reported, but of another member of the same superfamily. For example, apolipoprotein E was overexpressed in the work of Sekiya et al. (2003) but not in the induced DFs30. However, several members of the apolipoproteins (APOB, APOB48R, APOBEC3B, APOD) were significantly upregulated in DFs30 and therefore were included in Table 11b (bold).

Major transcription factors of adipogenesis were upregulated in common in differentiated MSCs and DFs30, such as the PPARγ, FoxO1, c-FOS and ZBTB16, however the transcription factor C/EBPD was not differentially expressed. The coactivator of the PPARγ, PPARγC1α (in bold) was also overexpressed.

Table 11b provides an overview of the comparison of the transcription profile of adipocytes deriving after adipogenic differentiation of human bone marrow MSCs versus the adipogenic induced DFs30 and DFs76.

Table 11b. Transcriptional profile of induced DFs30/DFs76 vs. adipocytes deriving from adipogenic differentiated human MSCs. All genes included, except for those in bold, were reported as markers of adipogenic induced MSCs (Sekiya et al., 2003). Genes in bold represent genes that were significantly upregulated in the induced DFs30 and not differentiated MSCs, but are either members of the same superfamily as the reported genes or are known to play a role in adipogenesis. Fold changes refer to untreated control fibroblasts of the corresponding age group and for every gene a p-value<0.05 was considered statistically significant . NE stands for no expression, where no significant regulation was observed.

Gene symbol	Gene description	Expression in induced DFs30	Expression in induced DFs76
	Metabolism/enzymes	(fold changes to control cells)	
ADH1B	alcohol dehydrogenase 1B	44.0	NE
ADH1C	alcohol dehydrogenase 1C	51.9	5.7
ADH1A	alcohol dehydrogenase 1A	NE	33.8
CHI3L1	chitinase 3-like 1	-7.3	NE
CHST2	carbohydrate sulfotransferase 2	NE	2.2
CHST4	**carbohydrate sulfotransferase 4**	**23.1**	**NE**
GCHFR	GTP cyclohydrolase I feedback regul.	2.0	NE
HAS1	hyaluronan synthase 1	4.4	3.8
HSD11B1	hydroxysteroid (11-b) dehydrogenase 1	2.2	-2.1
HSD11B2	hydroxysteroid (11-b) dehydrogenase 2	4.5	NE
IMPA2	inositol(myo)-1-monophosphatase 2	2.3	NE
LPL	lipoprotein lipase	8.2	12.2
MAOA	monoamine oxidase A	21.2	11.8
PCK1	phosphoenolpyruvate carboxykinase 1	-2.0	NE
PLA2G2A	phospholipase A2, group IIA	4.2	NE
PLA2G5	phospholipase A2, group V	2.2	NE
SCD5	stearoyl-CoA desaturase 5	2.6	2.3
TIMP4	TIMP metallopeptidase inhibitor 4	94.2	14.7
	Signaling genes		
IL18R1	interleukin 18 receptor 1	9.2	7.1
	Cell cycle genes		
G0S2	G0/G1switch 2	2.9	NE
	Extracellular matrix protein		
COL11A1	collagen, type XI, alpha 1	2.1	2.3
COMP	cartilage oligomeric matrix protein	2.2	7.2
IBSP	integrin binding sialoprotein	-12.2	NE
	Transcription genes		
c-FOS	FBJ osteosarcoma oncogene	2.6	8.2
FOXO1	forkhead box O1	5.0	4.1
PPARγ	peroxisome proliferator-activ. receptor γ	25.6	4.8
PPARγC1α	PPARγ, coactivator 1α	8.9	6.8
ZBTB16	zinc finger and BTB domain 16	40.6	NE
	Secreted genes		
ANGPT1	angiopoietin 1	2.5	2.4
APOB	**apolipoprotein B**	**24.2**	**NE**
APOB48R	**apolipoprotein B receptor**	**5.0**	**NE**
APOBEC3B	**apolipoprotein B editing enzyme,3B**	**2.0**	**NE**
APOD	**apolipoprotein D**	**8.2**	**7.4**

CRLF1	cytokine receptor-like factor 1	19.0	20.7
CXCL1	melanoma growth stimulating activity a	-2.2	NE
FABP5	fatty acid binding protein 5	7.9	NE
IGF1	insulin-like growth factor 1	2.5	7.8
IGF2	insulin-like growth factor 2	-3.7	3.6
IGF2BP3	**insulin-like growth factor2 bind. prot.3**	**2.1**	**NE**
IGFBP7	**insulin-like growth factor bind. prot.7**	**NE**	**3.4**
IGFBP2	insulin-like growth factor bind. prot.2	4.9	NE
NPTX1	neuronal pentraxin I	-3.2	NE
NPTX2	**neuronal pentraxin II**	**100.0**	**NE**
RBP4	retinol binding protein 4, plasma	12.5	NE
SERPINF2	serpin peptidase inhibitor, clade F, 2	10.1	NE
SPARCL1	SPARC-like 1 (hevin)	NE	6.7
TGF-β	transforming growth factor β3	-2.0	NE
	Other genes		
ACTG2	actin, gamma 2, smooth muscle, enteric	5.7	NE
AOC3	amine oxidase, copper containing 3	2.0	NE
CACNB2	calcium channel, voltage-dependent, b2	13.5	7.1
PTK2B	protein tyrosine kinase 2 beta	9.9	NE
PPL	periplakin	NE	4.2
HP	haptoglobin	7.8	NE
SAA1	serum amyloid A1	34.6	100.0

3.4.3. Gene expression analysis of the induced DFs76

3.4.3.1. Expression of differentially regulated genes in induced DFs76 compared with control DFs76

Microarray analysis showed 4,786 differentially regulated genes, among them 2,235 significantly upregulated and 2,551 significantly downregulated genes in induced DFs76 compared with control DFs76, whereas 36,109 genes remained unchanged (Fig. 3.4.3.1.).

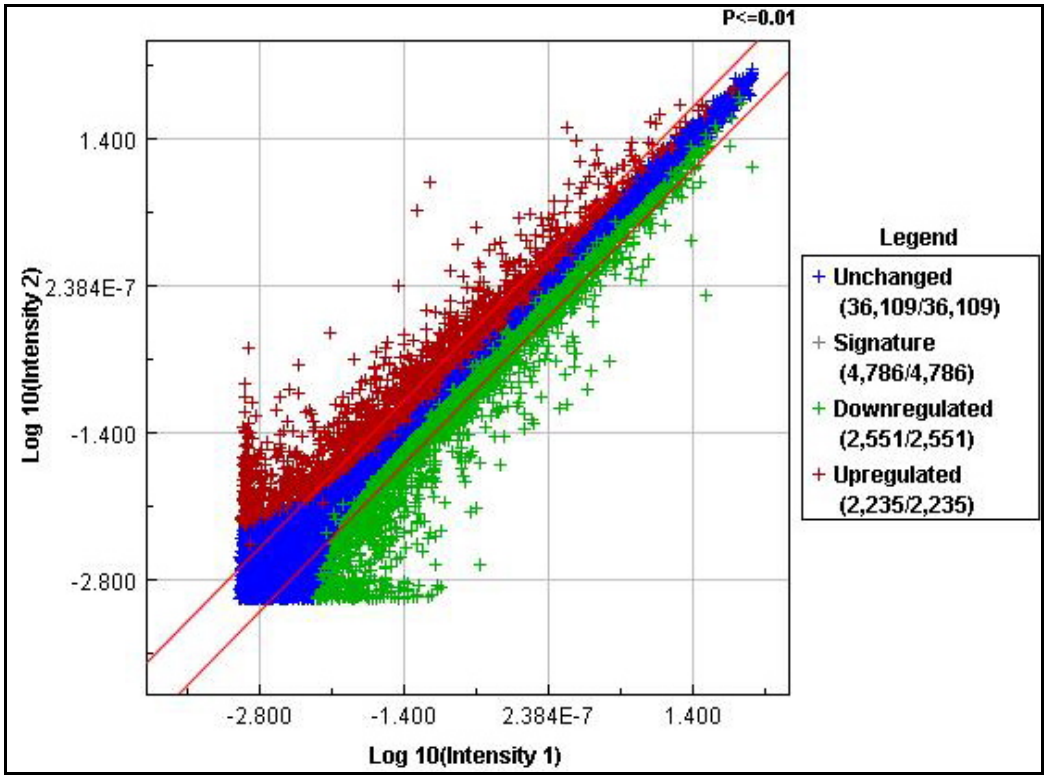

Figure 3.4.3.1. Scatter plot of signal intensities of all spots of induced DFs76 versus control DFs76 cells. The signal intensities of each feature represented by a dot are shown in double logarithmic scale. X-axis: control-log signal intensity; y-axis: sample-log signal intensity. Red diagonal lines define the areas of 2-fold differential signal intensities. Blue cross: unchanged genes. Red cross: significantly upregulated genes (p-value <0.01). Green cross: significantly downregulated genes (p-value <0.01). Grey cross (legend): summary of significantly up- and downregulated signatures.

3.4.3.2. Genes involved in cell differentiation and lipid metabolism were significantly upregulated in induced DFs76

In the functional grouping analysis, significantly regulated genes were annotated with information from various databases in order to find common features among the genes sharing similar expression characteristics. The annotations used were derived from Gene Ontology (GO). Among the 2,235 significantly upregulated genes, 159 key genes were involved in cell differentiation and 51 key genes in lipid metabolism (Fig. 3.4.6.). A certain number of genes, significantly less if compared to the induced DFs30, that regulate development (233), receptor signaling (193), cellular transportation (121), response to toxins (128), protein modification (105), cytoskeleton (75), transcription (118), cell proliferation (101) metabolism (79), as well as cell death (84) were upregulated.

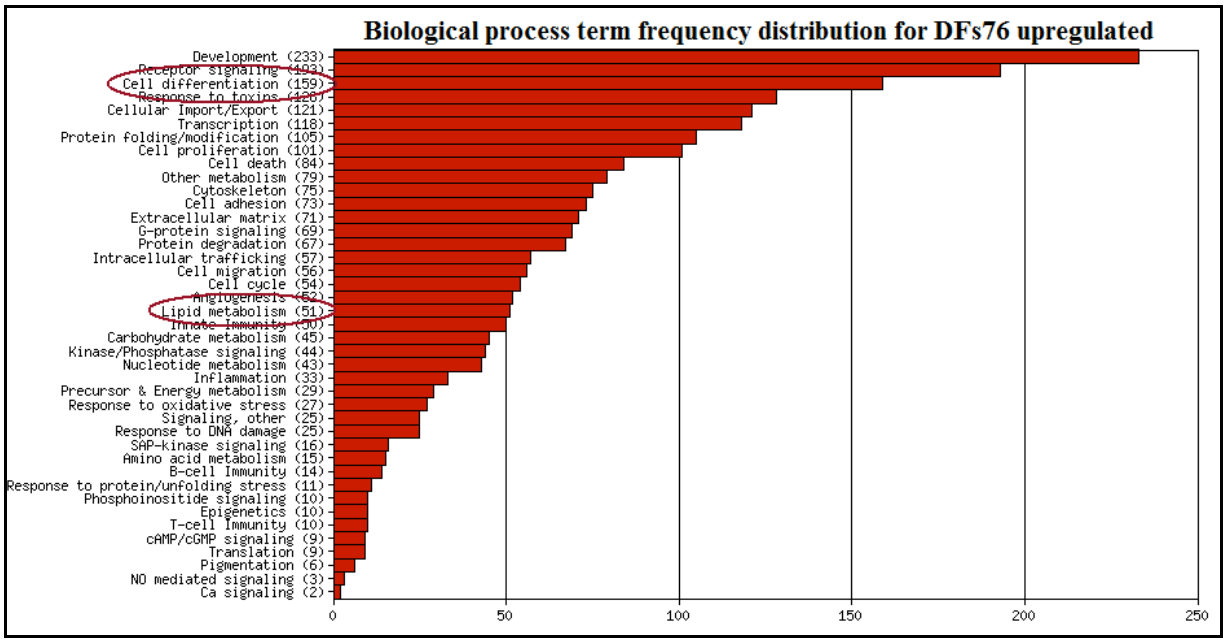

Fig. 3.4.3.2. Functional grouping analysis of at least two-fold upregulated genes. Frequency of upregulated genes in induced DFs76 compared to untreated control DFs76 in categories describing "biological processes". 159 genes implicated in cell differentiation and 51 genes implicated in lipid metabolism were found to be significantly upregulated (red circles).

The induced DFs76 showed an upregulation of key transcription factors for adipogenesis such as the PPARγ, PPARγ co-activator 1α, c-Fos and FoxO1. However, their expression was remarkably weaker in comparison to the corresponding fold changes in the induced younger DFs30 (Table 13). In contrast with younger fibroblasts, the subunit CEBPδ of the major adipogenic regulators CEBPs was found to be significantly upregulated in older fibroblasts

(3.2 fold-change). Furthermore, genes with a key role in lipid metabolism, such as lipogenesis (LPL, LPLR, SCD) were overexpressed but in a weaker manner than in DFs30. Moreover, secreted proteins regulating cell metabolism during adipogenesis were also significantly upregulated (apolipoproteins B and D), however, DFs76 exhibited no upregulation of the retinol binding protein compared to induced DFs30. Leptin and leptin receptor were also significantly overexpressed and leptin together with the GGT5, SERPINA3 and LPL were the only upregulated genes that exhibited a slightly stronger expression in induced DFs76 than in induced DFs30 (Table 13, in bold). A considerable amount of upregulated genes in younger fibroblasts could not be identified in induced older fibroblasts (i.e. FABP5, phospholipases, LDLR). A summary of genes implicated in lipid metabolism that showed a significant upregulation in induced DFs76 is presented in Table 12. Moreover, Table 13 provides an overview of the 22 upregulated genes implicated in lipid metabolism that were expressed in common in both adipogenic induced DFs30 and DFs76 and the corresponding fold changes.

Table 12. Selection of significantly upregulated genes (more than two-fold) implicated in lipid metabolism in adipogenic induced DFs76 compared to control DFs76 and their fold changes.

Gene symbol	Gene description	Fold changes	Gene symbol	Gene description	Fold changes
ABHD5	1-acylglyc.-3-phosph.O-acyltransf.5	5.3	LEP	leptin	3.4
ACOT11	acyl-CoA thioesterase 11	4.6	LEPR	leptin receptor	4.8
ACSL1	acyl-CoA synthetase long-chain 1	3.6	LPL	lipoprotein lipase	12.2
ACSM5	acyl-CoA synthetase medium-chain 5	13.6	LRP2	low dens. lipoprot. recept. 2	73.9
ALOX15B	arachidonate 15-lipoxygenase, type B	5.8	MCAT	ACP acyltransferase	3
APOD	apolipoprotein D	7.4	MLXIPL	MLX interacting protein-like	2.1
ASPG	asparaginase homolog	3.4	OSBPL10	oxysterol binding prot-like 10	2.5
B3GNT5	b-1,3-N-acetylglucosaminyltransfer.5	4.5	PIK3C2A	phosphoinositide-3-kinase, 2a	2.9
C9ORF3	chromosome 9 open reading frame 3	2	PIK3R1	phosphoinositide-3-kinase	3.6
CYP7B1	cytochrome P450, family 7, B 1	2.4	PPARγ	peroxis. prolif-activat recept. γ	4.8
DHCR24	24-dehydrocholesterol reductase	2.3	PPARγC1A	PPARγ coactivator 1α	6.8
EDN2	endothelin 2	8.2	PRKAG3	prot. kinase, AMP-activated g3	18.9
ELOVL3	elongat. of very long chain fatty acids	3.1	PTGIS	prostaglandin I2 synthase	2.1
FADS2	fatty acid desaturase 2	2.2	SCD	stearoyl-CoA desaturase	2.3
GGT5	gamma-glutamyltransferase 5	3.9	SERPINA3	serpin peptid. inhibit. clade A3	11.9
HAO2	hydroxyacid oxidase 2 (long chain)	4.7	SMPDL3A	sphingomyel. phosphodiest.3A	2.2
HNF1A	HNF1 homeobox A	2.1	SORBS1	sorbin and SH3 domain 1	3.6
HSD17B6	hydroxysteroid (17-b) dehydrogen.6	2.2	STRADA	STE20-related kinase adaptor a	32.8
IGFBP7	insulin-like growth factor bind. prot.7	3.4	TBXAS1	thromboxane A synthase 1	3
IRS1	insulin receptor substrate 1	2.2	TNF	tumor necrosis factor (memb.2)	3.8
IRS2	insulin receptor substrate 2	2.1	WDTC1	WD and tetratricopept. repeats1	2.2

Table 13. Significantly upregulated genes (>2-fold) implicated in lipid metabolism expressed in common in both induced DFs30 and DFs76 and the fold changes compared to corresponding control cells. In bold, genes that were more strongly expressed in induced DFs76 than DFs30.

Gene symbol	Gene description	Fold changes (to control)	
		DFs30	DFs76
ACSL1	acyl-CoA synthetase long-chain family member 1	3.1	3.6
ACSM5	acyl-CoA synthetase medium-chain family member 5	21.6	13.6
ALOX15B	arachidonate 15-lipoxygenase, type B	17	5.8
APOD	apolipoprotein D	8.2	7.4
B3GNT5	b-1,3-N-acetylglucosaminyltransferase 5	27.9	4.5
CYP7B1	cytochrome P450, family 7, subfamily B, polypeptide 1	2.9	2.4
DHCR24	24-dehydrocholesterol reductase	9.4	2.3
ELOVL3	elongation of very long chain fatty acids	4.8	3.1
GGT5	**gamma-glutamyltransferase 5**	**3.4**	**3.9**
HNF1A	HNF1 homeobox A	7.7	2.1
LEP	leptin	56	3.4
LEPR	**leptin receptor**	**3.2**	**4.8**
LPL	**lipoprotein lipase**	**8.2**	**12.2**
MCAT	ACP acyltransferase	3	3
MLXIPL	MLX interacting protein-like	5.6	2.1
PIK3R1	phosphoinositide-3-kinase, regulatory subunit 1 (alpha)	4.7	3.6
PPARG	peroxisome proliferator-activated receptor gamma	25.6	4.8
PPARGC1A	peroxisome proliferator-activated receptor gamma,coactivator1a	8.9	6.8
SCD	stearoyl-CoA desaturase (delta-9-desaturase)	2.6	2.3
SERPINA3	**serpin peptidase inhibitor, clade A, member 3**	**4.3**	**11.9**
SORBS1	sorbin and SH3 domain containing 1	24.2	3.6
TBXAS1	thromboxane A synthase 1	13.2	3

3.4.3.3. Signaling pathways of cell differentiation and adipogenesis showed a weaker differential expression in induced DFs76 versus induced DFs30

Major signaling pathways that play a crucial role in the cell differentiation process and adipogenesis, such as the insulin receptor, TGF-β, Wnt, Notch, phosphoinositide, FGF, Notch, BMP and steroid receptor signaling pathways proved to be significantly regulated in the induced DFs76 in comparison with the control DFs76. An analytical presentation of the fold changes in key regulatory genes for each pathway is shown in Table 14. The highest fold change (30.8) in DFs76 induced cells compared with control fibroblasts was observed in the Wnt signaling pathway and the gene coding the R-spondin homolog 1 (RSPO1), whereas the lowest (-30.7) in the protein-coding gene coiled-coil domain 88C also in the Wnt signaling pathway (CCDC 88C).

Table 14. Differential regulation of signaling pathways in induced DFs76 compared with control DFs76. In each pathway significantly regulated genes are presented with the corresponding fold changes (>2-fold). Grey font: downregulated genes; black font: upregulated genes.

Gene symbol	Gene description	Fold changes
	Insulin receptor signaling	
IL1B	interleukin 1, beta	-10.3
PTPRE	prot. tyros phosphatase, rec.E	-2.9
FOXO1	forkhead box O1	4.1
IGF2	insulin-like growth factor 2	3.6
IRS1	insulin receptor substrate 1	2.2
IRS2	insulin receptor substrate 2	2.1
PIK3R1	phosphoinositide-3-kinase, sub.1	3.6
PIK3R3	phosphoinositide-3-kinase, sub.3	6.3
SORBS1	sorbin and SH3 domain 1	3.6
	Wnt pathway	
CCDC88C	coiled-coil domain 88C	-30.7
WISP1	WNT1 ind. signal.pathw.prot.1	-9.8
NDP	Norrie disease	-5.8
WNT2	wingless-type member 2	-5
FZD8	frizzled homolog 8	-4.9
FZD10	frizzled homolog 10	-2.6
RSPO3	R-spondin 3 homolog	-2.5
SOX17	SRY box 17	-2.5
SFRP1	secreted frizzled-related prot. 1	-2.4
DACT1	dapper, antagonist of b-catenin1	-2.2
MAPK8	mitogen-activated prot. kinase 8	-2.1
SOX4	SRY box 4	-2.1
RSPO3	R-spondin 3 homolog	-2
APC2	adenomatosis polyposis coli 2	2.3
AXIN2	axin 2	2.4
BARX1	BARX homeobox 1	2.6
BC063022	frizzled homolog 4	2.6
CDH1	cadherin 1, type 1, E-cadherin	2.6
DIXDC1	DIX domain containing 1	2.2
DKK1	dickkopf homolog 1	3
FRZB	frizzled-related protein	2.1
HNF1A	HNF1 homeobox A	2.1
NKD2	naked cuticle homolog 2	3.4
ROR2	recept. tyrosine kin.-like orph. 2	3.7
RSPO1	R-spondin homolog 1	30.8
RUNX2	runt-related transcription factor 2	2.8
SFRP2	secreted frizzled-related protein 2	8.4
SIX3	SIX homeobox 3	12.2
TCF7L2	cadherin 1, type 1, E-cadherin	14
	FGF signaling	
FGF2	fibroblast growth factor 2	-5.7
FGF5	fibroblast growth factor 5	-4.2
FGF7	fibroblast growth factor 7	-2.1
THBS1	thrombospondin 1	-2.7

Gene symbol	Gene description	Fold changes
	TGFbeta signaling	
BMP7	bone morphogenetic prot.7	-2.7
CCL2	chemokine ligand 2	-2.8
GDF10	growth differentiation factor 10	-3.3
GDF15	growth differentiation factor 15	-3.2
ITGA8	integrin, alpha 8	-5.7
NOG	noggin	-2.8
SMURF2	SMAD spec E3 ubiquitin prot. lig.2	-3.4
THBS1	thrombospondin 1	-2.7
VWC2	von Willebrand factor C domain2	-7.2
ACVRL1	activin A receptor type II-like 1	2.7
BMP4	bone morphogenetic protein 4	2.2
COL1A2	collagen, type I, alpha 2	3.9
COL3A1	collagen, type III, alpha 1	4.2
FOS	FBJ murine osteosarcoma vir. oncog.	8.2
FSTL3	follistatin-like 3	2.5
ID1	inhibitor of DNA binding 1	2.8
KLF10	Kruppel-like factor 10	2.3
RGMA	RGM domain family, member A	2.8
TGFBR2	transforming growth factor, b rec II	2.6
	BMP signaling	
BMP7	bone morphogenetic protein 7	-2.7
FST	follistatin	-3
GREM2	gremlin 2	-2.1
NOG	noggin	-2.8
SMURF2	SMAD spec E3 ubiquitin prot lig 2	-3.4
VWC2	von Willebrand factor C domain 2	-7.2
ACVRL1	activin A receptor type II-like 1	2.7
BMP4	bone morphogenetic protein 4	2.2
FSTL3	follistatin-like 3	2.5
ID1	inhibitor of DNA binding 1	2.8
RGMA	RGM domain family, member A	2.8
	Phosphoinositide signaling	
CHRM2	cholinergic receptor, muscarinic 2	-11.4
TGM2	transglutaminase 2	-10.4
CCKBR	cholecystokinin B receptor	-3
HTR2B	5-hydroxytryptamine receptor 2B	-2.6
P2RY2	purinergic receptor P2Y, 2	-2.5
EDNRA	endothelin receptor type A	-2.4
DRD5	dopamine receptor D5	10.4
EDN2	endothelin 2	8.2
EDNRB	endothelin receptor type B	2.5
IGF1	insulin-like growth factor 1	7.8
NPR3	natriuretic peptide receptor C	7.5
PIK3C2A	phosphoinositide-3-kinase, class 2, a	2.9

FRS2	fibroblast growth factor rec. substr2	2		**Notch signaling**	
RUNX2	runt-related transcription factor 2	2.8	DNER	delta/notch-like EGF repeat	-4
	Steroid receptor signaling		DTX2	deltex homolog 2	-2.6
STRN3	striatin, calmodulin bind.prot.3	-2.3	KIT	v-**kit** Hardy-Zuckerman oncogene	-2.1
MLL2	mixed-lineage leukemia 2	-2.1	NRG1	neuregulin 1	-2.4
IGF1	insulin-like growth factor 1	7.8	CFD	complement factor D (adipsin)	3.7
KLF9	Kruppel-like factor 9	2.3	HES1	hairy and enhancer of split 1	4.5
PPARγC1A	PPARγ, coactivator 1α	6.8	JAG1	jagged 1	3.6

PPAR signaling pathway

The essential transcription factor of adipogenesis, the peroxisome proliferator activated receptor γ (PPARγ) was significantly upregulated in the induced DFs76. Furthermore, target genes of the PPARγ signaling pathway, such as the LPL, CAP, ACS, were identified to be significantly upregulated, however, they were less than those identified in the induced DFs30. Isoforms of the FABP ligands did not show any differential expression (Fig. 3.4.3.3.).

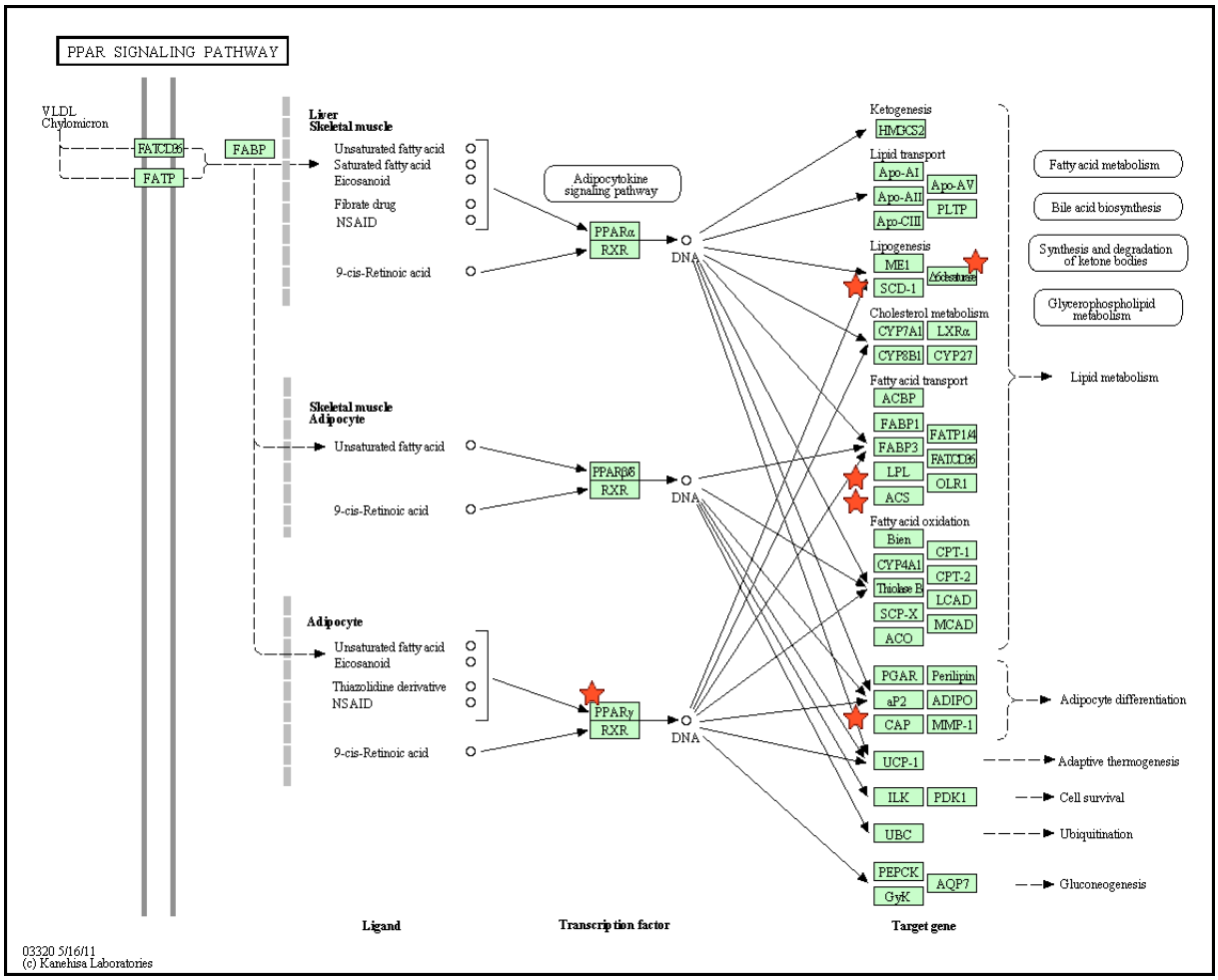

Fig. 3.4.3.3. The KEGG-pathway shows genes that are upregulated (red asterisk) in the PPAR signaling pathway in the adipogenic induced DFs76.

3.4.3.4. Comparison of the differential expression of key genes in major signaling pathways of the induced DFs30 versus DFs76

Moreover, the differences and similarities in the expression of key genes in the regulated major signaling pathways between the adipogenic induced DFs30 and DFs76 were explored (Table 15). A major difference was that no genes of the hedgehog pathway showed a differential expression in induced DFs76 compared to control DFs76, whereas younger fibroblasts showed a significant regulation of 4 genes of the pathway, either up- or downregulation (CREBBP, GLI1, CCMB1, CDC2). In most of the signaling pathways, genes implicated in cell differentiation and adipogenesis, which were identified in both young (DFs30) and old fibroblasts (DFs76), showed a stronger expression in the adipogenic induced DFs30 compared to adipogenic induced DFs76 (e.g. SORBS1, BMP4, ID1, DKK1, RUNX2, WNT2, CFD, GDF10, IGFBP2). Furthermore, induced DFs30 expressed a wider range of genes involved in adipogenesis that were either not significantly regulated in induced DFs76 (e.g. IGFBP3, Glypican, SMAD1 and 2) or they exhibited an opposite regulation of the one detected in DFs30 (e.g. TGM2 and Noggin were upregulated in DFs30 and downregulated in DFs76). In general, the TGF-β, Wnt and BMP signaling pathways exhibited the most abundant differential regulation in both adipogenic induced DFs30 and DFs76.

Table 15. Comparison of significantly regulated genes (>2-fold) implicated in major signaling pathways in induced DFs30 versus DFs76. Fold changes refer to the corresponding control cells. Negative values represent downregulated genes. n.e.: not expressed/no significant regulation.

Gene symbol	Gene description	Fold changes		Gene symbol	Gene description	Fold changes	
		DFs30	DFs76			DFs30	DFs76
	TGFbeta signaling				**Wnt pathway**		
BMP4	bone morphogenetic prot. 4	2.6	2.2	BARX1	BARX homeobox 1	6.6	2.6
BMP7	bone morphogenetic prot.7	n.e.	-2.7	CCDC88C	coiled-coil domain 88C	n.e.	-30.7
CCL2	chemokine ligand 2	-2.3	-2.8	CDH1	cadherin 1, type 1, E-cadherin	-2.3	2.6
FOS	FBJ mur. osteos. vir. oncog.	2.6	8.2	DKK1	dickkopf homolog 1	8.6	3
GDF10	growth different. factor 10	-16.4	-3.3	FRZB	frizzled-related protein	2.6	2.1
GDF5	growth differentiation fact. 5	5.9	n.e.	FZD10	frizzled homolog 10	n.e.	-2.6
GPC3	glypican 3	16	n.e.	FZD7	frizzled homolog 7 (Drosophila)	-2.8	n.e.
ID1	inhibitor of DNA binding 1	5.3	2.8	FZD8	frizzled homolog 8	n.e.	-4.9
ITGA8	integrin, alpha 8	-6.2	-5.7	HNF1A	HNF1 homeobox A	7.7	2.1
NOG	noggin	2.4	-2.8	ROR2	recept. tyrosine kin.-like 2	-	3.7
PEG10	paternally expressed 10	6	n.e.	RSPO1	R-spondin homolog	2	30.8
SMAD1	SMAD family member 1	-2.1	n.e.	RSPO3	R-spondin 3 homolog	n.e.	-2.5
SMAD2	SMAD family member 2	-3.4	n.e.	RUNX2	runt-related transcription factor 2	7	2.8
TGF-β3	transforming growth fact. β3	-2	n.e.	SIX3	SIX homeobox 3	n.e.	12.2
TGFβR2	transforming gr. fact.β recII	n.e.	2.6	SOX17	sex determining region Y-box 17	14	-2.5
THBS1	thrombospondin 1	-2.4	-2.7	TCF7L2	lymphoid enhancer-binding fact.1	-2.7	14

	BMP signaling		
ACVRL1	activin A rec. type II-like 1	2.4	2.7
BMP4	bone morphogenetic protein4	2.6	2.2
BMP7	bone morphogenetic protein7	n.e.	-2.7
CHRDL1	chordin-like 1	62.3	n.e.
FST	follistatin	-2.1	-3
GPC3	glypican 3	16	n.e.
ID1	inhibitor of DNA binding 1	5.3	2.8
NOG	noggin	2.4	-2.8
SMAD1	SMAD family member 1	-2.1	n.e.
ZFYVE16	zinc finger, FYVE domain 16	9.1	n.e.
	Insulin receptor signaling		
FOXO1	forkhead box O1	5	4.1
IGF1	insulin-like growth factor 1	2.5	7.8
IGF1R	insulin-like growth fact.1 rec.	-3.8	n.e.
IGF2	insulin-like growth factor 2	-2.3	3.6
IGFBP2	insulin-likegr.fact.bind.prot.2	4.9	3.4
IGFBP3	insulin-likegr.fact.bind.prot.3	2	n.e.
IL1B	interleukin 1, beta	-7.8	-10.3
PIK3R1	phosphoinositide-3-kin.,sub.1	4.7	3.6
PTPRE	prot. tyros phosphatase, rec.E	-6.8	-2.9
SORBS1	sorbin and SH3 domain 1	24.2	3.6
	FGF signaling		
FGF2	fibroblast growth factor 2	-2.5	-5.7
FGF12	fibroblast growth factor 12	5.3	n.e.
FGF18	fibroblast growth factor 18	-100	n.e.
FGF5	fibroblast growth factor 5	n.e.	-4.2
FGF7	fibroblast growth factor 7	n.e.	-2.1
FGF9	fibroblast growth factor 9	-30.4	n.e.
FGFR1	fibroblast growth factor rec 1	3.4	n.e.
FGFR2	fibroblast growth factor rec 2	-2.7	n.e.
RUNX2	runt-related transcript. fact.2	7	2.8
THBS1	thrombospondin 1	-2.1	-2.7
WNT4	wingless-type family, mem. 4	-100	n.e.
WISP1	WNT1 induc. signal.path. prot.1	2	-9.8
WNT16	wingless-type family member 16	9.3	n.e.
WNT2	wingless-type family member 2	-27.1	-5
WNT3	wingless-type family member 3	-2.2	n.e.
WNT4	wingless-type family member 4	-100	n.e.
	Notch		
CFD	complement factor D (adipsin)	4.5	3.7
DNER	delta/notch-like EGF repeat	14.8	-4
DTX2	deltex homolog 2	n.e.	-2.6
DTX4	deltex homolog 4	-3.8	n.e.
FOXC1	forkhead box C1	-3.1	n.e.
HES1	hairy and enhancer of split 1	-3	4.5
HEY1	hairy/enhancer-of-split	2.7	n.e.
JAG1	jagged 1	n.e.	3.6
NRG1	neuregulin 1	-12.5	-2.4
TP63	tumor protein p63	-5.2	n.e.
	Phosphoinositide signaling		
DRD1	dopamine receptor D1	-16	n.e.
DRD5	dopamine receptor D5	n.e.	10.4
EDN2	endothelin 2	8.2	n.e.
EDNRA	endothelin receptor type A	2.5	-2.4
EDNRB	endothelin receptor type B	100	2.5
HMGB2	high-mobility group box 2	2	n.e.
HTR2A	5-hydroxytryptamine receptor 2A	-2.2	n.e.
IGF1	insulin-like growth factor 1	2.5	7.8
NPR3	atrionatriuretic peptide receptor C	3.1	7.5
TGM2	transglutaminase 2	3	-10.4
	Steroid receptor signaling		
AR	androgen receptor	15.9	n.e.
FHL2	four and a half LIM domains 2	-4.6	n.e.
IGF1	insulin-like growth factor 1	2.5	7.8
KLF9	Kruppel-like factor 9	2.2	2.3
MLL2	mixed-lineage leukemia 2	-2.2	-2.1
PGR	progesterone receptor	7.7	n.e.
PIAS2	prot. inhibitor of activ. STAT2	2.1	n.e.
PPARγC1α	PPARγ, coactivator 1α	8.9	6.8

3.4.3.5. Comparison of the transcription profiles of induced DFs76 versus human adipocytes and adipocytes deriving from differentiated MSCs

In order to examine whether the adipogenic induced DFs76 expressed adipocyte-specific genes, their transcriptional phenotype was compared to that of human adipocytes (Table 11a) deriving from the subcutaneous abdominal fat from healthy women, as described elsewhere (Urs et al., 2004). A second comparison was conducted to the gene expression profile of adipocytes derived after adipogenic induction of human bone marrow-derived MSCs (Table 11b) described by Sekiya et al. (2003).

Adipogenic induced DFs76 vs human adipocytes

Urs et al. (2004) performed a study on gene expression profiling in human adipocytes using microarray technology and provided novel markers for the characterisation of human adipocytes. In total, 77 genes involved in metabolism/transport, transcription factors and binding proteins, signaling molecules and cellular matrix proteins were reported to be overexpressed in human adipocytes. Our results were compared one-to-one to the reported genes (Table 11a). 14 genes out of the 77 were found to be significantly regulated in the adipogenic induced DFs76, approximately 18% of the adipocyte markers reported by Urs et al. (2004). Induced DFs30 showed a greater affinity to human adipocytes (25%). Among them, two genes (GPD1 and MASP1) showed a downregulation in our cells, which was not consistent with the data of Urs et al. (2004). However, the overexpression of these genes in human adipocytes was reported as non-significant by the authors.

None of the members of the FABP or phospholipase families were expressed in induced DFs76 in contrast to human adipocytes and induced DFs30. In general, genes that showed a significant upregulation in both induced DFs30 and DFs76 exhibited a weaker expression in older fibroblasts (PPARγ, PPARγC1α, GLUL, SCD, IGFBP2) or were not expressed at all (i.e. ALDH6A1, APOB, DGAT1, LRP8, GPX3, HSD11B2, IL22R). However, induced DFs76 showed significant upregulation of most of the cellular matrix and cytoskeleton genes (3/4, COL1A2, MMP7, DPT), genes that were not regulated in younger fibroblasts. A complete absence of expression of signaling molecules was observed in older fibroblasts.

Interestingly, a number of the major transcription factors of adipogenesis, such as the PPARγ, IGFBP2, and TNFAIP2, were upregulated in the induced DFs76. In contrast to DFs30, induced DFs76 exhibited a significant upregulation of the transcription factor C/EBPD. The transcription activator of the c-fos promoter was not regulated in induced DFs76, in contrast to human adipocytes, however c-FOS was significantly upregulated both in induced DFs30 and DFs76 (in bold). Glutathione peroxidase 3, which was in common expressed in adipocytes and induced DFs30, was not expressed in DFs76.

Table 11a provides an overview of the comparison of the transcription profile of human adipocytes versus the adipogenic induced DFs30 and DFs76.

Adipogenic induced DFs76 vs. adipocytes from differentiated human MSCs

Sekiya et al. (2003) assayed gene expression during and at the end-point of adipogenesis of human MSCs and reported increases in expression of 65 genes, which were proposed as markers of adipogenesis. Our results were compared one-to-one to the reported genes (Table

11b). 23 out of the 65 proposed genes were regulated in the induced DFs76, approximately 35% of the reported markers of adipocytes deriving from adipogenic differentiated MSCs. Induced DFs30 showed a greater affinity to differentiated MSCs (66%). Among them, one gene (HSD11B1) was downregulated, which was not consistent with the data of Sekiya et al. (2003). None of the members of the FABP or phospholipase families were expressed in induced DFs76 in contrast to adipogenic differentiated MSCs and induced DFs30. In general, genes that showed a significant upregulation in both induced DFs30 and DFs76 exhibited a weaker expression in older fibroblasts (ADH1C, HAS1, MAOA, SCD5, TIMP4, IL18R, FoxO1, PPARγ, PPARγC1A, ANGPT1, APOD, CACNB2) or were not expressed at all (e.g. ADH1B, HSD11B2, IMPA2, G0S2, ZBTB16, IGFBP2, TGF-β, SERPINF2, HP). Exceptions to the above were the genes ADH1C, CHST2, LPL, c-FOS, CRLF1, IGF1, IGF2, SPARCL1, PPL and SAA1 that showed either a stronger expression in older fibroblasts or were expressed in older fibroblasts but not in the induced DFs30.

Major transcription factors of adipogenesis were upregulated in common in differentiated MSCs and DFs76, such as the PPARγ, FoxO1 and c-FOS, however in a weaker manner than in younger fibroblasts, except for c-FOS. Moreover, the transcription factor ZBTB16 was not regulated in the induced DFs76 in contrast to the induced DFs30.

Table 11b provides an overview of the comparison of the transcription profile of adipocytes deriving after adipogenic differentiation of human bone marrow MSCs versus the adipogenic induced DFs30 and DFs76.

3.4.4. Confirmation of microarray results via qRT-PCR

The microarray results were confirmed by qRT-PCR analysis. Four representative gene candidates that were found to be significantly upregulated in both DFs30 and DFs76 in the microarray analysis, which are of great importance in the process of adipogenesis and for the phenotype of adipocytes, were selected: the major adipogenesis player PPARγ, the lipoprotein lipase (LPL), the insulin growth factor binding protein 2 (IGFBP2) and leptin. Moreover, gene expression of the above-mentioned genes was also evaluated over time by analyzing their expression at two different time points, on the 8th and 23rd day of the adipogenic treatment (Fig. 3.4.4.).

qRT-PCR analysis data correlated well with the microarray results. Fold change values for adipogenic induced DFs30 and DFs76 were related to the corresponding untreated control fibroblasts, the latter being set to 1. IGFBP2 showed a significant upregulation both in young

(DFs30; day 8: 1.8, $p<0.01$ and day 23: 2.5, $p<0.01$) and in older fibroblasts (DFs76; day 8: 4.2 and Day 23: 6.0, $p<0.05$) that increased over time. Leptin exhibited the strongest upregulation over time in DFs30 (day 8: 5.3, $p<0.001$; day 23: 34.0, $p<0.001$), however in older fibroblasts, leptin expression showed a strong upregulation at the 8th day of the treatment and a significant decrease at the 23rd day of adipogenic treatment (day 8: 27.0, $p<0.001$; day 23: 2.3, $p<0.001$). The master regulator PPARγ expression was significantly upregulated in DFs30 at the 8th day (day 8: 3.4, $p<0.01$) and increased gradually until the 23rd day (day 23: 12.6, $p<0.001$), whereas in older fibroblasts, although at the 8th day PPARγ expression showed to be significantly increased (day 8: 3.5, $p<0.05$), its expression did not increase further and, on the contrary, it decreased later on (day 23: 1.5, $p<0.01$). Finally, LPL expression increased over time in DFS30 (day 8: 1.1; day 23: 1.6, $p<0.01$), whereas in DFs76 decreased (day 8: 2.1; day 23: 1.3, $p<0.01$). However, the expression ratios for both DFs30 and DFs76 at the 8th day of treatment did not reach a level of significance. At the 23rd day of treatment, LPL expression exhibited significant upregulation in both types of induced fibroblasts.

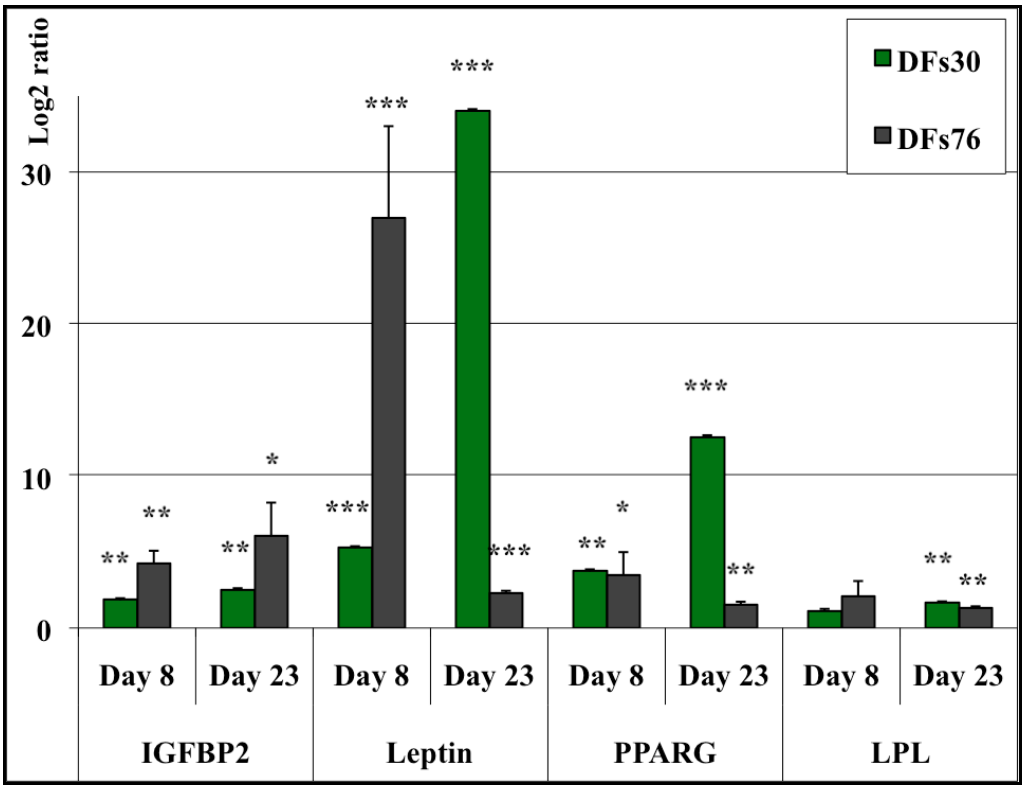

Fig. 3.4.4. Confirmation of microarray data via qRT-PCR. Examination of expression levels of selected genes: IGFBP2, leptin, PPARγ, LPL in DFs30 and DFs76. The figure shows the logarithmic ratios (log2) of induced DFs30 vs. untreated control DFs30 (green) and induced DFs76 vs control DFs76 (grey) at two different time points of the adipogenic induction (day 8 and day 23).
$p<0.05$: *, $p<0.01$: **, $p<0.001$: ***

«ἓν οἶδα ὅτι οὐδὲν οἶδα»

«As for me, I know one thing, that I know nothing»

Socrates

Greek philosopher, ca. 469 BC- ca. 399 BC

4. DISCUSSION

4.1. Stem cells and fibroblasts in tissue engineering

Tissue engineering has become one of the most intriguing, promising and fastest growing field in medical research over the past few decades and stem cells constitute one of its cornerstones. As research on stem cells evolves, new information arises daily regarding breakthrough technologies for isolation and expansion of stem cell populations and new stem cell niches in the human body. The revolutionary discovery of embryonic and perinatal stem cells gradually led to the discovery of adult stem cells in all human tissues and more recently to the bioengineered, induced stem cells. The evolution from considering cell differentiation as an irreversible process to accepting that cell fate may be manipulated even during advanced differentiation has given rise to a revolution in the field of regenerative science and gave hope for new clinical applications and therapeutic strategies, for example in organ and tissue transplantation.

Skin, the biggest human organ, is able to provide a niche for many different types of stem cells from all its compartments, namely epidermis-, dermis-, adipose-, hair follicle-derived stem cells, and sebaceous gland-derived progenitors (LoCelso et al., 2008; Yang et al., 2010; Yang and Cotsarelis, 2010; Toma et al., 2010). Among these stem cell populations, dermal fibroblasts have attracted a great amount of scientific interest and there are several reports in the literature describing the inherent plasticity of these cells (Toma et al., 2001; Bartsch et al., 2005; Chen et al., 2007). Skin fibroblasts are among the easiest human cell types to process and expand *in vitro* (Wong et al., 2007) and, therefore, their usage in cell-based therapies may facilitate the production of autologous tissues for the reconstruction of damaged tissues and organs. However, it still remains unclear whether dermal fibroblasts owe their plasticity to circulating stem cells and progenitor cells that they may be contained into fibroblast populations isolated from human tissues or whether fibroblasts are actually capable per se, as differentiated cells, to return to an undifferentiated state under the appropriate stimulus and further differentiate into new cell types.

In this work, the question whether human dermal fibroblasts are capable of differentiating along the mesenchymal lineage into adipocytes was addressed. In addition, the plasticity of dermal fibroblasts between young and older donors was investigated. Moreover, the transcriptional profile of these cells after adipogenic induction was examined. The results presented in this work strengthen the notion that skin fibroblasts are not the "terminally differentiated" cells they were previously considered to be and they still possess the ability to differentiate into cells that resemble the phenotype of adipocytes, while acquiring an adipogenic transcriptional profile.

4.2. Morphological changes and lipid accumulation capacity of human skin fibroblasts during differentiation towards an adipocyte-like phenotype

4.2.1. Dermal fibroblasts from all ages (FSFs, DFs30 and DFs76) are capable of intracellular lipid accumulation after adipogenic induction

In the present study, the possibility of inducing differentiation of human dermal fibroblasts towards an adipocyte cell-like phenotype was investigated. This was achieved by culturing fibroblasts in an induction medium containing factors that are known to promote adipogenesis, a technique that has been used in other groups in order to induce adipogenic differentiation in bone marrow-derived pluripotent MSCs (Pittenger et al., 1999). The phenotypical changes were confirmed via fluorescence, light and electron microscopy after 23 days of adipogenic treatment. At that time point dermal fibroblasts of different ages (FSFs, DFs30 and DFs76) accumulated lipid droplets in their cytoplasm that were positively stained with Nile red under fluorescence microscopy (Fig. 3.1.1. - 3.1.9.). This finding was reproducible in repeated experiments.

This observation is consistent with several reports that have been published in recent years describing an intrinsic differentiation capacity of human skin fibroblasts, which can be used to corroborate the findings of other groups (Chen et al., 2007; Junker et al., 2010).

Although fluorescence microscopy was only used as a screening method and the results were not further quantified, it was obvious that younger fibroblasts, namely FSFs and DFs30 showed a stronger lipid accumulation in a large number of cells than older fibroblasts (DFs76), which were also stained positively for Nile red but not to the same extend.

It is important to mention here that other groups have published somewhat controversial results concerning the differentiation capacity of fibroblasts (Pittenger et al., 1999; Wagner et al., 2005). For example, Pittenger et al. (1999), whose adipogenic induction protocol has also been used in the present work, used dermal fibroblasts in differentiation experiments of bone-marrow-derived MSCs as negative control. In these experiments, MSCs were driven to differentiate into adipocytes under the appropriate adipogenic stimulus, whereas skin fibroblasts did not exhibit any morphological changes or lipid accumulation. A possible explanation could be that Pittenger et al. (1999) used fibroblast cell lines, namely the Hs27 newborn skin fibroblasts and 1087Sk adult mammary tissue fibroblasts, which might have lost a part of their inherent plasticity and not primary cells as we used in our experiments. However, this may only be a partial explanation, as it has recently been shown that conditionally immortalized mouse embryonic fibroblasts using SV40 large T antigen retain their proliferative activity without compromising their multipotent differentiation potential (Huang et al., 2012).

4.2.2. Young fibroblasts acquire an adipocyte-like phenotype and accumulate more lipids than older fibroblasts which exhibit damaged cytoplasmic membranes

Flow cytometry after Nile red staining of induced fibroblasts was used to quantify the results acquired by fluorescence microscopy and confirmed the increased lipid accumulation in all induced fibroblasts. However, younger fibroblasts were capable of accumulating more lipids than older fibroblasts, thus providing evidence that dermal fibroblasts from older donors do not possess the same adipogenic differentiation potential as younger ones.

It has been reported that the decline of regeneration potential of a tissue is a hallmark of ageing and this may be a result of age-related changes of the tissue-specific residing stem cells and progenitor cells (Conboy et al., 2005; Zouboulis et al., 2008). Sharpless et al (2007) supported the notion that stem cell numbers and self-renewal ability may not be affected by ageing, but the function and differentiation capacity are the features that are mostly influenced (Sharpless and DePinho, 2007). Our results are consistent with this observation and with numerous further reports of the loss or decline of cell differentiation potential with increasing age of the donor (Joine et al., 2012; Klatte-Schulz et al., 2012; Lohmann et al., 2012; Zaim et al., 2012; Zhang et al., 2012).

Surprisingly, morphological examination of adipogenic induced fibroblasts via electron microscopy revealed that all fibroblasts from donors of different ages, including the DFs76, contained lipid droplets in their cytoplasm, thus providing evidence that even older fibroblasts are able to undergo differentiation into adipocytes by accumulating intracellular lipids. However, older dermal fibroblasts exhibited damaged membranes and complete loss of their cytoplasmic structure, whereas younger fibroblasts appeared normal with no significant changes of their cytoplasmic membranes. A possible explanation could be that older fibroblasts, even though they possess the ability to differentiate, they lack strength and capacity to respond to the induction pressure and at a certain point of the differentiation process their cytoplasmatic membranes are damaged, endoplasmatic lipids are released and therefore not detected by flow cytometry.

To our knowledge, there has been no publication reporting the electron microscopic morphology changes occurring in dermal fibroblasts from older donors during adipogenic induction *in vitro*. Zaim et al (2012) described a decrease in adipogenic, osteogenic, and neurogenic differentiation potential of human bone marrow-derived MSCs with age and a negative effect of long-term passaging on cell morphology and proliferation capacity. With increasing passage number, proliferation rate decreased and cells lost their typical morphology, however the morphological changes of aged cells during adipogenic differentiation were not examined.

4.3. Gene expression profiles of the adipogenic induced dermal fibroblasts

Human dermal fibroblasts from donors of different ages were induced to differentiate into adipocytes under the appropriate adipogenic stimulus. Subsequently, the gene expression profiles of the induced fibroblasts from the 30- and 76-year old donors were examined in order to identify adipocyte-specific genes associated with the successful differentiation of these cells into adipocyte-like cells. Gene expression analysis was performed via microarrays and the gene expression profiles of the induced cells were compared to the transcriptional profiles of the untreated control cells of the corresponding age group in order to identify differential gene expression. Differential regulation of major signaling pathways involved in adipogenesis was also examined. Moreover, in order to examine whether our adipogenic induced cells expressed adipocyte-specific genes, their transcriptional phenotype was compared with the gene expression profiles of normal human adipocytes and preadipocytes deriving from the subcutaneous tissue of healthy women, as reported in the literature with the

use of microarray analysis (Urs et al., 2004). To our knowledge, only a few studies on genome analysis in whole human adipose tissue using DNA array have been reported to date (Gabrielsson et al., 2000; Urs et al., 2004). The majority of the research groups investigating adipogenesis reported in the literature have used as cell model murine cell lines, such as the 3T3-L1 (Kim et al., 2007). However, although rodents are accepted as appropriate models of adipogenesis, differences in basic physiology in comparison to humans that may affect gene expression do exist. Therefore, in this work the transcriptional profile of human adipocytes and preadipocytes was selected as a standard cell population, expressing adipogenic markers, with which the gene expression profiles of our adipogenic induced cells were compared.

A second comparison of the induced dermal fibroblasts with adipocytes deriving from human bone-marrow MSCs after adipogenic differentiaton was also conducted. Human adipocyte development can be studied *in vitro* starting from MSC cultures, which can be induced to follow the process of adipogenesis (Rosen and MacDougald, 2006). Human MSCs and their adipogenic differentiation potential have been studied thoroughly by numerous research groups in the past decades (Pittenger et al., 1999; Hung et al., 2002) and therefore they comprise a well-established model of adipogenesis. Under cultivation in a defined adipogenic medium, human MSCs differentiate into adipocytes in the same pattern as the pre-adipocyte murine cell lines 3T3-L1 and 3T3-F442A by acquiring an adipocyte-like phenotype, thus accumulating intracellular lipids and expressing genes that are expressed during adipogenesis (Janderova et al., 2003). Sekiya et al. (2003) assayed gene expression during and at the end-point of adipogenesis of human MSCs and provided novel makers for adipocytes from differentiated MSCs.

Microarray analysis was performed at the end-point of differentiation and therefore mostly evaluates the phenotype maturity of the induced cells rather than the sequence of events taking place during differentiation. It is important to mention that although data are analogous, a one-to-one comparison of fold changes of the regulated genes in our experiments versus regulated genes reported in the literature is not possible, mainly because the analyses are critically dependent on the algorithms and parameters, such as the thresholds that each group used. Therefore, comparison of fold changes was not performed. Results of the microarray analysis and important, adipocyte-specific genes were further confirmed by qRT-PCR and their time course was also evaluated.

4.3.1. Analysis of the differential expression of genes involved in lipid metabolism in adipogenic induced DFs30 and DFs76

DFs30

Microarray analysis identified an overall significant differential expression of 9,308 genes between the adipogenic induced DFs30 versus control DFs30 (≥ 2-fold change, $p<0.01$), among them 4,722 genes were significantly upregulated. After performing functional grouping analysis via annotations deriving from Gene Ontology, 222 involved in cell differentiation and 115 key genes implicated in lipid metabolism were found to be significantly upregulated in induced DFs30 (Table 9). All genes referred to in Table 9 constitute hallmarks of lipid metabolism and the genes: ACSM5, APOB, B3GNT5, CYP19A1, SULT1B1, SORBS1, PPARγ and leptin showed the most abundant upregulation among them (>20 fold-change). APOB is expressed in primary adipocytes and binding of APOB with LDL to adipocytes via the LDL receptor inhibits intracellular noradrenaline-induced lipolysis in adipocytes and thus it constitutes a novel signaling molecule from the liver to peripheral fat deposits that may play a key role in the metabolic syndrome (Skogsberg et al., 2008). B3GNT5 was reported as the most feasible candidate for lactotriaosylceramide synthase, an important enzyme in the synthesis of lacto- or neolacto-series carbohydrate chains of glycolipids (Togayachi et al., 2001), SORBS1 gene is an important adaptor protein in the insulin-signaling pathway in many molecular and cellular biology studies (Yang et al., 2003), it is highly expressed at mRNA level in the adipose tissues and has been implicated in the pathogenesis of human disorders with insulin resistance (Lin et al., 2001). Leptin is a peptide hormone primarily made and secreted by mature adipocytes and plays a major role in the regulation of body weight (Singh et al., 2012). Its action through the leptin receptor, which was also significantly upregulated in adipogenic induced DFs30 (Table 9), inhibits food intake and regulates energy loss to maintain constancy of adipose mass. Severe obesity and diabetes mellitus type 2 have been associated with dysregulation or mutation on the gene encoding leptin or its regulatory units (Coppari and Bjorbaek 2012). Upregulation of leptin in induced DFs30 was also confirmed via qRT-PCR, which showed a significant upregulation throughout the study period (Fig. 3.4.8.).

Interestingly, the glucose transporter protein GLUT4 and the fatty acid binding protein FABP4, which have been reported to play a key role in lipid metabolism, were not differentially expressed in the adipogenic induced DFs30, thus indicating that maybe our adipogenic induced fibroblasts do not possess exactly the same phenotype as mature adipocytes or that adipogenesis was somehow not complete. However, other isoforms of the

same superfamily were significantly upregulated, namely the GLUT5 (2.3 fold-change) and FABP5 (7.9 fold-change). GLUT5 is a fructose transporter and its levels are increased by glucose and to a greater extent by fructose (Gouyon et al., 2003). In a study conducted by Stuart et al (2007) the expression of muscle GLUT5 in type 2 diabetes mellitus was quantified and was found to be dramatically increased in diabetic muscle (muscle homogenates from biopsies of vastus lateralis before and after treatment with pioglitazone), whereas pioglitazone treatment reversed this overexpression. FABP4 together with FABP5 constitute genes involved in fatty acid uptake, transport and metabolism in adipocytes and bind both long-chain fatty acid and retinoic acid. Therefore, the significant upregulation of FABP5 in the induced DFs30 gives further evidence for the successful differentiation of dermal fibroblasts in adipocytes (Urs et al., 2004; Sumner-Thomson et al., 2011).

DFs76

In older fibroblasts markedly less genes were regulated than in younger fibroblasts, in total 4,786, among them 2,235 showed an upregulation. In the distinct functional categories, DFs76 overexpressed a smaller number of genes than younger fibroblasts, i.e. 159 genes involved in cell differentiation and 51 genes involved in lipid metabolism. 22 genes were overexpressed in common in both young and older induced fibroblasts (Table 13), however, key genes did not show any significant regulation in DFs76 (e.g. RBP4, LDLR, FABP5, phospholipases, GLUT5). Retinol-binding protein 4 (RBP4) is a novel adipocytokine and a marker of adipose tissue mass and obesity (Friebe et al., 2011) that was not regulated in induced DFs76. The induction of the low density lipoprotein receptor (LDLR) has recently been reported as a potential means by which PPARγ ligands regulate lipid metabolism and insulin sensitivity in adipocytes. However, the gene encoding LDLR was not expressed in older induced fibroblasts (Chui et al., 2005). On the other hand, genes with a key role in lipogenesis (LPL, LPLR, SCD) were positively expressed in both young and old fibroblasts, however, older fibroblasts exhibited a weaker regulation. Both leptin and leptin receptor, as well as LPL showed an overexpression in both induced cell types and the upregulation of these genes was detected throughout the study time by qRT-PCR (Fig. 3.4.4.).

Leptin expression increased over time in DFs30 during induction and this result is in line with findings of MacDougald et al. (1995), who have reported a gradual increase in leptin expression levels during adipogenesis. In the induced DFs76, leptin expression exhibited a dramatic increase after the first 8 days of adipogenic induction. However, its expression did not increase further, as it would be expected in normal adipogenesis, but showed a rapid decrease on the last day of induction.

LPL expression also increased gradually in young fibroblasts, which correlates well with the microarray data and data of Rakar et al. (2011). However, older fibroblasts, were not able to further increase the expression of LPL, which was higher after the first days of induction compared to the expression levels detected on the last day of the adipogenic treatment.

Taken together, these findings provide evidence that adipogenic induced fibroblasts from both young and old donors express genes of lipid metabolism that are normally expressed in adipocytes and show an inclination towards adipose-related physiological phenotypes and mechanisms. However, although older fibroblasts may be able to enter the process of adipogenesis and express markers of mature adipocytes, they are not able to complete the lipidogenic process and, therefore, exhibits significantly smaller number of genes involved in lipid metabolism and weaker regulation of the genes expressed in common with younger fibroblasts.

4.3.2. Analysis of the regulated signaling pathways of adipogenesis in the adipogenic induced DFs30 and DFs76

PPAR signaling pathway

Expression of PPARγ was significantly higher in both young and old fibroblasts after adipogenic induction (Table 13) and these results were confirmed by qRT-PCR (Fig. 3.4.4.). Ectopical expression of PPARγ has been shown to be enough to convert fibroblasts into preadipose-like cells and upon application of activators or PPARγ ligands, these cells can differentiate into fat cells (Spiegelman et al., 1997). Further studies on PPARγ confirmed that PPARγ is both necessary and sufficient for fat formation (Farmer, 2006). Known targets of the PPARγ transcriptional activity (i.e. LPL, CAP) (Tontonoz et al., 1994) were also upregulated in induced fibroblasts, however there were more of them in younger fibroblasts than in older ones (Fig. 3.4.2.3. and Fig. 3.4.3.3.). Moreover, we identified a significant upregulation of the transcriptional factor PPARγC1α, which is the co-activator of PPARγ in both induced DFs30 and DFs76. PPARγC1α induces the expression of genes that promote the differentiation of preadipocytes to brown adipocytes and it has been implicated in increasing the oxidation of fatty acids via increasing mitochondrial capacity and function (Medina-Gomez et al., 2007).

Interestingly, at the end of the adipogenic treatment, induced DFs30 showed no significant regulation of αvυ of the isoforms of the transcription factors of the CEBP family and only older fibroblasts overexpressed the isoform CEBPδ. It is known that CEBPδ

together with CEBPβ increase dramatically during the first stages of adipogenesis upon stimulation *in vitro* by a hormonal differentiation cocktail (Ramji and Foka, 2002) and subsequently induce the expression of PPARγ and ECBPα. Moreover, it has been reported that the accumulation of CEBPδ reaches a maximal level during the first two days of adipocyte differentiation and declines sharply before the onset of CEBPα accumulation (Cao et al., 1991). Therefore, the overexpression of CEBPδ in older fibroblasts may indicate the arrest of adipogenesis in the first stages of the process in these cells and may also explain the weaker expression of the PPARγ in older fibroblasts than in younger ones. Absence of CEBP expression in DFs30 may explain the partial and not universal lipid accumulation in our young induced cells and it has also been reported by Rakar et al, (2011) that attempted an adipogenic differentiation of dermal fibroblasts.

Phosphoinositide signaling pathway/ Insulin signaling pathway

The insulin/IGF-1 and phosphoinositide signaling pathways promote adipocyte differentiation via complex signaling networks. Phosphoinositide 3-kinase (PI3K), a lipid kinase, catalyzes phosphorylation of the D3 position of phosphoinositides and is important in a wide variety of cellular processes, including intracellular trafficking, organization of the cytoskeleton, cell growth and transformation, and prevention of apoptosis (Toker and Cantley, 1997). However, it has recently been reported that PI3K is required for murine and human adipocyte differentiation (Aubin et al., 2007) and the ability of preadipocytes to differentiate into mature adipocytes depends on the activation of PIK3 (Sorisky and Gagnon, 2008). Furthermore, specific inhibitors of PI3K and the phosphoinositide pathway block the adipocyte differentiation of 3T3-L1 pre-adipocytes into adipocytes, thus proving the involvement of PI3K in adipogenesis (Tomiyama et al., 1995; Xia and Serrero, 1999). Moreover, hyperglycemia enhances an ERK-mediated PI3K/Akt-dependent up-regulation of PPARγ expression, as well as an increase of adipocyte formation and adipogenic induction of lipid accumulation in MSCs under adipogenic medium (Chuang et al., 2007). Our data are in line with these observations, as numerous genes involved in the phosphoinositide pathway were positively expressed in the adipogenic induced DFs30 (Table 10), including the regulatory subunit 1 of the PIK3 (Table 10). A number of genes involved in this pathway, including the regulatory subunits 1 and 3 of the PIK3, were also regulated in the adipogenic induced DFs76 (Table 14), however these were less numerous than in induced DFs30.

FoxO1 belongs to the forkhead family of transcription factors, which are characterized by a distinct forkhead domain, it is regulated by insulin via Akt-dependent phosphorylation and

nuclear exclusion and its role in adipogenesis is still not fully understood. Recently, it was reported that suppression of FoxO1 mRNA using silence-RNA technology in the murine 3T3-L1 preadipocyte cell line resulted in significant decrease in lipid droplet formation during adipogenic differentiation (Munekata and Sakamoto, 2009). Furthermore, downregulation of FoxO1 decreased the expression of the transcription factors PPARγ and CEBPα, whereas CEBPβ and CEBPδ during the early period of adipocyte differentiation were not affected, thus providing evidence that FoxO1 plays an essential role in adipocyte differentiation, especially at the very early stage of terminal adipocyte differentiation (Munekata and Sakamoto, 2009). Both young and old adipogenic induced fibroblasts exhibited a significant upregulation of FoxO1 (Table 15).

IGF1 was found to be upregulated in both induced DFs30 and DFs76, which correlates well with published data reporting that IGF1 promotes adipogenesis (Zhao et al., 2012) and increases preadipocyte replication and differentiation (Hausman et al., 2001). A somewhat controversial result was that the IGF1 receptor exhibited a negative regulation in DFs30 and was not differentially expressed in DFs76. Reduction of IGF1 receptor expression in adipose tissue has been shown to result in a smaller volume of adipose tissue (Holzenberger et al., 2001) and upregulation of the gene encoding the receptor would be expected. A possible explanation could be that the levels of IGF1 receptor decrease after terminal differentiation and therefore they show a negative regulation in DFs30 and no differential expression in DFs76 (Boucher et al., 2010).

TGFb signaling pathway/ BMP signaling pathway

Many of the TGFβ superfamily members, such as TGFβ, BMPs and SMADs regulate the differentiation of numerous cell types, including adipocytes. Numerous studies report that TGF-b is a cytokine that stimulates preadipocyte proliferation (Choy et al., 2000) and at the same time inhibits adipogenesis *in vitro* (Derynck and Miyazono, 2007). In accordance with these findings, TGFβ was significantly downregulated in the adipogenic induced DFs30, however, no differential expression was observed in the DFs76 (Table 15).

Although previous reports confirm dual roles for many members of the BMP superfamily (BMP2, -4, -6, -7, and -9) in regulating adipogenesis and osteogenesis (Kang et al., 2009), there have been extensive studies of BMP4 for its proadipogenic activity (Zamani and Brown, 2011). Exposure of multipotent MSCs to BMP4 commits these cells to the adipocyte lineage, allowing them to undergo adipose conversion (Tang et al., 2004). BMP4 expression was

significantly upregulated in both young and old induced fibroblasts, a slightly stronger expression was detected in the DFs30.

A recent study on the role of the BMP3 [or else known as growth differentiation factor 10 (GDF10)] in the process of adipogenesis in MSCs reported that regulation of BMP3 does not promote the commitment of MSCs to the adipocyte lineage or the differentiation of preadipocytes to adipocytes. These results correlate well with our findings, which showed a significant downregulation of GDF10 in both induced DFs30 and DFs76, whereas younger fibroblasts exhibited a stronger regulation (Stewart et al., 2010).

Wnt signaling pathway

The Wnt family of secreted glycoproteins has a significant influence on adipogenesis. Activation of the Wnt/β-catenin signaling pathway inhibits adipogenesis, while disruption of Wnt signaling leads to spontaneous adipogenesis (Chung et al., 2012). In a recent study on the role of the Wnt signaling pathway during adipogenic differentiation of human MSCs the expression of the canonical WNT2, 10B, 13, and 14 was decreased, whereas non-canonical WNT4 and 11 increased, and WNT5A was unchanged (Shen et al., 2011). WNT2 showed a downregulation in both young and old induced fibroblasts, though the negative expression of WNT2 was stronger in the DFs30 (Table 15). Moreover, further members of the pathway exhibited significant downregulation in young fibroblasts (WNT3 and 4), whereas no regulation was identified in the older ones. WNT4 normally antagonizes adipogenesis and was shown to be downregulated in the adipose tissue of rats on high carbohydrate diet (Shankar et al., 2010). In adipogenic induced DFs30, WNT4 was strongly downregulated (100 fold change) compared to untreated fibroblasts.

Dickkopf 1 (Dkk1), a Wnt antagonist is secreted by human preadipocytes and promotes adipogenesis. Dkk1 mRNA increases 6 h after onset of human adipogenesis and this is followed by an increase in Dkk1 protein levels (Christodoulides et al., 2006). Further studies strengthen the positive effect of the induction of Dkk1 in adipogenesis (Gustafson and Smith, 2012) and our results, in which significant overexpression of Dkk1 in both young and old fibroblasts was observed, are consistent with these results.

Hedgehog signaling pathway

Hedgehog signaling has been reported to direct the lineage differentiation of mesodermal stem cells either towards the adipogenic or osteogenic phenotypes. Blockade of endogenous hedgehog signaling with the hedgehog antagonist cyclopamine, enhances adipogenesis at the

expense of osteogenesis (James et al., 2010). Target genes of the pathway, such as the Ptc1 and Gli1 have been shown to decrease significantly in vitro during adipogenic differentiation (James et al., 2010) and this finding correlates with our results. Gli1 was found to be negatively expressed in the young adipogenic induced fibroblasts, however old fibroblasts regulated none of the members of the hedgehog signaling pathway.

4.3.3. Result analysis of the transcription profile comparison between adipogenic induced DFs30 and DFs76 versus human adipocytes

The acquired adipocyte-like transcriptional phenotype of the adipogenic induced fibroblasts was confirmed by comparing their gene expression profiles with human adipocytes. The expression profile of the young induced fibroblasts exhibited a greater similarity to that of human adipocytes (approximately 25% similar gene expression) compared to old fibroblasts (approximately 18% similar gene expression), thus providing evidence that young fibroblasts are more capable of adipogenic differentiation than fibroblasts from older donors (Table 11a). The metabolism genes LPL, SCD, APOD, CHST (-2, -4, -7), GLUL and the transcription factors PPARγ, PPARγC1α, IGFBP2 and IGF1 belong to the genes that were in common significantly upregulated in human adipocytes and adipogenic induced DFs30 and DFs76.

Human adipocytes respond to treatment with insulin by expressing lipid-metabolizing genes such as those coding for FABP (Hunt et al., 1986), LPL (Fried et al., 1993) and GPD1 (Moustaid et al., 1990) and younger fibroblasts showed a positive expression of all these genes after adipogenic treatment. Old fibroblast only exhibited an upregulation for the gene coding for LPL, whereas FABP was not regulated and GPD1 was significantly downregulated. LPL is expressed as a homodimer in adipose tissue and has the dual function of a hydrolase and a ligand factor for receptor-mediated lipoprotein uptake, whereas GPD1 is responsible for re-esterification of fatty acids to form triacylglycerol (Urs et al., 2004).

SCD encodes an enzyme involved in fatty acid biosynthesis, primarily the synthesis of oleic acid, and it has been shown recently that it is required for the induction and maintenance of PPARγ protein levels and adipogenesis in 3T3-L1 cells (Christianson et al., 2008). SCD expression was slightly stronger in adipogenic induced DFs30 than DFs76 (Table 11a).

CHST1 has been described by Urs et al. (2004) as a marker of human mature adipocytes, however no significant regulation of this isoform could be identified either in the young or in the old induced fibroblasts. However, three further isoforms of CHST were significantly upregulated (CHST-2, -4, -7) in both DFs30 and DFs76 and one isoform only in DFs30

(CHST-6). Among them, CHST4 showed the strongest regulation in both cell types compared to other isoforms, whereas DFs30 exhibited a stronger regulation of CHST4 compared to DFs76 (Table 11a). CHST-2 and -4, like CHST1, are involved in the glycosaminoglycan biosynthesis pathway.

Except for the major transcription factors of adipogenesis PPARγ, PPARγC1α and IGF1 (analysis in section 4.3.2.), IGFBP2 was also significantly upregulated in both DFs30 and DFs76. The biological actions of IGFs are closely regulated by the IGF-binding proteins and it has been shown that IGFBP2 is the principal IGFBP secreted by white preadipocytes during adipogenesis (Boney et al., 1994). This finding was also confirmed by qRT-PCR, which showed a gradual, significant increase in the expression of IGFBP2 during the adipogenic treatment of both DFs30 and DFs76.

IGFBP3 was also found to be differentially expressed in the induced DFs30, specifically a significant downregulation was identified (Table 11a). Although IGFBP3 was not reported by Urs et al. (2004) as a hallmark of human mature adipocytes, it has been recently shown that it inhibits adipocyte differentiation of murine 3T3-L1 cell line via impacting on the PPARγ system (Chan et al., 2009). The fact that IGBP3 was negatively expressed in young fibroblasts further supports the notion that young fibroblasts succeeded in differentiating into adipocyte-like cells. IGFBP3 was not differentially expressed in old fibroblasts.

Further genes that are known as novel adipocyte markers that were significantly upregulated in young fibroblasts and not in old fibroblasts after adipogenic treatment are the HSD11β (11β-hydroxysteroid dehydrogenase) and CTSG (cathepsin G). HSD11β1 plays a significant functional role in the initiation of 3T3-L1 adipogenesis (Liu et al., 2008) and cathepsin G is highly expressed in human adipose tissue as this has been detected by RT-PCR (Karlsson et al., 1998). Moreover, adipogenic induced DFs76 expressed only apolipoprotein D and no further members of the apolipoprotein family, whereas young fibroblasts expressed apolipoprotein B and D, as well as the receptor for apolipoprotein B.

4.3.4. Result analysis of the transcription profile comparison between adipogenic induced DFs30 and DFs76 versus adipocytes from differentiated human MSCs

The transcriptional phenotype of the adipogenic induced fibroblasts was compared further to the gene expression profile of adipocytes produced after adipogenic differentiation of human bone-marrow MSCs (Sekiya et al., 2003). As in the case of the comparison to human

adipocytes, young fibroblasts showed a greater similarity to the adipogenic differentiated MSCs (approximately 66% similar gene expression) than old fibroblasts (approximately 35% similar gene expression), thus strengthening the notion that dermal fibroblasts from younger donors are more capable of adipogenic differentiation than skin fibroblasts from older donors. Most importantly, considering the data from the two comparisons collectively, at least on gene expression level, our adipogenic induced cells were more similar to adipogenic differentiated MSCs than to human adipocytes. A possible explanation could be that both gene and microRNA expression profiles of MSCs have been reported to be highly similar to those of fibroblasts, accounting well for their extensive phenotypic and functional overlaps (Covas et al., 2007; Bae et al., 2009). Some authors have even described both MSCs and fibroblasts as members of the same family (Haniffa et al., 2009).

Genes involved in metabolism, such as the TIMP4, MAOA, HAS1 and ADH1 were significantly upregulated in both young and old fibroblasts. TIMP4 is specifically expressed in adipose tissue and adipocytes in humans according to tissue-wide gene expression analysis of UniGene (Pontius et al., 2003) and GNF Gene Atlas (Su et al., 2004) and is highly regulated during adipogenesis (Melendez-Zajgla et al., 2008; Mariman and Wang, 2010). Its expression was strongly regulated in adipogenic induced DFs30 (94 fold change), as well as in DFs76, however in a weaker manner (14.7 fold change).

MAOA encodes mitochondrial enzymes, which catalyze the oxidative deamination of amines and an adipogenesis-related increase of this gene has been described in human adipocytes (Bour et al., 2007). Both adipogenic induced fibroblasts showed a positive expression of MAOA, in young fibroblasts the expression was again stronger.
Extracellular matrix components COMP and COL11A1 were also significantly upregulated in our induced cells. The increased expression of these genes has been also reported in other studies (Burton et al., 2002, Nakamura et al., 2003, Hung et al., 2004).

An interesting point to mention is the expression of the serum amyloid A protein (SAA1), which has been reported to take place during adipogenic differentiation of human MSCs. The encoded protein, being a major acute phase protein that is highly expressed in response to inflammation and tissue injury, plays an important role in HDL metabolism and cholesterol homeostasis and high levels of this protein are associated with chronic inflammatory diseases such as the Alzheimer's and Crohn's disease. Adipocytes have been reported to express SAA1 mRNA and protein and its production at this site is regulated by nutritional status (Poitou et al., 2005). Recently, it has been described that SAA induces lipolysis by downregulating perilipin through ERK1/2 and PKA signaling pathways (Liu et al., 2011), however, the exact

biological function of SAA, particularly its role in glucose and lipid metabolism, has yet to be fully established.

4.4. Concluding remarks

The data presented in this work illustrate that human dermal fibroblasts are not the "terminally differentiated" cells they were considered to be until currently but that they possess an inherent ability to differentiate along the mesenchymal lineage towards an adipocyte-like transcriptional phenotype upon treatment with specific induction media. Our results are consistent with the findings of other groups, which have also used dermal fibroblasts that were driven to differentiate not only towards adipocytes, but also towards chondrocytes, osteocytes and endothelial cells (Chen et al., 2007; Junker et al., 2010; Rakar et al., 2011). The capacity of skin fibroblasts to be a multipotent cell population is a very appealing one in the context of regenerative medicine and our results further strengthen this notion.

The fibroblasts that have been used in this work were isolated from human dermal specimens and exhibited a typical fibroblast-like, spindle-shaped morphology during their cultivation. Contamination of our fibroblast cultures with other cell types, such as adipocytes, endothelial cells or neural cells could be excluded, because these are negatively selected as they need different optimal growth environments.

Several regulatory genes of adipogenesis and lineage specific genes were significantly regulated in both young and old fibroblasts under the appropriate adipogenic induction media. Supplementation of the media with factors such as indomethacin, IBMX, dexamethasone and insulin is considered safe and these factors have been widely used in multiple clinical applications. Other groups have used viral vectors in order to drive cell differentiation and to generate highly potentive cells (Takahashi and Yamanaka, 2006), however their use may increase the risk of tumorigenesis and mutagenesis (Wu and Dunbar, 2011). The approach of using induction media with soluble factors as an alternative to genetic modification of cells may represent a very promising solution.

Our results also show that skin fibroblasts from younger donors represent a preferable population for future cell-based therapies compared to older donors. We have shown that the adipogenic potential decreases significantly with age and although fibroblasts from older donors are capable to enter the process of adipogenesis, they do not manage to accomplish the generation of healthy and functional adipocyte-like cells. It has been long known that ageing

has a major impact on skin, which gradually loses its structural and functional characteristics. Wound healing, angiogenesis, lipogenesis, sweat production, immune function, and vitamin D synthesis are some of the skin functions that deteriorate with increasing age (reviewed by Zouboulis and Makrantonaki, 2011). Among the most important biologic processes involved in skin aging are alterations in DNA repair and stability, mitochondrial function, cell cycle and apoptosis, extracellular matrix, lipid synthesis, ubiquitin-induced proteolysis and cellular metabolism (reviewed by Zouboulis and Makrantonaki, 2011). The decline of the inherent plasticity of cells with ageing, which has also been shown by other groups (Joine et al., 2012; Klatte-Schulz et al., 2012; Lohmann et al., 2012; Zaim et al., 2012; Zhang et al., 2012) may represent another important biologic process of skin ageing.

Further studies exploring the features of the adipogenic differentiated fibroblasts are required in order to fully characterise these cells and to prove their functionality and stability as adipocytes, both *in vitro* and *in vivo*. In the present study we focused on detecting the ability of skin fibroblasts to differentiate along the same lineage from which they derive, the mesenchymal lineage. Current research is focusing on showing that fibroblasts are also capable of a transdifferentiation, thus meaning across different germ layers, however further studies are needed to investigate the full potency of dermal fibroblasts. The application of these differentiated cells *in vivo* is a crucial step, which will prove the therapeutic quality of these cells.

Following the results of the present work, adipocyte-like cells could be used in cases of extended lipodystrophy, for example in facial wasting rehabilitation in HIV-positive patients, in cases of lipoatrophy such as the steroid-induced lipoatrophy, as well as in scientific cosmetic dermatology in the treatment of skin ageing, or even in rare genetic disease wherein symptoms resembling aspects of ageing manifest at a very early age, such as the Hutchinson Gilford Progeria Syndrome.

5. ABBREVIATIONS

AdipoQ	adiponectin
AGPAT2	sn-1-acylglycerol-3-phosphate acyltransferase 2
AS	adult stem cells
BAT	brown adipose tissue
BMP	bone morphogenetic protein
CFD	adipsin
CS	cancer stem cells
CK	cytokeratin
CREBP	cAMP response element binding protein
DP	dermal papilla
DS	dermal sheath
DEJ	dermo-epidermal junction
DEX	dexamethasone
DFs30	dermal fibroblasts from 30 year old female donor
DFs76	dermal fibroblasts from 76 year old female donor
DMSO	dimethylsulfoxide
ES	embryonic stem
EGF	epidermal growth factor
FABP4	fatty-acid-binding protein 4
FACS	fluorescence activated cell sorting
FSFs	foreskin fibroblasts
FSC	forward scatter
FGF	fibroblast growth factor
GAPDH	glyceraldehyde 3-phosphate dehydrogenase
GLUT4	glucose transporter 4
HF	hair follicle
IBMX	1-methyl-3-isobutylxanthine
IFE	interfollicular epithelium/epidermis
IL-6	interleukin-6
IGF	insulin growth factor
IGFBP	insulin-like growth factor binding protein
iPS	induced pluripotent stem

LEP	leptin
LPL	lipoprotein lipase
MIX	methyl-isobutyl-xanthine
MMP	matrix metalloproteinase
MSC	mesenchymal stem cells
PAI-1	plasminogen activator inhibitor-1
PIK3	phosphoinositide 3-kinase
PPAR	peroxisome-proliferator-activated receptor
qRT-PCR	quantitative real time polymerase chain reaction
RIN	RNA integrity number
SD	standard deviation
SG	sebaceous gland
Shh	sonic hedgehog
SKP	skin-derived precursors
SREBP-1c	sterol regulatory element binding transcription factor 1c
SSC	side scatter
TIMP	tissue inhibitor of metalloproteinase
TGF	transforming growth factor
TNF-α	tumor necrosis factor-alpha
WAT	white adipose tissue
Wnt	wingless-type

6. REFERENCES

Ailles LE and Weissman IL. Cancer stem cells in solid tumors. Curr Opin Biotechnol 2007;18:460-466.

Al Battah F, De Kock J, Vanhaecke T, Rogiers V. Current status of human adipose-derived stem cells: differentiation into hepatocyte-like cells. ScientificWorldJournal. 2011;11:1568-1581.

Alt E, Yan Y, Gehmert S, et al. Fibroblasts share mesenchymal phenotypes with stem cells, but lack their differentiation and colony-forming potential. Biol Cell 2011;103:197-208.

Anderson DJ, Gage FH, Weissman IL. Can stem cells cross lineage boundaries? Nature 2001;7:393–395.

Arnold I and Watt FM. c-Myc activation in transgenic mouse epidermis results in mobilisation of stem cells and differentiation of their progeny. Curr Biol 2001;11:558–568.

Aubin D, Gagnon A, Sorisky A. Phosphoinositide 3-kinase is required for human adipocyte differentiation in culture. Int J Obes Relat Metab Disord 2005;29:1006–1009.

Bartsch G, Yoo JJ, De Coppi P, et al. Propagation, expansion, and multilineage differentiation of human somatic stem cells from dermal progenitors. Stem Cells Dev 2005;14:337–348.

Belicchi M, Pisati F, Lopa R, et al. Human skin-derived stem cells migrate throughout forebrain and differentiate into astrocytes after injection into adult mouse brain. J Neurosci Res 2004;77:475-486.

Bae S, Ahn JH, Park CW, et al. Gene and microRNA expression signatures of human mesenchymal stromal cells in comparison to fibroblasts. Cell Tissue Res 2009;335:565-573.

Bi D, Chen FG, Zhang WJ, et al. Differentiation of human multipotent dermal fibroblasts into islet-like cell clusters. BMC Cell Biol 2010;11:46.

Blanpain C and Fuchs E. Epidermal stem cells of the skin. Annu Rev Cell Biol 2006;22: 339-373.

Blanpain C, Horsley V, Fuchs E. Epithelial stem cells: turning over new leaves. Cell 2007;128:445-458.

Blanpain C, Lowry WE, Geoghegan A, Polak L, Fuchs E. Self- renewal, multipotency, and the existence of two cell populations within an epithelial stem cell niche. Cell 2004;118:635–648.

Blüher S, Kratzsch J, Kiess W. Insulin-like growth factor I, growth hormone and insulin in white adipose tissue. Best Pract Res Clin Endocrinol Metab 2005;19:577-587.

Boheler KR. Stem cell pluripotency: a cellular trait that depends on transcription factors, chromatin state and a checkpoint deficient cell cycle. J Cell Physiol 2009;221:10–17.

Boney CM, Moats-Staats BM, Stiles AD, D'Ercole AJ. Expression of insulin-like growth factor-I (IGF-I) and IGF-binding proteins during adipogenesis. Endocrinology 1994;135: 1863-1868.

Bongso A and Lee EH. Stem Cells: Their definition, classification and sources. In: Stem Cells-From Bench to Bedside. World Scientific Publishing, Singapore, 2005:Chapter 1: 4.

Boucher J, Tseng YH, Kahn CR. Insulin and insulin-like growth factor-1 receptors act as ligand-specific amplitude modulators of a common pathway regulating gene transcription. J Biol Chem 2010;285:17235-17245.

Bour S, Daviaud D, Gres S, et al. Adipogenesis-related increase of semicarbazide-sensitive amine oxidase and monoamine oxidase in human adipocytes. Biochimie 2007;89:916-925.

Braun KM, Niemann C, Jensen UB, Sundberg JP, Silva-Vargas V, Watt FM. Manipulation of stem cell proliferation and lineage commitment: visualisation of label-retaining cells in whole mounts of mouse epidermis. Development 2003;130:5241–5255.

Brendel C, Kuklick L, Hartmann O, et al. Distinct gene expression profile of human mesenchymal stem cells in comparison to skin fibroblasts employing cDNA microarray analysis of 9600 genes. Gene Expr 2005;12:245-257.

Broad TE and Ham RG. Growth and adipose differentiation of sheep preadipocyte fibroblasts in serum-free medium. Eur J Biochem 1983;135:33-39.

Burgeson RE, Chiquet M, Deutzmann R, et al. A new nomenclature for the laminins. Matrix Biol 1994;14:209-211.

Burton GR, Guan Y, Nagarajan R, McGehee RE Jr. Microarray analysis of gene expression during early adipocyte differentiation. Gene 2002;293:21-31.

Cao Z, Umek RM, McKnight SL. Regulated expression of three C/EBP isoforms during adipose conversion of 3T3-L1 cells. Genes Dev 1991;5:1538-1552.

Chan SS, Schedlich LJ, Twigg SM, Baxter RC. Inhibition of adipocyte differentiation by insulin-like growth factor-binding protein-3. Am J Physiol Endocrinol Metab 2009;296:E654-663.

Chang HY, Chi JT, Dudoit S, et al. Diversity, topographic differentiation, and positional memory in human fibroblasts. Proc Natl Acad Sci USA 2002;99:12877-12882.

Chen FG, Zhang WJ, Bi D, et al. Clonal analysis of nestin(-) vimentin(+) multipotent fibroblasts isolated from human dermis. J Cell Sci 2007;120:2875–2883.

Chen Z, Torrens JI, Anand A, Spiegelman BM, Friedman JM. Krox20 stimulates adipogenesis via C/EBPbeta-dependent and -independent mechanisms. Cell Metab 2005;1:93–106.

Chien CC, Yen BL, Lee FK, et al. In vitro differentiation of human placenta-derived multipotent cells into hepatocyte-like cells. Stem Cells 2006;24:1759.

Choy L, Skillington J, Derynck R. Roles of autocrine TGF-β receptor and Smad signaling in adipocyte differentiation. J Cell Biol 2000;149:667–682.

Christianson JL, Nicoloro S, Straubhaar J, Czech MP. Stearoyl-CoA desaturase 2 is required for peroxisome proliferator-activated receptor gamma expression and adipogenesis in cultured 3T3-L1 cells. J Biol Chem 2008;283:2906-2916.

Christodoulides C, Laudes M, Cawthorn WP, et al. The Wnt antagonist Dickkopf-1 and its receptors are coordinately regulated during early human adipogenesis. J Cell Sci 2006;119:2613-2620.

Chuang CC, Yang RS, Tsai KS, Ho FM, Liu SH. Hyperglycemia enhances adipogenic induction of lipid accumulation: involvement of extracellular signal-regulated protein kinase 1/2, phosphoinositide 3-kinase/Akt, and peroxisome proliferator-activated receptor gamma signaling. Endocrinology 2007;148:4267-4275.

Chui PC, Guan HP, Lehrke M, Lazar MA. PPARgamma regulates adipocyte cholesterol metabolism via oxidized LDL receptor 1. J Clin Invest 2005;115:2244-2256.

Chung SS, Lee JS, Kim M, et al. Regulation of Wnt/β-catenin signaling by CCAAT/enhancer binding protein β during adipogenesis. Obesity (Silver Spring) 2012;20:482-487.

Cinti S. Between brown and white: novel aspects of adipocyte differentiation. Ann Med 2011;43:104–115.

Clarke SL, Robinson CE, Gimble JM. CAAT/enhancer binding proteins directly modulate transcription from the peroxisome proliferator-activated receptor gamma 2 promoter. Biochem Biophys Res Commun 1997;240:99-103.

Claudinot SM, Nicolas H, Oshima H, Rochat A, Barrandon Y. Long-term renewal of hair follicles from clonogenic multipotent stem cells. Proc Natl Acad Sci USA 2005;102:14677–14682.

Clayton E, Doupe DP, Klein AM, Winton DJ, Simons BD, Jones PH. A single type of progenitor cell maintains normal epidermis. Nature 2007;446:185–189.

ClinicalTrials.gov [Internet]. Bethesda (MD): National Library of Medicine, NCT01217008, A Phase 1 Safety Study of GRNOPC1 in Patients With Neurologically Complete, Subacute, Spinal Cord Injury 2010; http://clinicaltrials.gov/ct2/show/study/NCT01217008.

Conboy IM, Conboy MJ, Wagers AJ, et al. Rejuvenation of aged progenitor cells by exposure to a young systemic environment. Nature 2005;433:760-764.

Coppari R and Bjørbæk C. Leptin revisited: its mechanism of action and potential for treating diabetes. Nat Rev Drug Discov 2012;11:692-708.

Cornelius P, MacDougald OA, Lane MD. Regulation of adipocyte development. Annu Rev Nutr 1994;14:99-129.

Cotsarelis G, Sun TT, Lavker RM. Label-retaining cells reside in the bulge area of pilosebaceous unit: implications for follicular stem cells, hair cycle, and skin carcinogenesis. Cell 1990;61:1329-1337.

Covas DT, Panepucci RA, Fontes AM, et al. Multipotent mesenchymal stromal cells obtained from diverse human tissues share functional properties and gene-expression profile with CD146+ perivascular cells and fibroblasts. Exp Hematol 2008;36:642-564.

Crigler L, Kazhanie A, Yoon TJ, et al. Isolation of a mesenchymal cell population from murine dermis that contains progenitors of multiple cell lineages. FASEB J 2007;21:2050-2063.

Cypess AM, Zhang H, Schulz TJ et al. Insulin/IGF-I regulation of necdin and brown adipocyte differentiation via CREB- and FoxO1-associated pathways. Endocrinology 2011;152:3680-3689.

Dalerba P, Cho RW, Clarke MF. Cancer stem cells: models and concepts. Annu Rev Med 2007;58:267-284.

De Luca M, Tamura RN, Kajiji S, et al. Polarized integrin mediates human keratinocyte adhesion to basal lamina. Proc Natl Acad Sci USA 1990;87:6888-6892.

Derynck R and Miyazono Ko. The TGF-β family. Cold Spring Harbor, NY: Cold Spring Harbor Laboratory Press 2007

Dick JE. Stem cell concepts renew cancer research. Blood 2008;112:4793-807.

Ding DC, Shyu WC, Lin SZ. Mesenchymal stem cells. Cell Transplant 2011;20:5-14.

Driskell RR, Clavel C, Rendl M, Watt FM. Hair follicle dermal papilla cells at a glance. J Cell Sci 2011;124:1179–1182.

Driskell RR, Giangreco A, Jensen KB, Mulder KW, Watt FM. Sox2-positive dermal papilla cells specify hair follicle type in mammalian epidermis. Development 2009;136:2815-2823.

El-Jack AK, Hamm JK, Pilch PF, Farmer SR. Reconstitution of insulin-sensitive glucose transport in fibroblasts requires expression of both PPARG and C/EBPα J Biol Chem 1999;274:7946–7951.

Farmer SR. Transcriptional control of adipocyte formation. Cell Metab 2006;4: 263–273.

Feldon SE, O'loughlin CW, Ray DM, Landskroner-Eiger S, Seweryniak KE, Phipps RP. Activated human T lymphocytes express cyclooxygenase-2 and produce proadipogenic prostaglandins that drive human orbital fibroblast differentiation to adipocytes. Am J Pathol 2006;169:1183-1193.

Fernandes KJ, McKenzie IA, Mill P, et al. A dermal niche for multipotent adult skin-derived precursor cells. Nat Cell Biol 2004;6:1082-1093.

Fernandes KJ, Toma JG, Miller FD. Multipotent skin-derived precursors: Adult neural crest-related precursors with therapeutic potential. Philos Trans R Soc Lond B Biol Sci 2008;363:185–198.

Fisher GJ, Varani J, Voorhees JJ. Looking older: fibroblast collapse and therapeutic implications. Arch Dermatol 2008;144:666-672.

Friebe D, Neef M, Erbs S, et al. Retinol binding protein 4 (RBP4) is primarily associated with adipose tissue mass in children. Int J Pediatr Obes 2011;6:e345-352.

Fried SK, Russell CD, Grauso NL, Brolin RE. Lipoprotein lipase regulation by insulin and glucocorticoid in subcutaneous and omental adipose tissues of obese women and men. J Clin Investig 1993;92: 2191-2198.

Fuchs E. Skin stem cells: rising to the surface. J Cell Biol. 2008;180:273-84.

Fuchs E and Horsley V. More than one way to skin.... Genes Dev 2008;22:976–985.

Gabrielsson BL, Carlsson B and Carlsson LMS. Partial genome scale analysis of gene expression in human adipose tissue using DNA array. Obes Res 2000;8:374–384.

Gat U, DasGupta R, Degenstein L, Fuchs E. De novo hair follicle morphogenesis and hair tumors in mice expressing a truncated beta-catenin in skin. Cell 1998; 95:605–614.

Genome Center Maastricht. Biomedical Genomics. A systems approach to the central dogma of biology in health and disease. 2007 Retrieved from http://biomedicalgenomics.org/RNA_quality_control.html

Gesta S, Tseng YH, Kahn CR. Developmental origin of fat: tracking obesity to its source. Cell 2007;131:242–256.

Ghazizadeh S and Taichman LB. Multiple classes of stem cells in cutaneous epithelium: a lineage analysis of adult mouse skin. EMBO J 2001;20:1215–1222.

Gimble JM, Katz AJ, Bunnell BA. Adipose-derived stem cells for regenerative medicine. Circ Res 2007;100:1249–1260.

Gore A, Li Z, Fung HL, et al. Somatic coding mutations in human induced pluripotent stem cells. Nature 2011;471:63-67.

Gouyon F, Onesto C, Dalet V, Pages G, Leturque A, Brot-Laroche E. Fructose modulates GLUT5 mRNA stability in differentiated Caco-2 cells: role of cAMP-signalling pathway and PABP (polyadenylated-binding protein)-interacting protein (Paip) 2. Biochem J 2003;375:167-174.

Greenspan P and Fowler SD. Spectrofluorometric studies of the lipid probe, nile red. J Lipid Res 1985;26:781-789.

Greenspan P, Mayer EP, Fowler SD. Nile red: a selective fluorescent stain for intracellular lipid droplets. J Cell Biol 1985;100:965-973.

Gregoire FM. Adipocyte differentiation: from fibroblast to endocrine cell. Exp Biol Med 2001;226:997-1002.

Gregoire FM, Smas CM, Sul HS. Understanding adipocyte differentiation. Physiol Rev 1998;78:783-809.

Guilak F, Estes BT, Diekman BO, Moutos FT, Gimble JM. 2010 Nicolas Andry Award: Multipotent Adult Stem Cells from Adipose Tissue for Musculoskeletal Tissue Engineering. Clin Orthop Relat Res 2010; 468:2530–2540.

Guilak F, Lott KE, Awad HA, et al. Clonal analysis of the differentiation potential of human adipose-derived adult stem cells. J Cell Physiol 2006; 206:229–237.

Gundry RL, Burridge PW, Boheler KR. Pluripotent stem cell heterogeneity and the evolving role of proteomic technologies in stem cell biology. Proteomics 2011;11:3947-3961.

Gustafson B and Smith U. The WNT inhibitor Dickkopf 1 and bone morphogenetic protein 4 rescue adipogenesis in hypertrophic obesity in humans. Diabetes. 2012;61:1217-1224.

Hajer GR, van Haeften TW, Visseren FL. Adipose tissue dysfunction in obesity, diabetes, and vascular diseases. Eur Heart J 2008;29:2959-2971.

Haniffa, MA, Collin, MP, Buckley, CD, Dazzi, F. Mesenchymal stem cells: the fibroblasts' new clothes? Haematologica 2009;94:258-263.

Hausman DB, DiGirolamo M, Bartness TJ, Hausman GJ, Martin RJ. The biology of white adipocyte proliferation. Obes Rev 2001;2:239-254.

Hee CK and Nicoll SB. Induction of osteoblast differentiation markers in human dermal fibroblasts: potential application to bone tissue engineering. Eng Med Biol Soc 2006;1:521-524.

Hematti P. Human embryonic stem cell-derived mesenchymal progenitors: an overview. Methods Mol Biol 2011;690:163-174.

Hoffman RM. The pluripotency of hair follicle stem cells. Cell Cycle 2006;5:232– 233.

Holzenberger M, Hamard G, Zaoui R, et al. Experimental IGF-I receptor deficiency generates a sexually dimorphic pattern of organ-specific growth deficits in mice, affecting fat tissue in particular. Endocrinology 2001;142:4469–4478.

Hong KM, Belperio JA, Keane MP, Burdick MD, Strieter RM. Differentiation of human circulating fibrocytes as mediated by transforming growth factor-beta and peroxisome proliferator-activated receptor gamma. J Biol Chem 2007;282:22910-22920.

Hoogduijn MJ, Gorjup E, Genever PG. Comparative characterization of hair follicle dermal stem cells and bone marrow mesenchymal stem cells. Stem Cells Dev 2006;15:49-60.

Horsley V, O'Carroll D, Tooze R, et al. Blimp1 defines a progenitor population that governs cellular input to the sebaceous gland. Cell 2006;126:597–609.

Huang da W, Sherman BT, Lempicki RA. Systematic and integrative analysis of large gene lists using DAVID bioinformatics resources. Nat Protoc 2009;4:44–57.

Huang E, Bi Y, Jiang W, et al. Conditionally immortalized mouse embryonic fibroblasts retain proliferative activity without compromising multipotent differentiation potential. PLoS One 2012;7:e32428.

Hung SC, Chang CF, Ma HL, Chen TH, Low-Tone Ho L. Gene expression profiles of early adipogenesis in human mesenchymal stem cells. Gene 2004;340:141-150.

Hung SC, Chen NJ, Hsieh SL, Li H, Ma HL, Lo WH. Isolation and characterization of size-sieved stem cells from human bone marrow. Stem Cells 2002;20:249-258.

Hunt CR, Ro JH, Dobson DE, Min HY, Spiegelman BM. Adipocyte P2 gene: developmental expression and homology of 5-flanking sequences among fat cell-specific genes. Proc Natl Acad Sci USA 1986;83:3786-3790.

Inoue K, Aoi N, Sato T, et al. Differential expression of stem-cell-associated markers in human hair follicle epithelial cells. Lab Invest 2009;89:844-856.

Ishii M, Koike C, Igarashi A, et al. Molecular markers distinguish bone marrow mesenchymal stem cells from fibroblasts. Biochem Biophys Res Commun 2005;332:297–303.

Ito M, Liu Y, Yang Z, et al. Stem cells in the hair follicle bulge contribute to wound repair but not to homeostasis of the epidermis. Nat. Med 2005;11:1351–1354.

Jääger K and Neuman T. Human dermal fibroblasts exhibit delayed adipogenic differentiation compared with mesenchymal stem cells. Stem Cells Dev 2011;20:1327-1336.

Jahoda CAB, Whitehouse CJ, Reynolds AJ, Hole N. Hair follicle dermal cells differentiate into adipogenic and osteogenic lineages. Exp Dermatol 2003;12:849–859.

James AW, Leucht P, Levi B, et al. Sonic Hedgehog influences the balance of osteogenesis and adipogenesis in mouse adipose-derived stromal cells. Tissue Eng Part A 2010;16:2605-2616.

Janderová L, McNeil M, Murrell AN, Mynatt RL, Smith SR. Human mesenchymal stem cells as an in vitro model for human adipogenesis. Obes Res 2003;11:65-74.

Jensen KB and Watt FM. Single-cell expression profiling of human epidermal stem and transit-amplifying cells: Lrig1 is a regulator of stem cell quiescence. Proc Natl Acad Sci USA 2006;103:11958-11963.

Jiang S, Zhao L, Purandare B, Hantash BM. Differential expression of stem cell markers in human follicular bulge and interfollicular epidermal compartments. Histochem Cell Biol 2010;133:455-465.

Jiang Y, Jahagirdar BN, Reinhardt RL, et al. Pluripotency of mesenchymal stem cells derived from adult marrow. Nature 2002;418:41-49.

Joannides A, Gaughwin P, Schwiening C, et al. Efficient generation of neural precursors from adult human skin: astrocytes promote neurogenesis from skin-derived stem cells. Lancet 2004;364:172-178.

Joiner DM, Tayim RJ, Kadado A, Goldstein SA. Bone marrow stromal cells from aged male rats have delayed mineralization and reduced response to mechanical stimulation through nitric oxide and ERK1/2 signaling during osteogenic differentiation. Biogerontology 2012;13:467-478.

Jones PH, Simons BD, Watt FM. Sic transit gloria: farewell to the epidermal transit amplifying cell? Cell Stem Cell 2007;1:371-381.

Jones PH and Watt FM. Separation of human epidermal stem cells from transit amplifying cells on the basis of differences in integrin function and expression. Cell 1993;73:713-724.

Junker JP, Sommar P, Skog M, Johnson H, Kratz G. Adipogenic, chondrogenic and osteogenic differentiation of clonally derived human dermal fibroblasts. Cells Tissues Organs 2010;191:105-118.

Kaji K, Norrby K, Paca A, Mileikovsky M, Mohseni P, Woltjen K. Virus-free induction of pluripotency and subsequent excision of reprogramming factors. Nature 2009;458:771-775.

Kanitakis J. Anatomy, histology and immunohistochemistry of normal human skin. Eur J Dermatol 2002;12: 390-399.

Kang Q, Song WX, Luo Q, et al. A comprehensive analysis of the dual roles of BMPs in regulating adipogenic and osteogenic differentiation of mesenchymal progenitor cells. Stem Cells Dev 2009;18:545–559.

Kapoor M, McCann M, Liu S, et al. Loss of peroxisome proliferator-activated receptor gamma in mouse fibroblasts results in increased susceptibility to bleomycin-induced skin fibrosis. Arthritis Rheum 2009;60:2822-2829.

Karlsson C, Lindell K, Ottosson M, Sjöström L, Carlsson B, Carlsson LM. Human adipose tissue expresses angiotensinogen and enzymes required for its conversion to angiotensin II. J Clin Endocrinol Metab 1998;83:3925-3929.

Karnovsky MJ. A formaldehyde-glutaraldehyde fixative of high osmolarity for use in electron microscopy. J Cell Biol 1965;27:137A.

Katz AJ, Llull R, Hedrick MH, Futrell JW. Emerging approaches to the tissue engineering of fat. Clin Plast Surg 1999;26:587-603.

Kim B, Yoon BS, Moon JH, et al. Differentiation of human labia minora dermis-derived fibroblasts into insulin-producing cells. Exp Mol Med 2012;44:26-35.

Kim JB, Sarraf P, Wright M, et al. Nutritional and insulin regulation of fatty acid synthetase and leptin gene expression through ADD1/SREBP1. J Clin Invest 1998;101:1-9.

Kim SJ, Lee KH, Lee YS, Mun EG, Kwon DY, Cha YS. Transcriptome analysis and promoter sequence studies on early adipogenesis in 3T3-L1 cells. Nutr Res Pract 2007;1:19-28.

Klatte-Schulz F, Pauly S, Scheibel M, et al. Influence of age on the cell biological characteristics and the stimulation potential of male human tenocyte-like cells. Eur Cell Mater 2012;24:74-89.

Krebsbach PH, Gu K, Franceschi RT, Rutherford RB. Gene therapy-directed osteogenesis: BMP-7-transduced human fibroblasts form bone in vivo. Hum Gene Ther 2000;11:1201-1210.

Kumamoto T, Shalhevet D, Matsue H, et al. Hair follicles serve as local reservoirs of skin mast cell precursors. Blood 2003;102:1654–1660.

Lechler T and Fuchs E. Asymmetric cell divisions promote stratification and differentiation of mammalian skin. Nature 2005;437:275–280.

Levy V, Lindon C, Zheng Y, Harfe BD, Morgan BA. Epidermal stem cells arise from the hair follicle after wounding. FASEB J 2007;21:1358–1366.

Lin WH, Chiu KC, Chang HM, Lee KC, Tai TY, Chuang LM. Molecular scanning of the human sorbin and SH3-domain-containing-1 (SORBS1) gene: positive association of the T228A polymorphism with obesity and type 2 diabetes. Hum Mol Genet 2001;10:1753-1760.

Liu LR, Lin SP, Chen CC, et al. Serum amyloid A induces lipolysis by downregulating perilipin through ERK1/2 and PKA signaling pathways. Obesity (Silver Spring). 2011;19:2301-2309.

Liu S, Liu S, Wang X, et al. The PI3K-Akt pathway inhibits senescence and promotes self-renewal of human skin-derived precursors in vitro. Aging Cell 2011;10:661-674.

Liu Y, Park F, Pietrusz JL, et al. Suppression of 11beta-hydroxysteroid dehydrogenase type 1 with RNA interference substantially attenuates 3T3-L1 adipogenesis. Physiol Genomics 2008;32:343-351.

Livak KJ and Schmittgen TD. Analysis of relative gene expression data using real-time quantitative PCR and the 2(-Delta Delta C(T)) Methods 2001;25:402-408.

Lo Celso C, Berta MA, Braun KM, et al. Characterisation of bipotential epidermal progenitors derived from human sebaceous gland: contrasting roles of c-Myc and b-catenin. Stem Cells 2008;26:1241–1252.

Lo Celso C, Prowse DM, Watt FM. Transient activation of β-catenin signalling in adult mouse epidermis is sufficient to induce new hair follicles but continuous activation is required to maintain hair follicle tumours. Development 2004;131:1787–1799.

Lohmann M, Walenda G, Hemeda H, et al. Donor age of human platelet lysate affects proliferation and differentiation of mesenchymal stem cells. PLoS One 2012;7:e37839. doi: 10.1371/journal.pone.0037839.

Lozito TP and Tuan RS. Mesenchymal stem cells inhibit both endogenous and exogenous MMPs via secreted TIMPs, J Cell Physiol 2011;226(2):385–396.

Lyle S, Christofidou-Solomidou M. et al. The C8/144B monoclonal antibody recognizes cytokeratin 15 and defines the location of human hair follicle stem cells. J Cell Sci 1998;111:3179–3188.

Lysy PA, Smets F, Sibille C, et al. Human skin fibroblasts: from mesodermal to hepatocyte-like differentiation. Hepatology 2007;46:1574.

MacDougald OA, Hwang CS, Fan H, Lane MD. Regulated expression of the obese gene product (leptin) in white adipose tissue and 3T3-L1 adipocytes. Proc Natl Acad Sci USA 1995;92:9034-9037.

Maherali N, Sridharan R, Xie W, et al. Directly reprogrammed fibroblasts show global epigenetic remodeling and widespread tissue contribution. Cell Stem Cell 2007;1:55–70.

Mariman EC and Wang P. Adipocyte extracellular matrix composition, dynamics and role in obesity. Cell Mol Life Sci 2010;67:1277-1292.

McGrath JA and Uitto J. Anatomy and organisation of human skin. In: Rook's Textbook of Dermatology. 8th ed. Blackwell Publishing 2010: pp. 3.1–3.6.

Medina-Gomez G, Gray S, Vidal-Puig A. Adipogenesis and lipotoxicity: role of peroxisome proliferator-activated receptor gamma (PPARgamma) and PPARgammacoactivator-1 (PGC1). Public Health Nutr 2007;10:1132-1137.

Melendez-Zajgla J, Del Pozo L, Ceballos G, Maldonado V. Tissue inhibitor of metalloproteinases-4. The road less traveled. Mol Cancer 2008;7:85.

Mitalipov S and Wolf D. Totipotency, pluripotency and nuclear reprogramming. Adv Biochem Eng Biotechnol. 2009;114:185-199.

Mizuno S and Glowacki J. Chondroinduction of human dermal fibroblasts by demineralized bone in three-dimensional culture. Exp Cell Res 1996;227:89-97.

Montserrat N, Ramirez-Bajo MJ, Xia Y, et al. Generation of induced pluripotent stem cells from human renal proximal tubular cells with only two transcription factors: OCT4 and SOX2. J Biol Chem 2012;287:24131-24138.

Moore KA and Lemischka IR. Stem cells and their niches. Science 2006;311:1880–1885.

Morrison RF and Farmer SR. Hormonal signaling and transcriptional control of adipocyte differentiation. J Nutr 2000;130:3116S-3121S.

Morrison SJ and Kimble J. Asymmetric and symmetric stem-cell divisions in development and cancer. Nature 2006;441:1068–1074.

Moustaid N, Lasnier F, Hainque B, Quignard-Boulange A Pairault J. Analysis of gene expression during adipogenesis in 3T3–F442A preadipocytes: insulin and dexamethasone control. J Cell Biochem 1990;42:243–254.

Munekata K and Sakamoto K. Forkhead transcription factor Foxo1 is essential for adipocyte differentiation. In Vitro Cell Dev Biol Anim 2009;45:642-651.

Nakamura T, Shiojima S, Hirai Y, et al. Temporal gene expression changes during adipogenesis in human mesenchymal stem cells. Biochem Biophys Res Commun 2003;303:306-312.

Narvaez D, Kanitakis J, Claudy A. Immunohistochemical study of CD34-positive dermal dendritic cells of normal human skin. Am J Dermatopathol 1996;18:283-288.

Niemela S, Miettinen S, Sarkanen JR and Ashammakhi N. Adipose Tissue and Adipocyte Differentiation: Molecular and Cellular Aspects and Tissue Engineering Applications. In: Ashammakhi N, Reis R and Chiellini F, eds. Topics in Tissue Engineering. 4th ed. Expertissues e-books, Oulu, Finland 2008;4:1-26.

Ntambi JM and Young-Cheul K. Adipocyte differentiation and gene expression. J Nutr 2000;130:3122S-3126S.

Ohyama M, Terunuma A, Tock CL, et al. Characterization and isolation of stem cell-enriched human hair follicle bulge cells. J Clin Invest 2006;116:249-260.

Okita K, Ichisaka T, Kobayashi T, et al. Generation of germline-competent induced pluripotent stem cells. Nature 2007;448:313–317.

Osborne TF. Sterol regulatory element-binding proteins (SREBPs): key regulators of nutritional homeostasis and insulin action. J Biol Chem 2000;275:32379-32382.

Oshima H, Rochat A, Kedzia C, Kobayashi K, Barrandon Y. Morphogenesis and renewal of hair follicles from adult multipotent stem cells. Cell 2001;104:233-245.

Park IH, Zhao R, West JA, et al. Reprogramming of human somatic cells to pluripotency with defined factors. Nature 2008;451:141–146.

Patrick CW Jr. Tissue engineering strategies for adipose tissue repair. Anat Rec 2001;263:361-366.

Pittenger MF, Mackay AM, Beck SC, et al. Multilineage potential of adult human mesenchymal stem cells. Science 1999;284:143-147.

Poitou C, Viguerie N, Cancello R, et al. Serum amyloid A: production by human white adipocyte and regulation by obesity and nutrition. Diabetologia 2005;48:519-528.

Pontius J, Wagner L, Schuler G. UniGene: a unified view of the transcriptome. In: Pontius J, Wagner L, Schuler G, editors. The NCBI handbook. Bethesda: National Center for Biotechnology Information; 2003.

Potten CS and Morris RJ. Epithelial stem cells in vivo. J Cell Sci Suppl 1988;10:45- 62.

Prigione A, Hossini AM, Lichtner B, et al. Mitochondrial-associated cell death mechanisms are reset to an embryonic-like state in aged donor-derived iPS cells harboring chromosomal aberrations. PLoS ONE 2011;6:e27352.

Quan TE, Cowper S, Wu SP, Bockenstedt LK, Bucala R. Circulating fibrocytes: collagen-secreting cells of the peripheral blood. Int J Biochem Cell Biol 2004;36:598–606.

Quatresooz P, Piérard-Franchimont C, Piérard GE. The thousand and one facets of skin stem cells. The future has found new roots. Rev Med Liege 2012;67:143-146.

Rakar J, Lönnqvist S, Sommar P, Junker J, Kratz G. Interpreted gene expression of human dermal fibroblasts after adipo-, chondro- and osteogenic phenotype shifts. Differentiation 2012;84:305-313.

Ramji DP and Foka P. CCAAT/enhancer-binding proteins: structure, function and regulation. Biochem J 2002;365:561–575.

Rosen ED, Hsu CH, Wang X, et al. C/EBPalpha induces adipogenesis through PPARgamma: a unified pathway. Genes Dev 2002;16:22-26.

Rosen ED and MacDougald OA. Adipocyte differentiation from the inside out. Nature reviews 2006;7:885-896.

Rosen ED and Spiegelman BM. Molecular regulation of adipogenesis. Annu Rev Cell Dev Biol 2000;16:145-171.

Rutherford RB, Gu K, Racenis P, Krebsbach PH. Early events: the in vitro conversion of BMP transduced fibroblasts to chondroblasts. Connect Tissue Res 2003;44:117-123.

Rutherford RB, Moalli M, Franceschi RT, Wang D, Gu K, Krebsbach PH. Bone morphogenetic protein-transduced human fibroblasts convert to osteoblasts and form bone in vivo. Tissue Eng 2002;8:441-452.

Saely CH, Geiger K, Drexel H. Brown versus white adipose tissue: a mini-review. Gerontology 2012;58:15-23.

Schwartz SD, Hubschman JP, Heilwell G, et al. Embryonic stem cell trials for macular degeneration: a preliminary report. Lancet 2012;379:713-720.

Sekiya I, Larson BL, Vuoristo JT, Cui JG, Prockop DJ. Adipogenic differentiation of human adult stem cells from bone marrow stroma (MSCs). J Bone Miner Res 2004;19:256-264.

Sellheyer K and Krahl D. Blimp-1: a marker of terminal differentiation but not of sebocytic progenitor cells. J Cutan Pathol 2010;37:362-370.

Seo MJ, Suh SY, Bae YC, Jung JS. Differentiation of human adipose stromal cells into hepatic lineage in vitro and in vivo. Biochem Biophys Res Commun 2005;328:258–264.

Shankar K, Harrell A, Kang P, Singhal R, Ronis MJ, Badger TM. Carbohydrate-responsive gene expression in the adipose tissue of rats. Endocrinology 2010;151:153-164.

Shao D and Lazar MA. Peroxisome proliferator activated receptor gamma, CCAAT/enhancer-binding protein alpha, and cell cycle status regulate the commitment to adipocyte differentiation. J Biol Chem 1997;272:21473-21478.

Sharpless NE and DePinho RA. How stem cells age and why this makes us grow old. Nat Rev Mol Cell Biol 2007;8:703-713.

Shen L, Glowacki J, Zhou S. Inhibition of adipocytogenesis by canonical WNT signaling in human mesenchymal stem cells. Exp Cell Res 2011;317:1796-1803.

Si YL, Zhao YL, Hao HJ, Fu XB, Han WD. MSCs: Biological characteristics, clinical applications and their outstanding concerns. Ageing Res Rev 2011;10:93-103.

Sieber-Blum M, Grim M et al. Pluripotent neural crest stem cells in the adult hair follicle. Dev Dyn 2004;231:258.

Singh P, Peterson TE, Sert-Kuniyoshi FH, et al. Leptin signaling in adipose tissue: role in lipid accumulation and weight gain. Circ Res 2012;111:599-603.

Skogsberg J, Dicker A, Rydén M, et al. ApoB100-LDL acts as a metabolic signal from liver to peripheral fat causing inhibition of lipolysis in adipocytes. PLoS One 2008;3:e3771.

Smas CM, Chen L, Zhao L, Latasa MJ, Sul HS. Transcriptional repression of pref-1 by glucocorticoids promotes 3T3-L1 adipocyte differentiation. J Biol Chem 1999;274:12632-12641.

Sorisky A and Gagnon A. Measurement of phosphoinositide 3-kinase and its products to study adipogenic signal transduction. Methods Mol Biol 2008;456:317-325.

Sorrell JM and Caplan AI. Fibroblast heterogeneity: more than skin deep. J Cell Sci 2004;117:667-675.

Spiegelman BM, Hu E, Kim JB, Brun R. PPAR gamma and the control of adipogenesis. Biochimie 1997;79:111-112.

Stern MM and Bickenbach JR. Epidermal stem cells are resistant to cellular aging. Aging Cell 2007;6:439-452.

Stewart A, Guan H, Yang K. BMP-3 promotes mesenchymal stem cell proliferation through the TGF-beta/activin signaling pathway. J Cell Physiol 2010;223:658-666.

Stuart CA, Howell ME, Yin D. Overexpression of GLUT5 in diabetic muscle is reversed by pioglitazone. Diabetes Care 2007;30:925-931.

Styner M, Sen B, Xie Z, Case N, Rubin J. Indomethacin promotes adipogenesis of mesenchymal stem cells through a cyclooxygenase independent mechanism. J Cell Biochem 2010;111:1042-1050.

Su AI, Wiltshire T, Batalov S, et al. A gene atlas of the mouse and human protein-encoding transcriptomes. Proc Natl Acad Sci USA 2004;101:6062–6067.

Sudo K, Kanno M, Miharada K, et al. Mesenchymal progenitors able to differentiate into osteogenic, chondrogenic, and/or adipogenic cells in vitro are present in most primary fibroblast-like cell populations. Stem Cells 2007;25:1610-1617.

Sumner-Thomson JM, Vierck JL, McNamara JP. Differential expression of genes in adipose tissue of first-lactation dairy cattle. J Dairy Sci 2011;94:361-369.

Sun N, Longaker MT, Wu JC. Human iPS cell-based therapy: considerations before clinical applications. Cell Cycle 2010;9:880-885.

Takahashi K and Yamanaka S. Induction of pluripotent stem cells from mouse embryonic and adult fibroblast cultures by defined factors. Cell 2006;126:663-676.

Takahashi K, Tanabe K, Ohnuki M, et al. Induction of pluripotent stem cells from adult human fibroblasts by defined factors. Cell 2007;30:861-872.

Tang QQ, Otto TC and Lane MD. Commitment of C3H10T1/2 pluripotent stem cells to the adipocyte lineage. Proc Natl Acad Sci USA 2004;101:9607–9611.

Thomson JA, Itskovitz-Eldor J, Shapiro SS, et al. Embryonic stem cell lines derived from human blastocysts. Science 1998;282:1145-1147.

Tirino V, Desiderio V, Paino F, et al. Cancer stem cells in solid tumors: an overview and new approaches for their isolation and characterization. FASEB J 2013;27:13-24.

Tobin DJ, Gunin A, Magerl M, Paus R. Plasticity and cytokinetic dynamics of the hair follicle mesenchyme during the hair growth cycle: implications for growth control and hair follicle transformations. J Invest Dermatol 2003;8:80–86.

Togayachi A, Akashima T, Ookubo R, et al. Molecular cloning and characterization of UDP-GlcNAc:lactosylceramide beta 1,3-N-acetylglucosaminyltransferase (beta 3Gn-T5), an essential enzyme for the expression of HNK-1 and Lewis X epitopes on glycolipids. J Biol Chem 2001;276:22032-22040.

Toker A and Cantley LC. Signalling through the lipid products of phosphoinositide-3-OH kinase. Nature 1997;387:673–676.

Toma JG, Akhavan M, Fernandes KJ, et al. Isolation of multipotent adult stem cells from the dermis of mammalian skin. Nat Cell Biol 2001;3:778–784.

Toma JG, McKenzie IA, Bagli D, Miller FD. Isolation and characterization of multipotent skin-derived precursors from human skin. Stem Cells 2005;23:727–737.

Tomiyama K, Nakata H, Sasa H, Arimura S, Nishio E, Watanabe Y. Wortmannin, a specific phosphatidylinositol 3-kinase inhibitor, inhibits adipocytic differentiation of 3T3-L1 cells. Biochem Biophys Res Commun 1995;212:263–269.

Tontonoz P, Hu E, Spiegelman BM. Stimulation of adipogenesis in fibroblasts by PPAR gamma 2, alipid-activated transcription factor. Cell 1994;79:1147-1156.

Trivedi NR, Cong Z, Nelson AM, et al. Peroxisome proliferator-activated receptors increase human sebum production. J Invest Dermatol 2006;126:2002–2009.

Tsuji W, Inamoto T, Yamashiro H, et al. Adipogenesis Induced by Human Adipose Tissue-Derived Stem Cells. Tissue Eng Part A 2009;15:83-93.

Tumbar T, Guasch V, Greco V, et al. Defining the epithelial stem cell niche in skin. Science 2004;303:359–363.

Uitto J. Collagen. In: Fitzpatrick TB, Eisen AZ, Wolff K, Freedbrg IM, Austen KF, editors. Dermatology in General Medicine. New York: McGraw-Hill; 1993;299–314.

Urs S, Smith C, Campbell B, et al. Gene expression profiling in human preadipocytes and adipocytes by microarray analysis. J Nutr. 2004;134:762-770.

Vaculik C, Schuster C, Bauer W, et al. Human dermis harbors distinct mesenchymal stromal cell subsets. J Invest Dermatol. 2012;132:563-574.

Verfaillie CM. Multipotent adult progenitor cells: an update. Novartis Found Symp 2005;265:55-61.

Watt FM and Jensen KB. Epidermal stem cell diversity and quiescence. EMBO Mol Med 2009;1:260-267.

Wei J, Ghosh AK, Sargent JL, et al. PPARγ downregulation by TGFß in fibroblast and impaired expression and function in systemic sclerosis: a novel mechanism for progressive fibrogenesis. PLoS One 2010;5:e13778.

Welter JF, Penick KJ, Solchaga LA. Assessing adipogenic potential of mesenchymal stem cells: a rapid three-dimensional culture screening technique. Stem Cells Int 2013;2013:806525.

Wernig M, Meissner A, Foreman R, et al. In vitro reprogramming of fibroblasts into a pluripotent ES-cell- like state. Nature 2007;448:318–324.

Wong VW, Levi B Rajadas J, Longaker MT, Gurtner GC. Stem cell niches for skin regeneration. Int J Biomater 2012; 926059.

Wong T, McGrath JA, Navsaria H. The role of fibroblasts in tissue engineering and regeneration. Br J Dermatol 2007;156:1149-1155.

Wróbel A, Seltmann H, Fimmel S, et al. Differentiation and apoptosis in human immortalized sebocytes. J Invest Dermatol 2003;120:175-181.

Wu C and Dunbar CE. Stem cell gene therapy: the risks of insertional mutagenesis and approaches to minimize genotoxicity. Front Med 2011;5:356-371.

Wu Z, Bucher NL, Farmer SR. Induction of peroxisome proliferator-activated receptor gamma during the conversion of 3T3 fibroblasts into adipocytes is mediated by C/EBPbeta, C/EBPdelta, and glucocorticoids. Mol Cell Biol 1996;16:4128-4136.

Xia X and Serrero G. Inhibition of adipose differentiation by phosphatidylinositol 3-kinase inhibitors. J Cell Physiol 1999;178:9–16.

Yang CC and Cotsarelis G. Review of hair follicle dermal cells. J Dermatol Sci 2010;57:2.

Yang L and Peng R. Unveiling hair follicle stem cells. Stem Cell Rev 2010;6:658–664.

Yang WS, Lee WJ, Huang KC. mRNA levels of the insulin-signaling molecule SORBS1 in the adipose depots of nondiabetic women. Obes Res 2003;11:586-590.

Yang YI, Kim HI, Choi MY, et al. Ex vivo organ culture of adipose tissue for in situ mobilization of adipose-derived stem cells and defining the stem cell niche. J Cell Physiol 2010;224:807–816.

Young HE and Black AC Jr. Adult stem cells. Anat Rec A Discov Mol Cell Evol Biol 2004;276:75-102.

Young HE, Steele TA, Bray RA, et al. Human reserve pluripotent mesenchymal stem cells are present in the connective tissues of skeletal muscle and dermis derived from fetal, adult, and geriatric donors. Anat Rec 2001;264:51–62.

Yu J, Vodyanik MA, Smuga-Otto K, et al. Induced pluripotent stem cell lines derived from human somatic cells. Science 2007;318:1917-1920.

Zaim M, Karaman S, Cetin G, Isik S. Donor age and long-term culture affect differentiation and proliferation of human bone marrow mesenchymal stem cells. Ann Hematol 2012;91:1175-1186.

Zainuddin A, Makpol S, Chua KH, Abdul Rahim N, Yusof YA, Ngah WZ. GAPDH as housekeeping gene for human skin fibroblast senescent model. Med J Malaysia. 2008;63:73-74.

Zamani N and Brown CW. Emerging Roles for the Transforming Growth Factor-β Superfamily in Regulating Adiposity and Energy Expenditure. Endocr Rev 2011;32:387–403.

Zhang J, An Y, Gao LN, Zhang YJ, Jin Y, Chen FM.The effect of aging on the pluripotential capacity and regenerative potential of human periodontal ligament stem cells. Biomaterials 2012;33:6974-6986.

Zhao P, Deng Y, Gu P, et al. Insulin-like growth factor 1 promotes the proliferation and adipogenesis of orbital adipose-derived stromal cells in thyroid-associated ophthalmopathy. Exp Eye Res 2013;107:65-73.

Zhao MT, Whitworth KM, Zhang X, et al. Deciphering the mesodermal potency of porcine skin-derived progenitors (SKP) by microarray analysis. Cell Reprogram 2010;12:161-173.

Zouboulis CC. Acne and sebaceous gland function. Clin Dermatol 2004;22:360-366.

Zouboulis CC, Adjaye J, Akamatsu H, Moe-Behrens G, Niemann C. Human skin stem cells and the ageing process. Exp Gerontol 2008;43:986-997.

Zouboulis CC and Makrantonaki E. Clinical aspects and molecular diagnostics of skin aging. Clin Dermatol 2011;29:3-14.

Eidesstattliche Versicherung

„Ich, ‚Vasiliki Zampeli, versichere an Eides statt durch meine eigenhändige Unterschrift, dass ich die vorgelegte Dissertation mit dem Thema: [INVOLVEMENT OF HUMAN FIBROBLASTS IN ADIPOSE TISSUE DEVELOPMENT] selbstständig und ohne nicht offengelegte Hilfe Dritter verfasst und keine anderen als die angegebenen Quellen und Hilfsmittel genutzt habe.
Alle Stellen, die wörtlich oder dem Sinne nach auf Publikationen oder Vorträgen anderer Autoren beruhen, sind als solche in korrekter Zitierung (siehe „Uniform Requirements for Manuscripts (URM)“ des ICMJE -*www.**icmje**.org*) kenntlich gemacht. Die Abschnitte zu Methodik (insbesondere praktische Arbeiten, Laborbestimmungen, statistische Aufarbeitung) und Resultaten (insbesondere Abbildungen, Graphiken und Tabellen) entsprechen den URM (s.o) und werden von mir verantwortet.

Die Bedeutung dieser eidesstattlichen Versicherung und die strafrechtlichen Folgen einer unwahren eidesstattlichen Versicherung (§156,161 des Strafgesetzbuches) sind mir bekannt und bewusst.“

Datum Unterschrift

7. CURRICULUM VITAE

Mein Lebenslauf wird aus datenschutzrechtlichen Gründen in der elektronischen Version meiner Arbeit nicht veröffentlicht.

8. ACKNOWLEDGMENTS

At this point I would like to express my sincere gratitude and gratefulness towards my supervisor, Prof. Dr. med. Christos C. Zouboulis, for giving me the chance to work in his laboratory and whose expertise, understanding, and patience made possible for me to accomplish this work.

None of the results described in this work would have been possible without the help and contribution of fellow colleagues and collaborators. A very special thanks goes out to Dr. rer. nat. Sabine Fimmel and Dr. Carola Mueller for their support and irreplaceable advice. Especially, I wish to thank Dipl.-Ing. Anke Herrmann and Dipl.-Ing. Bjoern Hermes, who definitely became something more than colleagues over the years working in the laboratory. Your insights, comments and most of all your support in all my struggles and frustrations in my new beginning in this country were invaluable and I am only grateful for having you in my life as my closest and dearest friends.

My greatest appreciation and friendship goes to Dr. med. Evgenia Makrantonaki, to whom I could always address any scientific question of mine and talk about my problems and excitments. Thank you for questioning my ideas, helping me think rationally but most of all for your support in difficult times.

I am grateful to Prof. Dr. Mehdi Shakibaei for the production of light and electron microscopic images, thus making possible to achieve a higher quality in this work. My gratitude is also extended to Prof. Dr. Efstathios S. Gonos, Director of Research IBRB/NHRF (National Hellenic Research foundation) and Dr. Niki Chondrogianni for providing me with primary fibroblasts when needed, thus making these experiments possible.

My work would have been impossible without the generous financial support of the “Kurt and Eva Herrmann Stipendium”, which was awarded in 2010 from the “Alfred Marchionini Foundation for the promotion of Medical Science”.

A good support group is essential to surviving such an experience as completing a doctoral thesis and I am more than grateful for having some unique friends by my side during this time that helped me to keep in sane and even persuaded me not to give up at some points. Maria and Melanie, I cannot thank you enough for being such precious and supporting friends over the past years. You made my life in Berlin a wonderful journey and nothing would have been the same without you.

I consider myself to be extremely lucky to have also made some new good friends when I begun working as a dermatology resident in Dessau. Giving up my life in Berlin was

definitely not an easy decision and Dr. med. Verena Eubel, Dr. med. Anja Jung and PD Dr. med. Undine Lippert helped me out and with their warm support made me feel welcome in a whole new working and living environment.

This thesis is definitely dedicated to my family. To my grandmother who has always encouraged me and advised me to be patient when I run to her for advice and to my sister for her unconditional love and the countless hours she spent patiently listening to my complaints and concerns, not only during my thesis time but throughout my life. But above all, this thesis is dedicated to my parents, without whom none of this would have ever been possible. Through their hard work, patience and personal sacrifices they provided me with essential qualities and stable foundations and taught me persistence, strength and self respect. They both never stopped being proud of me and believing in me, even in times when I questioned myself. There are not enough words to express my love and gratitude to you; you are the reason that makes want to be a better person.

Last, but not least, I would like to thank Menelaos Tsiakiris. He has been a great and true supporter over the good and especially bad times. Thank you for sticking with me over the past years, for appreciating me and for putting up with my “cyclothymia”. This work would have never been possible without your unconditional love and patience, even in times that we have not seen each other over longer periods.